UNCLASSIFIED
SECURITY CLASSIFICATION OF THIS PAGE (When Data Entered)

AD771580

REPORT DOCUMENTATION PAGE

1. REPORT NUMBER: AFRPL-TR-73-105	2. GOVT. ACCESSION NO.
3. RECIPIENT'S CATALOG NUMBER: AD-771580	
4. TITLE (and Subtitle): ENGINEERING PROPERTIES OF ROCKET PROPELLANTS	5. TYPE OF REPORT & PERIOD COVERED: FINAL - 19 January 1971 through 16 September 1973
	6. PERFORMING ORG. REPORT NUMBER: R-9357
7. AUTHOR(s): R.C. Mitchell, R.W. Melvold, and J. Quaglino	8. CONTRACT OR GRANT NUMBER(s): F04611-71-C-0035
9. PERFORMING ORGANIZATION NAME AND ADDRESS: Rocketdyne Division, Rockwell International, 6633 Canoga Avenue, Canoga Park, California 91304	10. PROGRAM ELEMENT, PROJECT, TASK AREA & WORK UNIT NUMBERS
11. CONTROLLING OFFICE NAME AND ADDRESS: Air Force Rocket Propulsion Laboratory, Edwards, California 93523	12. REPORT DATE: November 1973
	13. NUMBER OF PAGES: ~~156~~ 158
14. MONITORING AGENCY NAME & ADDRESS (if different from Controlling Office)	15. SECURITY CLASS. (of this report): UNCLASSIFIED
	15a. DECLASSIFICATION/DOWNGRADING SCHEDULE

16. DISTRIBUTION STATEMENT (of this Report)

Approved for Public Release; Distribution Unlimited

Phase 3 - results of evaluation and completion of data for selected liquid propellants

17. DISTRIBUTION STATEMENT (of the abstract entered in Block 20, if different from Report)

18. SUPPLEMENTARY NOTES

Details of illustrations in this document may be better studied on microfiche.

19. KEY WORDS (Continue on reverse side if necessary and identify by block number)

Adiabatic Compressibility; Card-Gap Tests; Critical Properties; Density Measurements; Detonation Propagation; Detonation Sensitivity; Flash Point; Gas Solubility Measurements; Heat of Formation; Heat of Vaporization; Melting Point Temperature Measurements; Normal Boiling Point; Propellant Formulation and Chemical Analysis; Propellant Storability and Compatibility; Sonic Velocity Measurements;

20. ABSTRACT (Continue on reverse side if necessary and identify by block number)

The results of a 32-month program on the analytical and experimental characteristics of the physical properties of selected propellants are presented in three phases. In Phase I, a continual review of the literature was conducted to ensure the acquisition and documentation of current propellant properties data. Phase II experimental efforts resulted in measurements of: (1) melting points of mixtures of fluorotrinitromethane and tetranitromethane with N_2O_4; (2) HDA, N_2O_4, and N_2H_4-UDMH(50-50) densities as a function of composition and temperature; (3) HDA sonic velocity (and calculations of adiabatic compressibilities) as

DD FORM 1 JAN 73 1473

UNCLASSIFIED
SECURITY CLASSIFICATION OF THIS PAGE (When Data Entered)

19. KEY WORDS (Continued)

Thermal Stability Measurements; Vapor and Equilibrium Pressure Measurements; Viscosity Measurements; Carbonyl Diisocyanate (CDI); CDI; Chlorine Pentafluoride (ClF_5); Chlorine Trifluoride (ClF_3); DCFO ($C_4N_4O_2$); DCFO Mixtures; Dicyanofuroxan (DCFO); Florox (ClF_3O); Fluorotrinitromethane (FTM); FTM; Fuming Nitric Acids; HDA; High Density Acid (HDA); Hydrazine (N_2H_4); Hydrazine Mixtures; Hydrazine, monomethyl ($CH_3N_2H_3$); Hydrazine Nitrate ($N_2H_5NO_3$); Hydrazine, Unsymmetrical Dimethyl; Malonitrile ($C_3H_2N_2$); Malonitrile Mixtures; MHF-3; MHF-5; MHF-7; Mixed Oxides of Nitrogen; MMH; MON-1; Nitrogen Tetroxide; Nitrogen Tetroxide Mixtures; Tetranitromethane (TNM); TNM; UDMH; UDMH Mixtures;

20. ABSTRACT (Continued)

functions of composition and temperature; (4) HDA vapor and equilibrium pressure as a function of composition (with calculations of normal boiling points and heats of vaporization); (5) viscosity of HDA (as a function of composition); (6) nitrogen gas solubility in MMH, N_2H_4, and N_2H_4-UDMH(50-50); (7) detonation propagation and sensitivity of CDI, DCFO, malonitrile, and DCFO Bottoms; (8) CDI and DCFO flash point; (9) CDI thermal stability; (10) malonitrile adiabatic compression sensitivity; (11) compatibility of AF-E-124D O-rings in IRFNA and selected construction materials in HDA; and (12) CDI reaction (possibly a polymerization) as a function of time, temperature, and container materials. In addition, chemical analyses and evaluation of the effects of storage were made on MHF-5, ClF_5, and N_2O_4 samples from long-term storability tests conducted at AFRPL. Also, long-term storability tests were continued with Florox, ClF_5, ClF_3, MHF-3, and MHF-5 in selected metals. Phase III efforts resulted in the reduction, evaluation, and correlation of all data from the experimental efforts, estimation of pseudocritical properties and heat of formation of HDA, and preparation of physical property data sheets for HDA. Physical property data sheets for nitrous oxide are also given.

"When U. S. Government drawings, specifications, or other data are used for any purpose other than a definitely related Government procurement operation, the Government thereby incurs no responsibility nor any obligation whatsoever, and the fact that the Government may have formulated, furnished, or in any way supplied the said drawings, specifications, or other data, is not to be regarded by implication or otherwise, or in any manner licensing the holder or any person or corporation, or conveying any rights or permission to manufacture, use, or sell any patented invention that may in any way be related thereto."

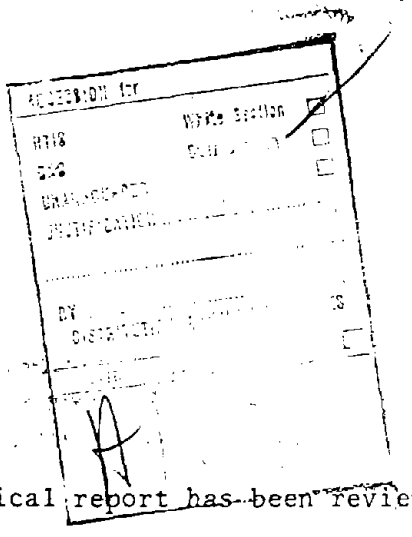

This technical report has been reviewed and is approved.

FOR THE COMMANDER:

CHARLES E. SIEBER, Lt. Colonel, USAF
Chief, Liquid Rocket Division

FOREWORD

This is the final report submitted under G.O. 09332 in compliance with Contract F04611-71-C-0035, Section H, Sub-Item 1AB and Line Item B004 of DD Form 1423. The research reported herein, which covers the period of 19 January 1971 through 16 September 1973, was sponsored by the Air Force Rocket Propulsion Laboratory, Research and Technology Division, Air Force Systems Command, Edwards, California, with Mr. F. S. Forbes acting as the Air Force Project Engineer.

This program was conducted by the Propellant Technology and Applied Mathematics unit of the Rocketdyne Advanced Programs Department, with Dr. E. A. Lawton and Dr. B. L. Tuffly serving, in turn, as the Program Manager and Mr. M. T. Constantine and Dr. R. C. Mitchell serving as the Responsible Project Scientists.

This report has been assigned the Rocketdyne identification number R-9357.

The following personnel have contributed to the work described in this report:

Phase I: Literature Survey

M. T. Constantine
R. C. Mitchell

Phase II: Experimental Determinations

N. S. Fujikawa	(Chemical Analysis)
J. V. Leece	(Compatibility)
R. W. Melvold	(Melting Point, Density, Vapor Pressure, Gas Solubility, Viscosity, Compatibility)
J. Quaglino	(Density, Equilibrium Pressure, Sonic Velocity, Viscosity, Propellant Compatibility, and Storability)
F. D. Raniere	(Propellant Stability)
Dr. J. Sinor	(Propellant Stability)
E. A. Welz	(Chemical Analysis)

Phase III: Evaluation and Compilation of Data

R. C. Mitchell
J. Q. Weber

TABLE OF CONTENTS

LIST OF ILLUSTRATIONS

TABLES

INTRODUCTION

In April 1965 under Contract AF04(611)-10546, Rocketdyne initiated analytical and experimental efforts designed as the initial step of an Air Force program to eliminate liquid propellant property data gaps. The requirements for such a program were clearly indicated by the history of propellant development where the acquisition of essential propellant properties data has frequently lagged, delaying development of propulsion systems using the propellants. Thus, out of necessity, many propulsion system development programs have used estimated or extrapolated propellant properties data (some of which have later proved to be misleading and inadequate), or have included propellant characterization studies as a part of the development program (which have proven to be costly and inefficient because of the time limitation).

The initial program to anticipate and alleviate these potential problem areas in Air Force propulsion systems development was a 12-month effort, directed at a rational and systematic physical characterization of selected liquid rocket propellants over applicable temperature and pressure ranges. To meet this overall objective, the program was conducted in three interrelated phases (Ref. 1). Phase I consisted of a literature survey to review and document available liquid propellant properties data. Experimental efforts under Phase II resulted in the measurement of: (1) the thermal conductivity of 50 N_2H_4-50 $(CH_3)_2N_2H_2$ and $CH_3N_2H_3$; (2) IRFNA and ClF_5 sonic velocity (and calculation of compressibility); (3) ClF_3 and $CH_3N_2H_3$ specific heat, and correction of ClF_5 specific heat data; (4) ClF_3 phase properties; and (5) the design and assembly of apparatuses for measurement of inert gas solubility in liquids and liquid viscosities at extended temperatures and pressures. Phase III analytical efforts included the assembly and evaluation of physical property data on MHF-1, MHF-3, ClF_3, and ClF_5 for future correlation and summary publication.

These analytical and experimental efforts were continued to meet additional liquid propellant property requirements under Contract AF04(611)-11407. In the 24-month, three-phase follow-on program (Ref. 2) under this contract, the

review of the literature was extended to ensure the acquisition and documentation of all liquid propellant properties data. Expansion of the experimental efforts resulted in the measurement of: (1) P-V-T properties (in the critical region) of ClF_3 and ClF_3O, and saturated liquid densities of ClF_3, INTO, and $CH_3N_2H_3$; (2) sonic velocities in ClF_5, ClF_3, N_2O_4, and MHF-3; (3) surface tensions of MHF-3 and MHF-5; (4) nitrogen and helium gas solubilities in ClF_5 and ClF_3; (5) specific heats of $(CH_3)_2N_2H_2$, 50 w/o N_2H_4-50 w/o $(CH_3)_2N_2H_2$, ClF_3, MHF-3, and MHF-5; (6) thermal conductivities of $(CH_3)_2N_2H_2$, MHF-3, MHF-5, and ClF_5; and (7) viscosities of ClF_5 and ClF_3. In addition, evaluation and assembly of selected data from the literature survey and the experimental efforts provided complete physical property bibliographies on B_2H_6 and N_2H_4, and assembly of N_2H_4 and N_2O_4 physical property data sheets.

The same approach was continued under Contract FO4611-68-C-0087 (Ref. 3, 4) to fill needs for additional liquid propellant properties. The literature review was conducted during the entire 28-month duration of the program. Experimental measurements were made in the areas of: (1) melting points of MHF-7 and MON-25; (2) triple point temperature of Florox; (3) liquid densities of Florox, HDA (high-density IRFNA, containing approximately 44.0 w/o N_2O_4), MOR-5, and MHF-7; (4) vapor pressures of HDA, Florox, MOR-5, and MHF-7; (5) surface tensions of N_2O_4 and MON-25; (6) specific heats of MON-25, Florox, MOR-5, and MHF-7; (7) viscosities of Florox, MOR-5, and MHF-7; (8) thermal conductivities of ClF_5; (9) sonic velocities in MON-25, Florox, N_2H_4, MMH, UDMH, 50 N_2H_4-50 UDMH, MHF-3, MHF-5, and MHF-7; and (10) thermal stability of 77 w/o N_2H_4-23 w/o $N_2H_5N_3$. Evaluation and assembly of selected data from the literature survey and the experimental efforts resulted in physical property data sheets for MMH, cyanogen, MON, fuming nitric acids, Florox, MOR-5, and MHF-7. A bibliography was also prepared on ClF_5/ and ClF_3/ materials interactions.

The total progress achieved during the related efforts under these three previous programs has resulted in the empirical establishment of much of the essential data required to fill gaps in the physical properties of many present-day and near-term rocket propellants. However, with the continual

advancement of the technology and the utilization of new propellants and application concepts, many requirements for additional propellant physical and engineering properties data have been established. As a result of these new requirements, a three-phase analytical and experimental extension of the previous systematic propellant property characterization efforts under Contracts AF04(611)-10546, AF04(611)-11407, and F04611-68-C-0087 was continued under Contract F04611-71-C-0035. The period of performance under this contract was extended by two additional increments (to meet new propellant data requirements) to a total span of 32 months. Phase I effort in this program represented a continual review of the literature to document reported propellant properties and to locate data gaps. Phase II effort was directed at the continued experimental determination of unavailable and/or questionable engineering data for selected oxidizers and fuels in an order related to current Air Force requirements. Phase III included the compilation, correlation, and evaluation of the data obtained from Phases I and II, the presentation of the valid data in annual technical reports and data sheets for incorporation in the CPIA propellant handbook. This report describes each phase of this program and summarizes the results and accomplishments achieved during the entire period of performance.

PHASE I: LITERATURE SEARCH

OBJECTIVE

The Phase I objective represented a continual review of the current propellant-related literature and efforts of other investigators in the field to acquire reported liquid propellant properties data and to locate data gaps and inconsistencies. This survey was designed to include selected fuels, oxidizers, monopropellants, pressurizing gases, and related materials as the needs for supplemental data would arise.

RESULTS AND ACCOMPLISHMENTS

A formal survey of current propellant literature, initiated under Contract AF04(611)-10546 (Ref. 1) and continued under Contract AF04(611)-11407 (Ref. 2) and Contract F04611-68-C-0087 (Ref. 4), was continued as Phase I of this program. The survey included the acquisition, review, and documentation of all available physical and engineering properties data on liquid propellants of interest to the Air Force.

The total literature survey was accomplished through the use of three different techniques. One part of the effort included a survey of all reports received by Rocketdyne through normal distribution channels. Each of these reports was surveyed with respect to subject matter, and reports containing potential liquid propellant information were selected for detailed review. All pertinent data contained in these reports were documented for potential future use.

This report survey was supplemented by a continual survey of current releases of Chemical Abstracts, NASA CSTAR Abstracts, CPIA Chemical Propulsion Abstracts, DDC Technical Abstract Bulletin, the NBS Cryogenic Data Center's Current Awareness Service, and propellant manufacturers' bulletins. Any pertinent information located through these sources that had not been acquired previously by Rocketdyne was obtained and reviewed in detail.

To ensure a complete awareness of all available data (and data sources) related to rocket propellants, the third technique involved selective use of the

federally sponsored information analysis centers whose services are available to the rocket propulsion industry. The many resources available through these centers were employed when a summary of sources of specific information and data was required on a particular propellant.

During the performance of this program, more than 6000 reports were surveyed. Of this total, more than 500 reports were reviewed in detail for pertinent propellant information.

As part of Phase I, comprehensive searches of the chemical and propulsion literature were conducted to locate all available physical properties data for high density fuming nitric acid (HDA). Sources checked included the chemical and propulsion abstract sources listed above, plus personal contacts with other companies who have an interest in this propellant.

PHASE II: EXPERIMENTAL DETERMINATIONS

OBJECTIVE

The objective of Phase II was the experimental characterization of essential properties of selected liquid propellants. This phase essentially constituted a 31-month continuation of the efforts initiated under Phase II of Contracts AF04(611)-10546 (Ref. 1), AF04(611)-11407 (Ref. 2), and F04611-68-C-0087 (Ref. 4). Selection of the propellants and properties that were experimentally characterized was related to the unavailability of required data and relative importance of the data to the Air Force. Initial efforts emphasized the completion of those propellant properties recommended for initial characterization under the previous programs. Additional efforts continued in an order related to the importance of the data to the Air Force (as determined by the Air Force Project Engineer).

The selected properties were determined over the liquidus temperature range and over a pressure range of 14.7 to 1000 psi, where practical. Changes to the selected list were made at various times during the program through mutual agreement of Rocketdyne and the Air Force Contracting Officer. Standard test methods were used when available. Wherever unique or new test methods were used, their use was approved by the Air Force Contracting Officer.

RESULTS AND ACCOMPLISHMENTS

During the program, Phase II efforts were directed at the measurement of melting point, density, vapor pressure (with calculation of normal boiling point and heat of vaporization), equilibrium pressure, inert gas solubility, viscosity, sonic velocity (and calculation of adiabatic compressibility), thermal stability, detonation propagation, flash point, plus materials compatibility and storability of selected propellants.

The apparatus and techniques used in these measurements were essentially those used previously in similar efforts conducted for the Air Force (Ref. 1 through 4), with one exception. An improved apparatus for the measurement of gas solubility, developed under in-house funding, was used to improve the

quality, economics, and accuracy of these measurements. In addition, standard techniques were used to evaluate thermal stability and storability.

The efforts and results in each of these areas of property characterization are described in the following paragraphs. Included in the discussions are details of the changes in experimental apparatus or methods instituted during the current program, as well as background information about the major apparatus and methods used previously.

Melting Point

Melting point measurements were conducted on several oxidizer blends to determine the extent of N_2O_4 melting point lowering that could be achieved through formulation of suitable mixtures of N_2O_4 with selected additives. The oxidizer blends studied in the course of this program consisted of separate mixtures of N_2O_4 with the additives tetranitromethane (TNM) and fluorotrinitromethane (FTM), in varying amounts.

The standard melting point sample cell consists of a glass ampoule closed by a Teflon needle valve, and fitted with an internal thermowell and a solenoid-activated reciprocating stirrer. The output from a copper-constantan thermocouple in the thermowell (filled with Dupont Freon E-2, used as a heat transfer medium) is fed to a calibrated recorder with which the temperature of the sample is monitored. Recorder calibration was accomplished by measuring both the ice-water point and an emf signal fed to the recorder through an accurate potentiometer. The sample cell is inserted through a cork into an unsilvered-strip Dewar containing a rapidly circulating GN_2 bath. Cell cooling is accomplished by allowing LN_2 to boil off in the lower portion of the Dewar, while heating is provided by thermal losses. The samples are cooled with stirring until they freeze and then they are warmed (with stirring). The temperature at which the last solid melts (usually determined by visual observation) is noted as the melting point. Triplicate measurements were made on each sample. All of the melting point measurements were made on samples under their own vapor pressure.

Melting point determinations were conducted on two N_2O_4-TNM formulations and two N_2O_4-FTM formulations. The red-brown N_2O_4 used to prepare these mixtures was propellant N-1 (described in the Chemical Formulation section) with 99.9 w/o N_2O_4 and 0.01 w/o H_2O equivalent. Their respective compositions, experimental melting points, and theoretical melting points appear in Table 1. The experimental melting points are plotted in Fig. 1. In all cases, a slight supercooling was observed when freezing the samples.

TABLE 1. MELTING POINTS OF SELECTED N_2O_4 MIXTURES

Oxidizer Blend	Additive	Melting Point		Theoretical Melting Point*
	w/o	C	F	C
N_2O_4-TNM	10.0	-13.1	8.4	-13.3
N_2O_4-TNM	20.0	-14.8	5.4	-15.8
N_2O_4-FTM	10.1	-13.5	7.7	-13.6
N_2O_4-FTM	20.1	-15.3	4.5	-16.6
N_2O_4**	None	-11.25	11.75	--
TNM**	None	14.2	57.6	--
FTM**	None	-41.9	-43.4	--

*Estimated from equation 1, for very dilute solutions

**Literature values (Ref. 2 for N_2O_4, Ref. 5 for TNM and Ref. 6 for FTM)

Theoretical melting points were calculated from the usual freezing point depression expressions based on the Clapeyron-Clausius equation. If the solid, which separates upon freezing the solution, is pure solvent it is found that for very dilute solutions

$$\Delta T = K_f m \qquad (1a)$$

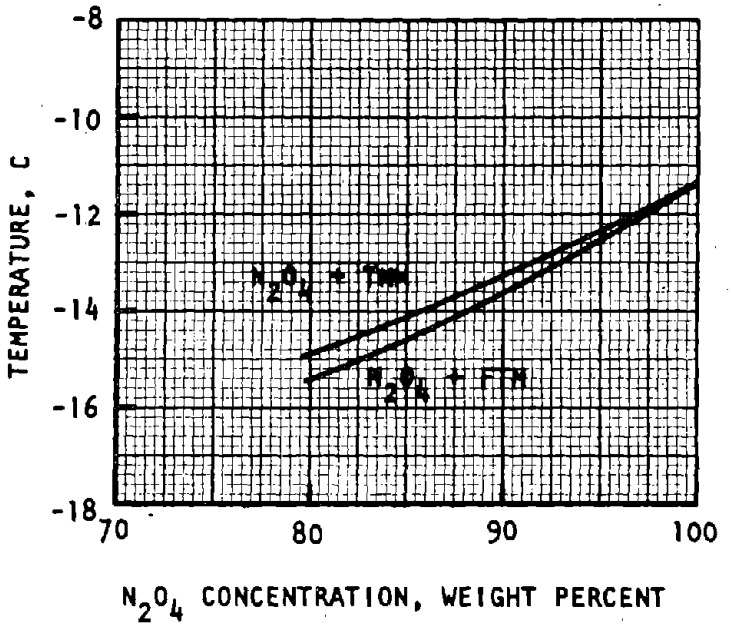

Figure 1. Melting Points of Selected Mixtures with N_2O_4

where m is the molality of the solution (g-mole/1000 g solvent), and K_f is the molal depression constant defined by

$$K_f = \frac{RT_o^2}{1000\ell_f} \qquad (1b)$$

in which ℓ_f is the heat of fusion per gram, and T_o is the freezing point of the solvent. The depression of the freezing point is thus proportional to the molality of the solution; however, the essential condition is that the solution be dilute. In this case, as with relatively concentrated solutions, deviations are observed, as is to be expected. Nevertheless, it would appear that the additives did no more than lower the N_2O_4 melting point nominally.

It would be desirable to have a mixture with a melting point in the range of about -18 to -29 C(0 to -20 F). Unfortunately, this does not appear attainable with practical amounts of additives.

Experimentally, the oxidizer additive was transferred into the sample cell (in a fume hood) using a glass syringe with a stainless-steel needle. Once loaded with the additive, the sample cell was immersed in LN_2, and subsequently evacuated. The approximate N_2O_4 volume was then loaded into the sample cell. Before removing it from the fume hood, the cell and its contents were allowed to warm slowly and mix. The cell was then removed and placed in the special melting point apparatus, and measurements were conducted. The approximate volume of mixture in the cell was 6 ml in the case of 20 w/o additive and 12 ml in the case of 10 w/o additive. The composition of each mixture was calculated on the basis of accurate sample cell weighings before and after loading each component.

Normal Boiling Point

The normal boiling points [i.e., the temperature at which the vapor pressure of the material is 1 atm (14.696 psia)] of HDA mixtures were calculated from their vapor pressure correlations as given in the Vapor and Equilibrium Pressure section. The normal boiling point of the nominal HDA (54.8 w/o HNO_3-44.0 w/o NO_2-0.5 w/o H_2O-0.7 w/o HF) was calculated as 24.7 C (76.5 F).

Critical Properties

Experimental values for the critical constants of HDA do not exist. It would not be possible to obtain reliable values because of the decomposition of nitric acid. Consequently, pseudocritical properties were estimated for this mixture.

Pseudocritical temperature and pressure were estimated by Kay's Rule (Ref. 7) and the pseudocritical compressibility factor was estimated by the analogous Leland-Mueller rule (Ref. 8). Pseudocritical volume was calculated from the other constants. HDA is considered to be an extremely non-ideal solution because of the associative nature of its components. For example, the N_2O_4 may be partly present as NO_2, $(NO_2)_2$, or $NO_2 \cdot HNO_3$, in various degrees, depending upon the temperature. In addition, it was necessary to estimate the critical properties of the major component, nitric acid, since no data could be found.

It is unlikely that such data exist, because of the rapid decomposition of anhydrous nitric acid at elevated temperatures. Consequently, there is more than average uncertainty in the estimated values.

The critical temperature of nitric acid was estimated by the methods of Lydersen (Ref. 9, 10) and Gates and Thodos (Ref. 11). The latter value, 624 K, was adopted because the former, 486 K, seemed peculiarly low. Critical pressure (94 atm) was estimated by Reidel's method (Ref. 12), and critical compressibility (0.238) was estimated by the boiling point correlation of García-Bárcena (Ref. 13).

In applying Kay's Rule to HDA, there is uncertainty as to the most appropriate value to use for the molecular weight of N_2O_4 (46, 92, or some intermediate value). Thus, the rule was applied using the extreme values. Pseudocritical pressure and compressibility were surprisingly insensitive to the molecular weight of N_2O_4 and even the temperatures were close (ΔT = 31 K). Values are summarized in Table 2 . There is no good reason to select either extreme; therefore, they were averaged to obtain the recommended values given in Table 2.

TABLE 2. PSEUDOCRITICAL CONSTANTS OF HDA

Constant	Assumption		Recommended Values
	N_2O_4 present as NO_2 (MW = 46.005)	N_2O_4 present as N_2O_4 (MW = 92.001)	
P_c, atm	97.4	97.1	97.2
T_c, K	524	555	540
Z_c	0.235	0.235	0.235
V_c, cc/g-mole	104	110	107

Density

Experimental measurements were performed to expand the available density data on N_2O_4, N_2H_4-UDMH (50-50), and HDA formulations. Hydrometer measurements were

also conducted on HDA to determine "bouyancy effects" that could be used to correlate hydrometer readings to actual density values. The densities of brown N_2O_4 and MON-1 were determined as a function of temperature from 6 to 78 C (43 to 173 F) and composition. The density of N_2H_4-UDMH (50-50) was determined as a function of temperature and composition (four formulations within the MIL Specification limits) over the temperature range of 0 to 59 C (32 to 138 F). Density measurements on three HDA formulations over a temperature range of 1 to 71 C (35 to 160 F) extended previously available data (Ref. 4) to account for composition variations. HDA hydrometer measurements were conducted at 15.56 C (60 F) and compared with density measurements at that temperature to determine a hydrometer correction factor.

Two different experimental apparatuses, an all-metal variable-volume densimeter and a Pyrex capillary pycnometer (closed), were used in the density measurements. A diagram of the variable-volume apparatus, which was constructed from the design of Poole and Nyberg (Ref. 15), is presented in Fig. 2. This densimeter (previously described in Ref. 2 and 4) operates on the principle that a sudden rise in pressure (sensed by the pressure transducer) will occur when all vapor in the variable-volume propellant cell is forced to condense by mechanical reduction of the cavity volume containing both liquid and vapor. The volume of the cell (and thus the contained liquid) at this point is indicated by the position of the micrometer attached to the bellows and a prior calibration of the micrometer (defining the micrometer setting-cell volume relationship of the apparatus) with a liquid of known density. The density of the sample at this point is then calculated from the weight of the propellant sample and the indicated volume.

The apparatus is constructed entirely of 321 stainless steel and is capable of withstanding pressures up to 1500 psi. The volume range provided by the stainless-steel bellows permits density measurements over a wide range of temperatures without change of the propellant sample size. The densimeter was placed in a constant-temperature bath for temperature selection and regulation to ±0.1 F. The temperature of the propellant sample was measured by a chromel-alumel thermocouple taped to the densimeter and was recorded during the density measurement after the propellant sample had reached thermal equilibrium with the environmental bath.

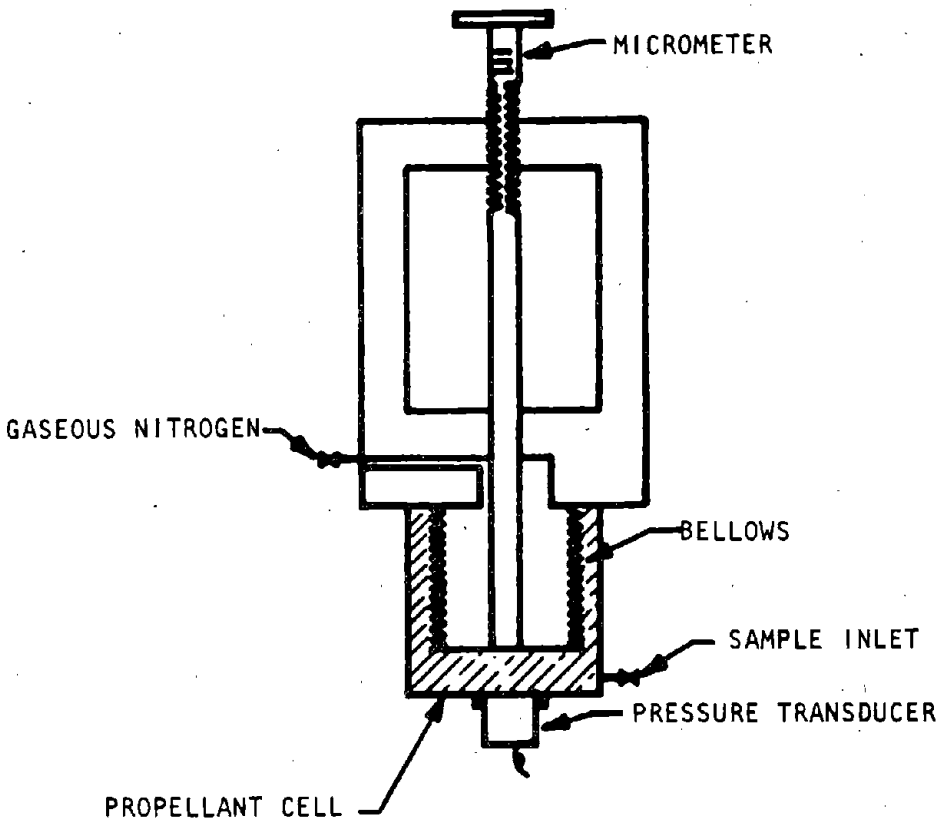

Figure 2. Poole-Nyberg Densimeter

The Pyrex capillary pycnometers used in the density measurements are of two basic types. The first are those converted from 10- or 25-ml volumetric flasks. The necks of the flasks were replaced with 4-inch sections of 2-mm bore capillary tubing, which were etched with reference lines and sealed with Fischer-Porter needle valves. The second type are those using a heavy wall Pyrex glass sample bulb to reduce non-linearities in the calibration curves caused by slight flexing of a thinner-wall bulb. Each pycnometer of the second type incorporates a 2-1/2-inch section of 1.0-mm bore capillary tubing, etched with a reference line, and sealed with a Kontes Teflon valve. For measurements below room temperature, both pycnometer types employed an expansion bulb in the upper portion above the capillary tubing. A Gaetner cathetometer was used to measure meniscus levels above or below the reference line. These deviations of the meniscus level were recorded to $\pm 5 \times 10^{-4}$ cm. As in the measurements with the densimeter, a constant-temperature bath maintained the desired temperature level of the propellant samples to ±0.1 F. A Mettler analytical balance was used to determine the sample weights to ±0.1 mg.

Hydrometer measurements were conducted with a short-stem hydrometer in conjunction with a 1.4-inch internal diameter cylinder.

Density of N_2O_4. As a result of density measurements obtained experimentally on N_2O_4 and MON-1, the resulting values (described subsequently) were correlated as a function of temperature from 6.2 to 78.2 C (43.1 to 172.8 F) and composition (0 to 1.17 w/o NO) through use of a least-squares curve-fit computer program. The correlation is represented by the following expressions:

$$\rho_{(g/cc)} = 1.4901 - 1.80169 \times 10^{-3} T_{(C)} - 2.71835 \times 10^{-5} T_{(C)}^2 + 5.093 \times 10^{-7} T_{(C)}^3 - 3.614 \times 10^{-9} T_{(C)}^4 - 2.9839 \times 10^{-3} N_{(w/o)} \quad (2a)$$

and

$$\rho_{(lb/cu\ ft)} = 94.29 - 0.0094 T_{(F)} - 1.17924 \times 10^{-3} T_{(F)}^2 + 8.2033 \times 10^{-6} T_{(F)}^3 - 2.1496 \times 10^{-8} T_{(F)}^4 - 0.1863 N_{(w/o)} \quad (2b)$$

where

ρ = density, g/cc or lb/cu ft

T = temperature, C or F

N = NO concentration, weight percent

The standard errors of estimate of these expression are 0.0010 g/cc and 0.063 lb/cu ft, respectively. It can be noted that there is no dependence on water composition in this correlation. It was found that the effect of water was negligible (within the specification range of 0 to 0.17 w/o), as described below.

Data for various mixtures of nitrogen tetroxide and nitric oxide were collected and evaluated previously (Ref. 4). During this program, these data (from Ref. 16 through 22) were reevaluated, and the valid data, including Rocketdyne data for saturated liquid, were correlated with a single equation as a function of both temperature (from freezing points to 105 C) and NO content (0 to 30 w/o NO):

$$\rho_{(g/cc)} = 1.4905 - 2.124 \times 10^{-3} T_{(C)} - 5.01 \times 10^{-6} T^2_{(C)} - 3.250 \times 10^{-3} N_{(w/o)} + 1.804 \times 10^{-5} N^2_{(w/o)} + 1.458 \times 10^{-5} N_{(w/o)} T_{(C)} + 3.852 \times 10^{-7} N^2_{(w/o)} T_{(C)} - 2.226 \times 10^{-7} N_{(w/o)} T^2_{(C)} \quad (3)$$

This correlation was compared with that developed for the new data (Eq. 2a for 0 to 1.17 w/o NO) by making a new curvefit on the new data with the density effect of NO "backed out" by means of Eq. 3 . This represented the new data just as well as the specific curvefit (Eq. 2a) , with standard errors of estimate of 0.0010 g/cc in each case. When a term was added for water content, the curvefit was not improved and the maximum contribution of the water term to density was only 0.0001 g/cc (one tenth of the standard error). Thus it was concluded that water does not have a significant effect on N_2O_4 density within the MIL specification range.

The final correlation (Eq. 2a) is represented graphically in Fig. 3 for red-brown N_2O_4 (i.e., zero NO concentration). The curves for other N_2O_4 compositions within the MIL specification range, which can be evaluated from the

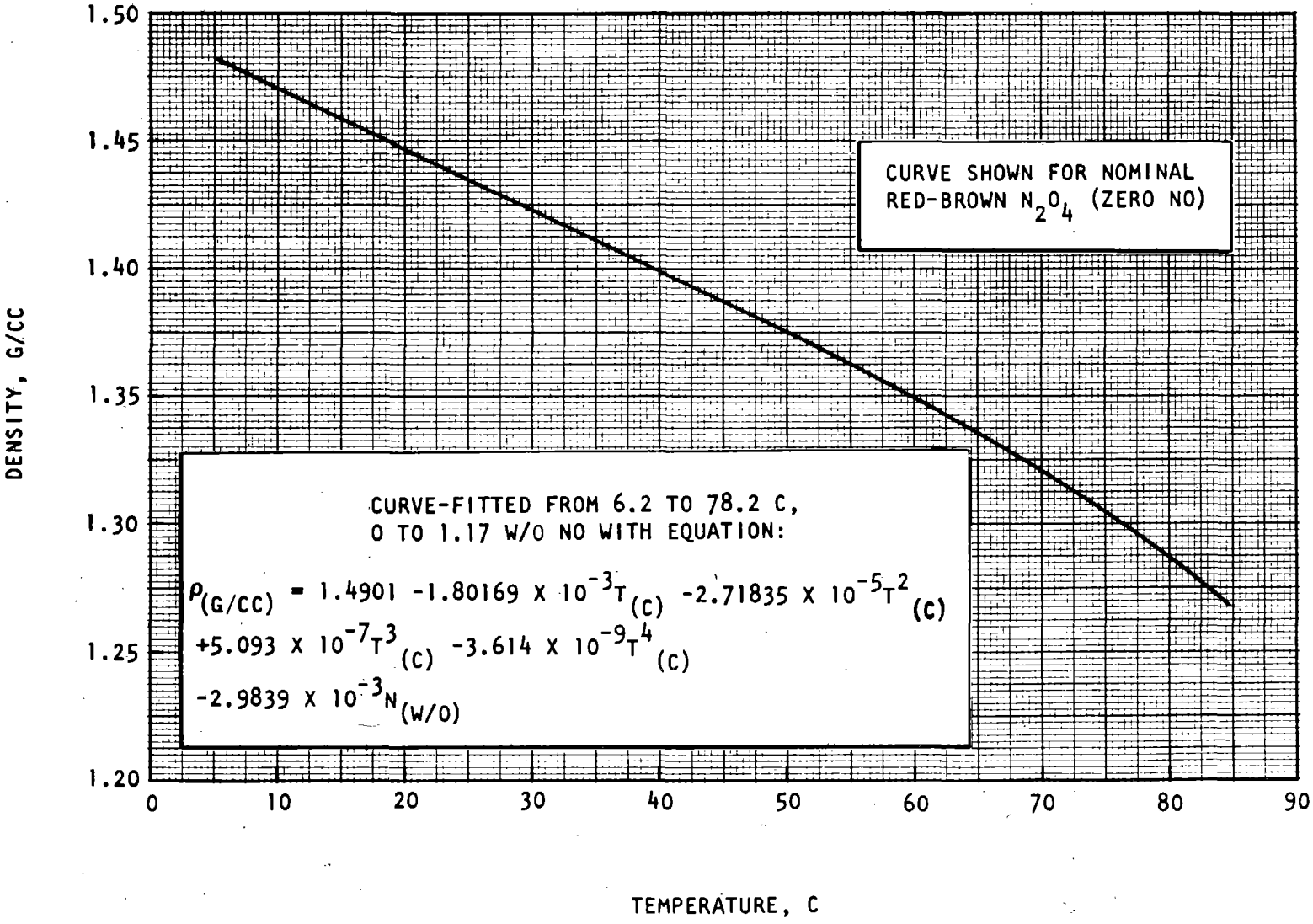

Figure 3. Density of Saturated Liquid Nitrogen Tetroxide

correlation, are not shown in Fig. 3 because they would be almost indistinguishable from each other. For example, the difference in density between red-brown N_2O_4 (zero NO) and MON-1 with maximum NO (1.0 w/o) is only 0.003 g/cc. The difference in MON-1 density over the MIL specification range of NO concentration (0.6 to 1.0 w/o) is only 0.0012 g/cc.

Density measurements were conducted on brown N_2O_4 (composition: 99.9 w/o N_2O_4, 0.01 w/o H_2O equivalent) over the temperature range 6.2 to 78.2 C (43.1 to 172.8 F). Sixteen values were obtained using the Poole-Nyberg densimeter and four using a 10-ml glass pycnometer of the volumetric-flask type. The results are listed in Table 3. A correlation of the resulting data by a least-squares curve-fit computer program resulted in the following expressions of density as a function of temperature:

$$\rho_{(g/cc)} = 1.4903 - 2.0517 \times 10^{-3} T_{(C)} - 6.0813 \times 10^{-6} T^2_{(C)}$$

with a standard error of estimate of 0.0014 g/cc.

Experimentally, the N_2O_4 loadings of the pycnometer were made directly from a vacuum line, and the pycnometer was calibrated using distilled water. A correction was applied to the pycnometer values for the amount of N_2O_4 in the vapor phase at each of the four temperatures involved. The densimeter, which had previously been passivated and cleaned with N_2O_4, was loaded with N_2O_4 indirectly through use of a tared loading cylinder for better accuracy. Again, all N_2O_4 transfers were performed using the vacuum line.

Density measurements were conducted on an NO-enriched N_2O_4 composition (1.17 w/o NO, 0.07 w/o H_2O) over the temperature range 22.3 to 74.2 C (72.1 to 165.6 F). A total of 16 individual data points were generated from two measurement sets using the Poole-Nyberg densimeter. These values are listed in Table 4. A least-squares computer curve-fit of the data resulted in the following expression of density as a function of temperature:

$$\rho_{(g/cc)} = 1.4883 - 2.180 \times 10^{-3} T_{(C)} - 4.109 \times 10^{-6} T^2_{(C)}$$

The standard error of estimate is 0.001 g/cc.

TABLE 3. EXPERIMENTAL DENSITY OF RED-BROWN NTO*

Temperature		Observed Density,	Calculated Density, Equations 2a and 2b	
C	F	g/cc	g/cc	lb/cu ft
6.2	43.1	1.478	1.478	92.28
7.2	45.0	1.4766**	1.476	92.14
9.3	48.7	1.471	1.471	91.86
12.4	54.4	1.464	1.464	91.42
15.6	60.0	1.4569**	1.457	90.97
15.6	60.0	1.457	1.457	90.97
18.6	65.5	1.450	1.450	90.52
21.7	71.0	1.443	1.443	90.07
22.3	72.1	1.441	1.441	89.98
24.5	76.1	1.434	1.436	89.64
25.0	77.0	1.4349**	1.435	89.56
28.0	82.4	1.428	1.427	89.11
29.4	85.0	1.4242**	1.424	88.89
30.3	86.5	1.421	1.422	88.76
33.8	92.9	1.415	1.413	88.21
42.6	108.6	1.391	1.392	86.88
47.9	118.3	1.380	1.378	86.05
58.7	137.6	1.350	1.351	84.33
66.1	151.0	1.331	1.330	83.05
78.2	172.8	1.290	1.291	80.61

* SAMPLE COMPOSITION: 99.9 w/o N_2O_4, 0.01 w/o H_2O equivalent

** Measurements conducted with 10-ml capillary pycnometer; all other measurements conducted with Poole-Nyberg densimeter.

TABLE 4. EXPERIMENTAL DENSITY OF NO-RICH MON-1*

Temperature		Observed Density,	Calculated Density, Equations 2a and 2b	
C	F	g/cc	g/cc	lb/cu ft
21.9	71.4	1.439	1.439	89.82
22.3	72.1	1.439	1.438	89.76
24.3	75.7	1.433	1.433	89.45
28.6	83.5	1.422	1.422	88.80
34.2	93.6	1.407	1.409	87.94
34.8	94.6	1.407	1.407	87.85
39.8	103.7	1.395	1.395	87.08
41.2	106.1	1.391	1.392	86.87
46.3	115.4	1.379	1.379	86.08
47.6	117.6	1.376	1.376	85.89
54.2	129.6	1.360	1.359	84.84
57.2	134.9	1.350	1.351	84.36
60.3	140.5	1.342	1.343	83.85
64.2	147.6	1.331	1.332	83.17
71.2	160.2	1.313	1.311	81.87
74.2	165.5	1.303	1.302	81.28

* SAMPLE COMPOSITION: 98.5 w/o N_2O_4, 1.17 w/o NO, <0.01 w/o Cl-, 0.07 w/o H_2O

Experimentally, the N_2O_4 vacuum system was first refurbished, and then a 500-ml stainless-steel cylinder unit was cleaned, helium leak-checked, and attached to the vacuum line preparatory to formulating the mixture. The N_2O_4 was loaded in increments by gravity flow through a transparent Teflon sight tube into the cylinder, immersed in LN_2. The NO was then added by volume expansion in several stages. A 100-psig pressure gauge attached to the cylinder was used to monitor pressure during the mixing operation. Following the successful mixing operation, in which approximately 1.2 w/o additional NO was added to the original N_2O_4, an accurately weighed NO-rich MON-1 sample was then transferred on a vacuum line to the Poole-Nyberg densimeter. The densimeter was removed and placed in an oven where density measurements were conducted. In order to back pressure the densimeter bellows, a new GN_2 pressurization system was assembled.

Density of N_2H_4-UDMH (50-50). Experimental density measurements were conducted on four selected N_2H_4-UDMH (50-50) formulations (described in the Propellant Formulation and Chemical Analyses section as A-1, A-2, A-3, A-4) over the temperature range of 0 to 59 C (32 to 138 F). Samples of the N_2H_4-UDMH (50-50) formulations were loaded into 25-ml pycnometers (of both types) within a dry box under approximately one atmosphere of gaseous nitrogen. The resulting data (shown in Table 5 with corresponding chemical analyses of the formulations) were correlated as a function of temperature and composition through the use of a least-squares curve-fit computer program. The correlation, which covers a range of 0 to 59 C (32 to 138 F), 46.6 to 50.3 w/o UDMH and 0.3 to 1.9 w/o water, is represented by the following expressions:

$$\rho_{(g/cc)} = 1.0249 - 9.550 \times 10^{-4} T_{(C)} - 2.165 \times 10^{-3} U_{(w/o)} + 1.715 \times 10^{-3} W_{(w/o)} \quad (4a)$$

and

$$\rho_{(lb/cu\ ft)} = 65.042 - 3.3123 \times 10^{-2} T_{(F)} - 0.1351\ U_{(w/o)} + 0.1071\ W_{(w/o)} \quad (4b)$$

where ρ = density, g/cc or lb/cu ft

T = temperature, C or F

U = UDMH concentration, weight percent

W = water concentration, weight percent

TABLE 5. DENSITY DATA FOR SATURATED LIQUID N_2H_4-UDMH (50-50)*

Formulation	Temperature		Density		
	F	C	Measured, g/cc	Calculated From Eq. 4a, g/cc	Calculated From Eq. 4b, lb/cu ft
A-1	32.0	0.0	0.9231	0.9239	57.68
	77.0	25.0	0.8996	0.9000	56.19
	138.0	58.9	0.8676	0.8676	54.16
A-2	32.0	0.0	0.9174	0.9165	57.22
	77.0	25.0	0.8928	0.8926	55.78
	138.0	58.9	0.8603	0.8603	53.71
A-3	32.0	0.0	0.9279	0.9272	57.89
	77.0	25.0	0.9040	0.9034	56.40
	138.0	58.9	0.8720	0.8710	54.38
A-4	32.0	0.0	0.9233	0.9236	57.66
	77.0	25.0	0.8983	0.8997	56.17
	138.0	58.9	0.8667	0.8673	54.15

* SAMPLE COMPOSITIONS:

Formulation	Composition, w/o			
	UDMH	N_2H_4	H_2O	OSI
A-1	46.9	52.6	0.3	0.2
A-2	50.3	49.1	0.3	0.3
A-3	46.6	51.3	1.9	0.2
A-4	48.3	49.6	1.9	0.2

The standard errors of estimate of these expressions are 0.0008 g/cc and 0.05 lb/cu ft, respectively. A graphical representation of the nominal N_2H_4 UDMH (50-50) formulation as described by Eq 4a is shown in Fig 4.

Density of HDA. Density measurements were conducted on three selected HDA formulations [described in the Propellant Formulation and Chemical Analyses section as nominal (HDA-N1), high H_2O (HDA-HW1), and high NO_2 (HDA-HN)] using the Poole-Nyberg densimeter. The samples were loaded into the apparatus under their own vapor pressure using a vacuum line. The results of these measurements, presented in Table 6, were correlated through use of a least-squares curve-fit computer program with the following expressions of density as a function of temperature and composition:

$$\rho_{(g/cc)} = 1.7889 - 1.8391 \times 10^{-3} T_{(C)} - 5.82 \times 10^{-6} T_{(C)}^2 - 2.420 \times 10^{-3} N_{(w/o)} - 1.750 \times 10^{-2} W_{(w/o)} \quad (5a)$$

and

$$\rho_{(lb/cu\ ft)} = 113.61 - 5.660 \times 10^{-2} T_{(F)} - 1.12 \times 10^{-4} T_{(F)}^2 - 0.1511\ N_{(w/o)} - 1.093\ W_{(w/o)} \quad (5b)$$

where ρ = density, g/cc or lb/cu ft

T = temperature, C or F

N = NO_2 concentration, weight percent

W = water concentration, weight percent

The standard errors of estimate of these equations are 0.0017 g/cc and 0.106 lb/cu ft, respectively, over a temperature range of 1 to 68 C (34 to 155 F) and composition variations of 43.4 to 45.6 w/o NO and 0.4 to 1.7 w/o H_2O. These correlations are shown graphically in Appendix A. Density data previously obtained (Ref. 4) were not included in this correlation because these new data were obtained with propellant formulations for which the composition could be much more accurately controlled.

HDA Hydrometer Measurements. Hydrometer measurements were made on HDA to determine the "buoyancy effects" or correlations of hydrometer readings to actual density values.

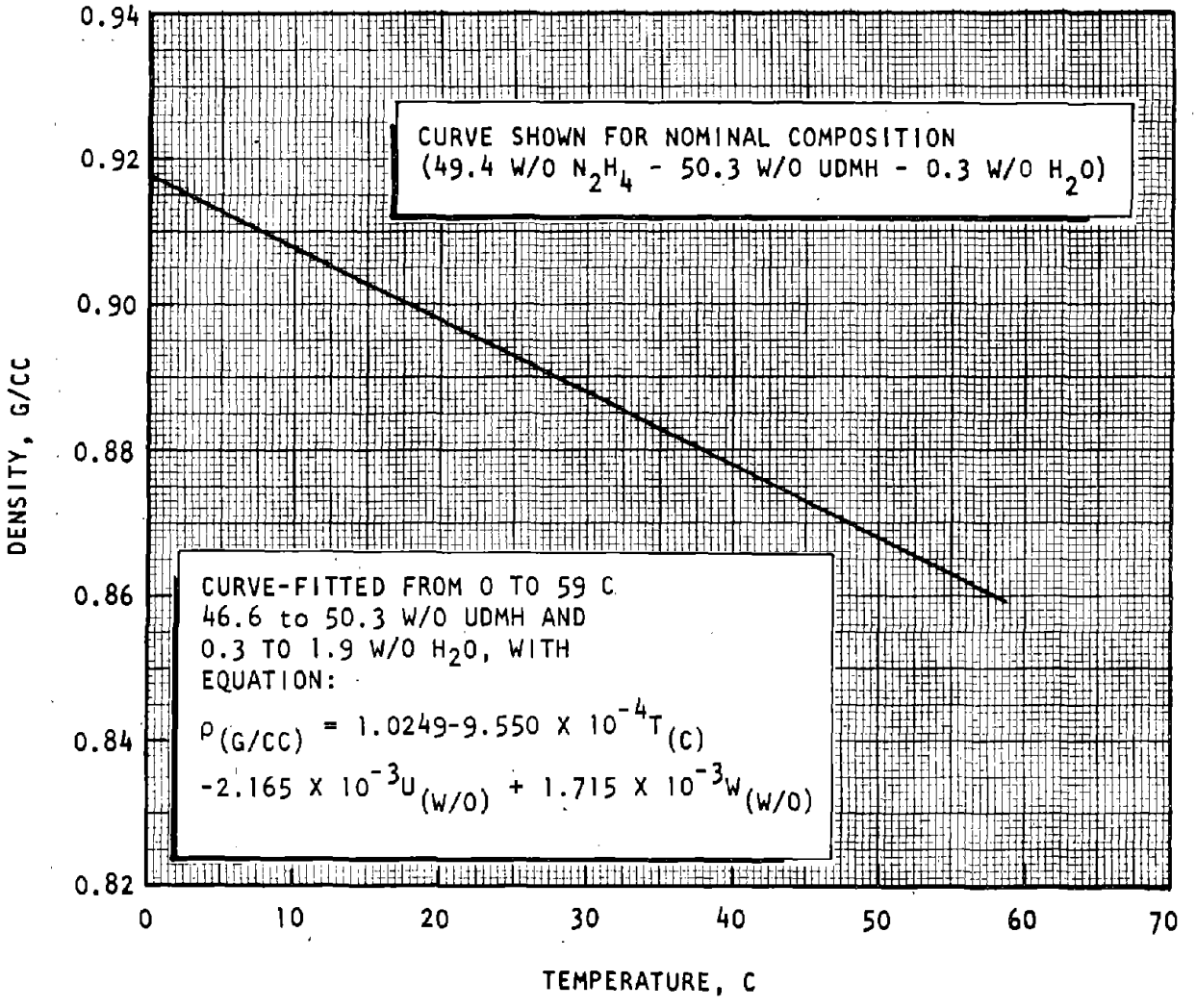

Figure 4. Density of Saturated Liquid N_2H_4-UDMH (50-50)

TABLE 6. DENSITY DATA FOR SATURATED LIQUID HDA*

Formulation	Temperature		Density		
	F	C	Measured, g/cc	Calculated From Eq. 5a, g/cc	Calculated From Eq. 5b, lb/cu ft
HDA-N1	33.8	1.0	1.670	1.674	104.5
	59.8	15.4	1.645	1.646	102.7
	80.2	26.8	1.623	1.622	101.3
	100.0	37.8	1.596	1.598	99.7
	121.8	49.9	1.570	1.569	98.0
	140.0	60.0	1.548	1.544	96.4
	153.8	67.7	1.524	1.524	95.1
HDA-HN	35.0	1.7	1.670	1.668	104.2
	60.0	15.6	1.641	1.642	102.5
	69.2	20.7	1.631	1.631	101.8
	80.1	26.7	1.618	1.618	101.0
	100.1	37.8	1.594	1.594	99.5
	120.0	48.9	1.569	1.568	97.9
	140.0	60.0	1.539	1.540	96.2
	147.6		1.528	1.529	95.5
	150.0	65.6	1.525	1.526	95.3
HDA-HW1	35.8	2.1	1.652	1.650	103.0
	60.2	15.7	1.625	1.624	101.4
	80.1	26.7	1.600	1.601	99.9
	100.1	37.8	1.576	1.576	98.4
	120.1	48.9	1.548	1.550	96.8
	139.9	60.0	1.522	1.523	95.1
	155.0	68.3	1.500	1.501	93.7

*SAMPLE COMPOSITIONS:

Formulation	Composition, w/o					
	HNO_3	NO_2	H_2O	HF	Fe_2O_3	Particulates
HDA-N1	55.0	44.0	0.4	0.4	0.03	0.2
HDA-HN	53.4	45.6	0.4	0.4	0.03	0.2
HDA-HW1	54.3	43.4	1.7	0.4	0.03	0.2

A sample from the nominal formulation of HDA was transferred to the chilled cylinder (surrounded by dry ice), the hydrometer was immersed, and the container was capped with aluminum foil. After the cylinder was transferred to a 15.56 C (60 F) bath and allowed to equilibrate, the foil cap was removed and the hydrometer was read after a two-minute period. Additional readings were taken over a period of 105 minutes. The hydrometer reading (taken by observing the graduations from below the liquid surface) on HDA after two minutes of temperature equilibration was 1.638 based on the H_2SO_4 calibrations. After 10 minutes the reading was 1.639; this remained constant through the remainder of the 105-minute observation period. The density of the same HDA formulation, as determined by densimeter measurements at 15.56 C (60 F) was 1.645 g/cc. Therefore, a correction factor of 0.006 to 0.007 (depending on the time of observation) should be added to the hydrometer readings to obtain actual density of HDA. (Using the CCl_4 calibrations, a reading of 1.634 would be observed for the same conditions.) Visual inspection of the hydrometer after the measurements revealed some surface etching of the glass.

Hydrometers are inherently the least accurate method of determining density. When they are floated in a liquid, a small amount of the liquid rises above the stem to form a meniscus. This liquid adhering to the stem, above the general level of the liquid in which the instrument is floating, has the same effect as adding to the mass of the hydrometer; thus increasing the depth of immersion. The influence of surface tension on hydrometers can be considerable, and can markedly change hydrometer readings when traces of impurities are absorbed on the liquid surface. Measurements in the HDA can be further affected by the volatility of NO_x components that give local temperature and density variations. It was concluded that hydrometer measurements in HDA are at best only accurate to two decimal places.

In the experimental investigation of HDA "bouyancy effects," short and long stem hydrometers were calibrated with CCl_4 and 73-percent H_2SO_4 in cylinders with internal diameters of 1.0, 1.4, and 1.9 inches. Since ASTM standards (D287-64 and D1298-67) require the ID of the cylinder containing the hydrometer to be at least one inch greater than the hydrometer OD, these sizes were evaluated for surface tension effects. The calibration liquids chosen bracket the surface tension of HDA ($\sigma \sim 33$ dyne/cm), since CCl_4 and 73-percent

H_2SO_4 have surface tension values of approximately 27 and 55 dyne/cm, respectively. The density of these calibrating liquids was determined using a Westphal balance. All determinations were conducted at 15.56 ±0.1 C (60 ±0.1 F). In addition, on the basis of the calibrations and limited quantity of propellant, the short stem hydrometer with the 1.4-inch ID cylinder was selected for the measurements with HDA.

Sonic Velocity

Sonic velocity measurements were conducted in HDA under saturated liquid conditions over selected temperature ranges. The resulting data were also used to calculate the adiabatic compressibility of HDA (as noted in the Adiabatic Compressibility section). Sonic velocity measurements in HDA were made in the experimental apparatus that has been described previously in Ref. 2 and 4 and is illustrated in Fig. 5. This apparatus accurately measures the distance that sound waves of a known frequency travel through a test fluid. The interferometer, which is capable of withstanding pressures to 1000 psia and temperatures to 200 F, is constructed of type 347 stainless steel. The dial gage, which provides precise linear location data, also enables the differentiation between the reflected signal (and its harmonics) and reflections from the metallic interferometer body. Displayed pips, from true reflections, move on the oscilloscope as the reflector is moved, while spurious signals remain stationary.

The measurements are conducted by initiation of a 5-megahertz radio frequency signal from the pulsed oscillator, which is fed simultaneously to the oscilloscope and a quartz piezoelectric crystal (with 5-megahertz resonant frequency) attached to the bottom of the interferometer. The sound waves, emanating from the crystal, travel through the bottom of the interferometer, through a known distance of test liquid to a reflector, and then back to the crystal. The initial and reflected waves are displayed on the oscilloscope, thus allowing measurement of the time required for the ultrasonic waves to traverse the known distance of test fluid.

During the determinations, the interferometer was immersed in a constant-temperature bath and allowed to reach thermal equilibrium at a selected temperature level before a measurement was conducted. The equilibrium temperature was then measured using a chromel-alumel thermocouple (with a type 316 stainless-steel sheath) immersed in

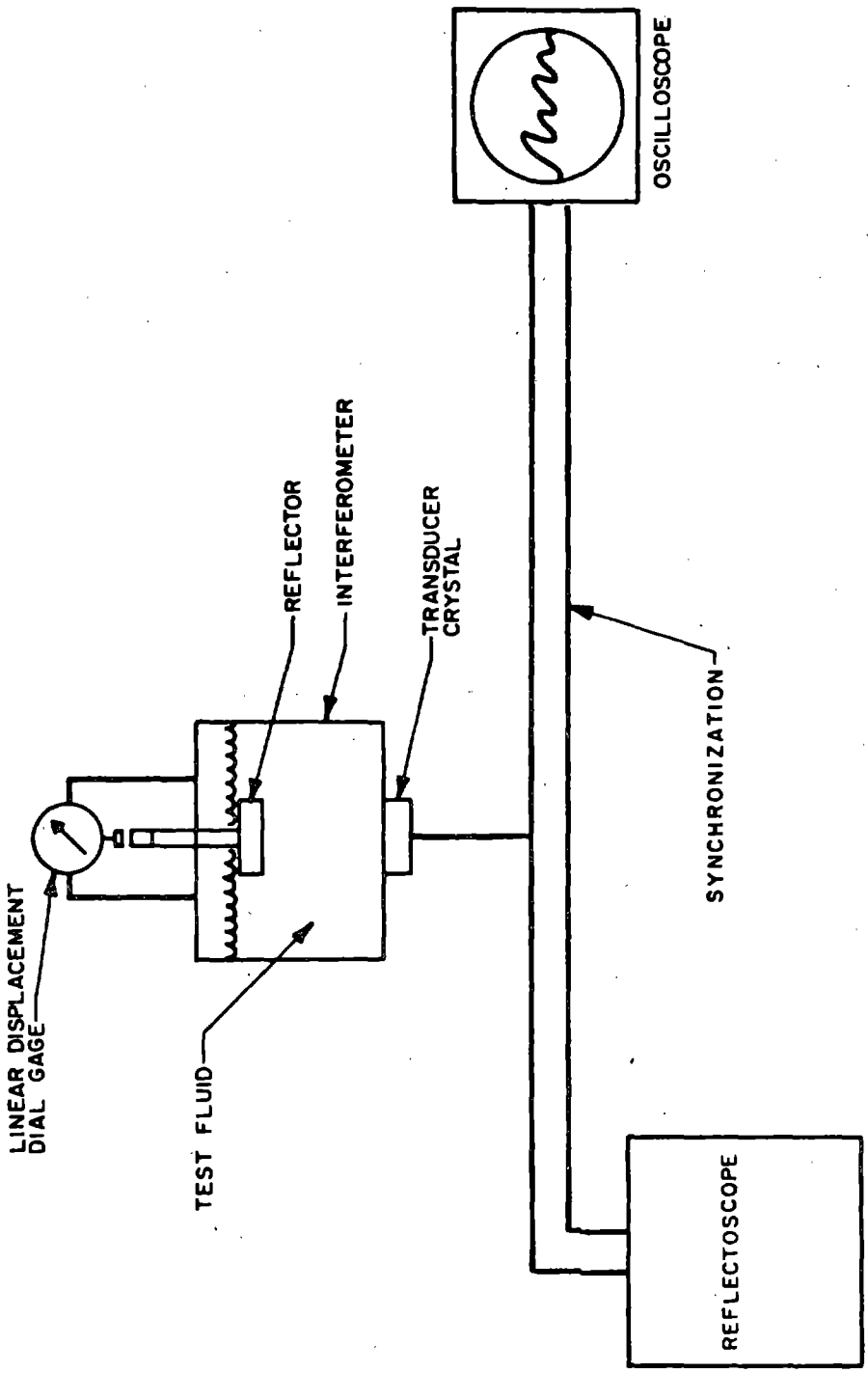

Figure 5. Sonic Velocity Apparatus

the test fluid. The sonic velocity apparatus was calibrated over a temperature range of 1 to 60 C (34 to 140 F) with distilled water and absolute methanol as test fluids. The data obtained from sonic velocity measurements in these fluids with this apparatus were compared with literature values for these fluids (Ref. 23 and 24) to obtain a calibration factor.

Sonic velocity measurements were made in three different HDA formulations over a temperature range of 1 to 60 C (34 to 140 F) under saturated liquid conditions. The resulting data in Table 7 were curve-fitted with the following expressions of sonic velocity as a function of temperature and composition:

$$c_{(m/sec)} = 2180.0 - 3.523T_{(C)} - 1.45 \times 10^{-2}T^2_{(C)} - 14.977\, N_{(w/o)} - 40.6\, W_{(w/o)} \quad (6a)$$

and

$$c_{(ft/sec)} = 7343 - 5.482T_{(F)} - 1.47 \times 10^{-2}T^2_{(F)} - 49.14\, N_{(w/o)} - 133\, W_{(w/o)} \quad (6b)$$

where

c = sonic velocity, m/sec or ft/sec
T = temperature, C or F
N = NO_2 concentration, weight percent
W = water concentration, weight percent

The standard errors of estimate for these equations are 6.3 m/sec and 20.6 ft/sec, respectively, over composition ranges of 43.4 to 45.6 w/o NO_2 and 0.4 to 1.7 w/o H_2O. These correlations are presented graphically in Appendix A.

TABLE 7. SONIC VELOCITY DATA FOR SATURATED LIQUID HDA*

Formulation	Temperature		Sonic Velocity		
	F	C	Measured, m/sec	Calculated From Eq. 6a, m/sec	Calculated From Eq. 6b, ft/sec
HDA-N1	37.7	3.2	1493	1493	4900
	60.2	15.7	1445	1446	4744
	80.5	27.0	1403	1399	4591
	100.1	37.8	1348	1351	4432
	121.1	49.5	1296	1295	4248
	138.9	59.4	1244	1244	4083
HDA-HN	34.3	1.3	1474	1476	4843
	60.2	15.7	1412	1422	4666
	80.3	26.8	1374	1376	4514
	100.0	37.8	1333	1327	4354
	120.2	49.0	1282	1273	4178
	140.0	60.0	1217	1217	3994
HDA-HW1	34.2	1.2	1464	1455	4774
	60.1	15.6	1402	1401	4596
	80.3	26.8	1350	1354	4444
	100.3	38.0	1301	1305	4281
	120.3	49.1	1260	1252	4107
	140.5	60.3	1185	1195	3919

* SAMPLE COMPOSITIONS:

Formulation	Composition, w/o					
	HNO_3	NO_2	H_2O	HF	Fe_2O_3	Partic.
HDA-N1	55.0	44.0	0.4	0.4	0.03	0.2
HDA-HN	53.4	45.6	0.4	0.4	0.03	0.2
HDA-HW1	54.3	43.4	1.7	0.4	0.03	0.2

Adiabatic Compressibility

Using the experimental sonic velocity data resulting from this program (as discussed in the Sonic Velocity section) and liquid density data (also from this program), the adiabatic compressibility of HDA was calculated from the thermodynamic relationship:

$$\beta_s = \frac{1}{\rho\, c^2}$$

where

β_s = adiabatic compressibility of the liquid
ρ = density of the liquid
c = velocity of sound in the liquid

The resulting correlation is given by the following equations:

$$\beta_{s(atm^{-1})} = 6.097 \times 10^{-7} - 2.9506 \times 10^{-7} T_{(C)} + 9.126 \times 10^{-10} T^2_{(C)} + 1.718 \times 10^{-11} T_{(C)}^3 + 5.7924 \times 10^{-7} N_{(w/o)} + 1.727 \times 10^{-6} W_{(w/o)} + 9.808 \times 10^{-9} N_{(w/o)} T_{(C)} + 2.84 \times 10^{-8} W_{(w/o)} T_{(C)}$$

and

$$\beta_{s(psia)} = 4.115 \times 10^{-7} - 1.1765 \times 10^{-8} T_{(F)} - 8.107 \times 10^{-14} T_{(F)}^2 + 2.005 \times 10^{-13} T_{(F)}^3 + 2.755 \times 10^{-8} N_{(w/o)} + 8.318 \times 10^{-8} W_{(w/o)} + 3.708 \times 10^{-10} N_{(w/o)} T_{(F)} + 1.074 \times 10^{-9} W_{(w/o)} T_{(F)}$$

The standard errors of estimate for these equations are 8.7×10^{-8} atm^{-1} and 5.9×10^{-9} $psia^{-1}$, respectively. These expressions are valid for temperatures from

1 to 60 C (34 to 140 F), N_2O_4 concentrations from 43.4 to 45.6 w/o, and H_2O concentrations from 0.4 to 1.7 w/o. The correlations are shown graphically in Appendix A.

Vapor and Equilibrium Pressure

Vapor pressure measurements were conducted on four HDA formulations (described in the Propellant Formulation and Chemical Analyses section as HDA-N1, HDA-N2, HDA-HW1, and HDA-HN) over the temperature range of -17 to 129 C (1 to 264 F). The resultant values were then correlated as a function of composition and temperature. Equilibrium pressure measurements were also conducted on three of the HDA formulations (HDA-N1, HDA-HW1, and HDA-HN) at 60 C (140 F). The equilibrium pressure cylinders were loaded to obtain ullages of 90, 50, 20, and 3 v/o at test temperature.

The apparatus used in the vapor pressure measurements consisted of a 10-milliliter, type 304 stainless-steel cylinder with immersion thermocouple, pressure transducer, and type 316 stainless-steel Hoke sample valve. The thermocouple, a chromel-alumel junction with type 316 stainless steel sheath, was sealed into the cylinder with a swedge fitting, thus permitting direct measurement of the temperature of the cylinder contents. The thermocouple was calibrated at the melting and boiling points of water. The type 316 stainless-steel pressure transducer (either a Taber 0-50 psia or CEC 0-2000 psia model, depending on the pressure range) was calibrated with a Heise gage over the temperature and pressure ranges of intended use. As the temperature of each liquid sample was increased or decreased in increments through heating or cooling of the apparatus in a regulated (to ±0.1 C) temperature bath or Delco precision oven, the pressure of the sample was recorded at the attainment of equilibrium temperature at each of the selected levels.

The equilibrium pressure measurements on HDA were conducted in type 304 stainless-steel Hoke cylinders of 10-ml capacity, which were fitted with type 304 stainless-steel Hoke needle valves and type 316 stainless-steel pressure transducers. The pressure range of the transducers was 0-2000 psia, and was selected for the range of equilibrium pressures exhibited by other fuming nitric acids.

Vapor Pressure of HDA. One hundred-eight vapor pressure data points were obtained on the four formulations measured. They are listed in Table 8, 9, and 10. The experimental data from vapor pressure measurements on four HDA formulations (HDA-N1, HDA-N2, HDA-HW1 and HDA-HN) were correlated as a function of temperature and composition by a least-squares curve-fit computer program. The resulting equations, covering the temperature range of -17 to 129 C (1 to 264 F), NO_2 (N) ranges of 43.2 to 45.6 w/o NO_2, and H_2O (W) ranges of 0.4 to 1.7 w/o H_2O, are:

$$\log_{10}P_{(atm)} = 10.7662 - \frac{4702.28}{T_{(K)}} - 5.43556 \times 10^{-2}N_{(w/o)} + 2.5549 \times 10^{-2}W_{(w/o)} + 28.5036 \frac{N_{(w/o)}}{T_{(K)}} + \frac{282926.}{T^2_{(K)}}$$

and

$$\log_{10}P_{(psia)} = 11.9347 - \frac{8464.86}{T_{(R)}} - 5.43838 \times 10^{-2}N_{(w/o)} + 2.5548 \times 10^{-2}W_{(w/o)} + 51.3221 \frac{N_{(w/o)}}{T_{(R)}} + \frac{916700.}{T^2_{(R)}}$$

The standard error of estimate is equivalent to 4.0 percent in pressure. Graphs of the expressions, evaluated for the nominal composition, are shown in Appendix A.

Only the initial set of data obtained over the high temperature range of each of the samples was used in the final data correlation. Data obtained from subsequent runs with the same sample at high temperatures were significantly higher than the established vapor pressure curve. This implies reaction and/or decomposition was taking place in the stainless-steel vapor pressure cell at elevated temperatures. In addition, further measurements established a pressure buildup of ~8 psi/hr when the loaded vapor pressure cell with the 0-2000 psia CEC transducer was held at 240 F for any length of time.

TABLE 8. VAPOR PRESSURE OF HDA-N1 FORMULATION*

Temperature		Observed Pressure,	Calculated Pressure	
C	F	psia	psia	atm
1.7	35.1	6.3	5.7	0.39
10.5	50.9	8.9	8.2	0.56
18.6	65.4	11.9	11.4	0.78
23.9	75.1	14.5	14.2	0.97
24.9	76.9	14.5	14.8	1.01
25.1	77.2	14.5	14.9	1.01
25.7	78.2	15.8	15.2	1.03
37.6	99.7	23.5	24.3	1.65
38.0	100.4	24.0	24.7	1.68
41.9	107.5	28.0	28.8	1.96
45.0	113.0	32.1	32.3	2.20
47.5	117.5	35.0	35.5	2.41
50.4	122.7	39.5	39.6	2.69
51.1	123.9	41.0	40.6	2.76
55.4	131.8	47.7	47.8	3.25
63.3	145.9	62.0	63.5	4.32
66.2	151.1	70.0	70.4	4.79
69.8	157.7	82.0	80.2	5.46
78.4	173.1	111.5	107.9	7.34
85.8	186.4	148.0	138.6	9.43
90.6	195.0	169.0	162.4	11.05
91.1	195.9	171.5	165.1	11.23
102.0	215.6	238.5	235.1	15.99
102.2	215.9	239.5	236.4	16.08
113.2	235.7	235.5	333.0	22.65
122.6	252.7	451.0	442.6	30.11
123.3	253.9	460.0	451.5	30.71

*SAMPLE COMPOSITION: 55.0 w/o HNO_3, 44.0 w/o NO_2, 0.4 w/o HF, 0.4 w/o H_2O, 0.2 w/o Particulates

TABLE 9. VAPOR PRESSURE OF HDA-N2 FORMULATION*

Temperature		Observed Pressure,	Calculated Pressure,		Temperature		Observed Pressure,	Calculated Pressure,	
C	F	psia	psia	atm	C	F	psia	psia	atm
-17.2	1.0	2.2	2.3	0.15	18.7	65.7	10.8	10.6	0.72
-16.9	1.6	2.3	2.3	0.15	19.1	66.4	11.0	10.6	0.73
-13.7	5.9	2.5	2.6	0.18	21.2	70.1	11.9	11.8	0.80
-14.1	6.7	2.6	2.6	0.18	22.6	72.7	12.5	12.5	0.85
-13.3	8.1	2.6	2.7	0.18	24.2	75.6	12.9	13.3	0.90
-11.3	11.6	2.9	2.9	0.20	24.9	76.8	14.0	13.7	0.93
-11.2	11.9	2.9	3.0	0.20	25.0	77.0	13.3	13.8	0.94
-10.9	12.4	3.0	3.0	0.20	26.1	78.9	14.1	14.4	0.98
-8.5	16.7	3.3	3.3	0.22	26.2	79.1	14.5	14.4	0.98
-7.4	18.6	3.5	3.5	0.24	28.7	83.7	15.1	16.0	1.09
-6.2	20.9	3.6	3.7	0.25	28.9	84.1	15.5	16.1	1.10
-4.2	24.4	4.1	4.0	0.27	29.1	84.4	16.0	16.3	1.11
-4.0	24.8	4.0	4.0	0.27	29.9	85.9	16.0	16.8	1.14
-0.7	30.7	4.6	4.7	0.32	30.9	87.7	16.7	17.5	1.19
-0.7	30.7	4.8	4.7	0.32	33.1	91.5	18.1	19.0	1.29
1.1	33.9	5.0	5.0	0.34	33.5	92.3	18.9	19.4	1.32
2.8	37.0	5.5	5.4	0.37	34.4	93.9	19.4	20.1	1.37
3.7	38.7	5.6	5.6	0.38	34.6	94.2	19.4	20.2	1.37
5.9	42.7	6.2	6.2	0.42	37.1	98.7	22.7	22.3	1.52
6.1	43.0	6.4	6.3	0.43	37.3	99.2	22.9	22.6	1.54
9.2	48.6	7.4	7.1	0.48	37.5	99.5	22.2	22.7	1.54
9.5	49.1	7.2	7.2	0.49	38.9	102.1	23.9	24.0	1.63
12.3	54.2	8.3	8.1	0.55	41.0	105.8	26.1	26.0	1.77
12.6	54.7	8.6	8.2	0.56	43.3	109.9	28.3	28.4	1.93
15.3	59.5	9.3	9.2	0.63	44.0	111.2	29.4	29.3	1.99
17.0	60.8	9.8	9.5	0.65					

*SAMPLE COMPOSITION: 55.7 w/o HNO_3, 43.2 w/o NO_2, 0.54 w/o HF, 0.46 w/o H_2O, 0.1 w/o Particulates

TABLE 10. VAPOR PRESSURE OF HDA-HW1 AND HDA-HN FORMULATIONS*

Formulation	Temperature		Observed Pressure, psia	Calculated Pressure	
	C	F		psia	atm
HDA-HW1	1.6	34.8	5.5	5.7	0.39
	8.8	47.9	7.5	7.8	0.53
	12.6	54.6	8.9	9.1	0.62
	18.3	64.9	11.3	11.6	0.79
	24.6	76.2	14.9	15.0	1.02
	26.9	80.4	17.5	16.4	1.12
	36.8	98.3	25.0	24.4	1.66
	37.5	99.5	24.3	25.1	1.71
	38.2	100.8	24.9	25.8	1.76
	47.9	118.3	37.1	37.5	2.55
	48.4	119.1	37.9	38.1	2.59
	49.3	120.7	43.0	39.4	2.68
	67.6	153.7	77.5	77.4	5.27
	69.6	157.3	86.5	83.1	5.65
	82.3	180.2	136.5	129.3	8.80
	96.6	205.9	215.0	208.1	14.16
	111.4	232.5	326.0	332.7	22.63
	125.6	258.1	474.0	511.9	34.82
	128.7	263.6	519.0	560.1	38.10
HDA-HN	1.9	35.4	6.9	6.8	0.46
	9.5	49.1	8.8	9.3	0.63
	17.7	63.9	12.1	12.9	0.88
	24.6	76.3	16.0	17.0	1.16
	29.4	85.0	19.0	20.5	1.39
	39.9	103.8	29.5	30.4	2.07
	48.9	120.0	44.5	42.5	2.89
	65.3	149.5	83.0	76.2	5.18
	81.7	179.0	145.0	132.8	9.03
	98.7	209.6	238.5	229.5	15.61
	117.5	243.5	394.5	406.8	27.67

*SAMPLE COMPOSITIONS:

Formulation	HNO_3, w/o	NO_2, w/o	HF, w/o	H_2O, w/o	Particulates, w/o
HDA-HW1	54.3	43.4	0.4	1.7	0.2
HDA-HN	53.4	45.6	0.4	0.4	0.2

Experimentally, the data were measured using the Taber and the CEC pressure transducers, both of which were calibrated at several temperatures before the experimental run. All loadings of the vapor pressure apparatus were performed using a vacuum line. The vapor pressure cell used in the measurements was disassembled, cleaned, reassembled, and leak-checked between loadings.

Equilibrium Pressure of HDA. Equilibrium pressure measurements were made on three HDA formulations (HDA-N1, HDA-HW1, and HDA-HN) at 60 C (140 F). Equilibrium pressure measurements conducted on samples of the propellant-grade HDA-N1 formulation showed that no significant deviations from the vapor pressure were noted during the first week of testing. However, during the second and third week, gradual pressure rises of 0.7 to 1.4 atm/week (10 to 20 psi/week) were observed. After the three-week test period, maximum pressures of 5 atm (75 psia) were attained in bombs loaded to ullages of 23, 50, and 90 v/o. The maximum pressure in the 5-percent ullage bomb was 6.5 atm (95 psia).

Measurements on the HDA-HW1 formulation showed that the two bombs loaded at ullages of 21 and 51 v/o remained at relatively constant pressures during 24 days at 60 C (140 F), attaining final pressures of 5.4 and 4.7 atm (80 and 70 psia), respectively. The bomb loaded to 90 v/o ullage developed internal pressure at the rate of about 0.13 atm/day (2 psi/day), then leveled off at 5.4 atm (80 psia). The fourth bomb, loaded at 3 v/o ullage, developed pressure at the rate of about 2 atm/day (30 psi/day) after a six-day induction period. The rate of pressure increase dropped off to about 1.4 atm/day (20 psi/day); then to about 0.7 atm/day (10 psi/day) during the final three days; attaining a final pressure of approximately 33 atm (485 psia).

The final pressures on the samples of HDA-HN exhibited the same general trends as the tests with propellant-grade HDA-N1 and HDA-HW1. The bombs loaded to 19 and 50 v/o ullages built up less pressure than the bomb loaded to 90 v/o ullage, and the highest pressure buildup was in the bomb loaded to 2 v/o ullage, as expected. Final pressures of approximately 5.5 atm (80 psia) were obtained in the 19, 50, and 90 v/o ullage bombs, while the pressure in the 2 v/o ullage bomb reached 50 atm (740 psia). When the bombs were cooled to

ambient temperature after the run at 60 C (140 F), a residual pressure of 1.4 to 1.7 atm (20 to 25 psia) was measured in each bomb.

Some general conclusions drawn from the three sets of equilibrium pressure runs are:

1. Pressure build-up appears to start within one week from test initiation.
2. The build-up appears to be a result of HDA reaction with the container walls.
3. At 60 C (140 F), tests with ullages of 20, 50, and 90 v/o result in a total pressure increase of about 1 atm (15 psi) in the first week, and then remain constant over the remaining period.
4. High pressure buildups, 6.5 to 50 atm (95 to 740 psia), were noted in all low ullage (2 to 5 v/o) tests. The pressures in these tests continued to rise throughout the test period although the pressure rise rate decreased with time. A possible explanation for the extremely high pressure levels may be liquid compression due to the achievement of a zero ullage through corrosion build-up on the wall.

Experimentally, the bombs were loaded with propellant using tared secondary transfer vessels and a vacuum line. The proper amounts of propellant to be loaded were determined by calculations (based on previous volume calibrations) such that ullages of 90, 50, 20, and 3 v/o would be obtained at the test temperature. The pressure transducers attached to each of the four bombs were monitored by a multipoint recorder that was switched on for 15 minutes every hour by an interval timer.

Heat of Formation

The heat of formation of HDA (54.8 w/o HNO_3, 44.0 w/o N_2O_4, 0.5 w/o H_2O, 0.7 w/o HF) was estimated using the heats of formation of the components, N_2O_4,

H_2O, and HF, and their heats of solution with each other. An estimate was made of the possible uncertainty in the calculation, using a conservative approach to arrive at the greatest possible uncertainty. Where uncertainties in individual enthalpies had to be estimated, unusually large values were chosen. Absolute values of the individual uncertainties were summed to calculate the total uncertainty. It should be noted that enthalpy values associated with H_2O and HF are not very critical since these components are present in small quantities.

The heat of formation of HDA was found to be 43.3 ±0.8 Kcal/100g, where 0.8 Kcal/100g is the estimate of the maximum uncertainty that could be expected. Even this pessimistic value for the uncertainty is still small for 100 g of material, and would have a small effect on theoretical performance parameters. The probable uncertainty is substantially less than this pessimistic value. Consequently, it was decided to recommend use of this estimated value for HDA heat of formation, for the present time, rather than making an experimental determination.

The individual values used in making this estimate are summarized in Table 11 and discussed in the remainder of this section.

TABLE 11. ENTHALPY CONTRIBUTIONS OF HDA COMPONENTS AND HEAT OF FORMATION OF HDA

Component	Composition w/o	Molecular weight	Moles/100 g HDA	Enthalpy Contribution (Kcal/100 g HDA) Low	Nominal	High
HNO_3	54.8	63.0129	0.86966	-36.14	-36.06	-35.97
N_2O_4	44.0	92.011	0.47820	-3.41	-2.98	-2.55
H_2O	0.5	18.0153	0.02775	-1.83	-1.62	-1.51
HF	0.7	20.0064	0.03499	-2.68	-2.59	-2.51
HDA Heatof formation (Kcal/100 g)				-44.06	-43.25	-42.54
Selected Value of HDA Heat of Formation: -43.3 ± 0.8 Kcal/100 g						
Empirical Formula (basis of 100 g HDA): $H_{0.96015}N_{1.82606}O_{4.54953}F_{0.03499}$						

Discussion of Estimation Procedure. The general approach employed was to start with the best available values for heat of formation of the pure components in HDA, then to calculate or estimate from known data their heats of solution or reaction in the HDA mixture. The heats of formation of pure compounds, used in these calculations, are shown in Table 12.

TABLE 12. HEATS OF FORMATION OF PURE COMPOUNDS AT STANDARD CONDITIONS

Compound	Heat of formation, liquid at 25 C (Kcal/g-mole)	Uncertainty (Kcal/g-mole)	Reference
HNO_3	-41.46	±0.09	25
N_2O_4	-4.68	±0.4	25
H_2	-68.32	±0.01 (est.)	26
HF	-71.99	±0.2	26
N_2O_3	+12.02	±2.0 (est.)	26
HNO_2	-27.6	±2.3 (est.)	26

For convenience in making estimates of heats of formation for other mixtures similar to HDA, a special set of heats of formation for the HDA components in solution were derived, combining the pure components heats of formation with the heats of solution and reaction. The heat of formation that was assigned to HNO_3 is the JANNAF value for the pure compound. With this approach, once the special set of heats of formation has been worked out, it is easy to compute the heat of formation of another mixture (as long as the composition is similar to that of HDA). The derivation of these special heats of formation of N_2O_4, H_2O, and HF, which include heats of interaction, are discussed in the following sections.

N_2O_4 is not known to react with HNO_3; i.e., no reaction can be written. A small heat of solution, -1.56 Kcal/g-mole N_2O_4, has been measured (Ref. 27 and 28). Calorimetric equipment was not used; however, large quantities (~100 g) were involved and temperature rises were in the range of 14 to 16 C. Therefore,

heat loss effects should have been minor. The assignment of an uncertainty of ±0.5 Kcal/g-mole to the above value seems exceptionally pessimistic since it corresponds to an error of about 5 C in temperature rise. Combining the above value for the heat of N_2O_4 in HNO_3, -1.56 ±0.5 Kcal/g-mole N_2O_4, with the heat of formation of N_2O_4, -4.68 ±0.4 Kcal/g-mole, leads to the following values for N_2O_4, dissolved in HDA.

Low	Nominal	High	
-7.14	-6.24	-5.34	Kcal/g-mole

These values, converted to the basis of 100 g HDA, were shown in Table 11.

Although H_2O would exhibit an exothermic heat of solution in HNO_3, it will react with the N_2O_4 in HDA. The reaction of H_2O with excess N_2O_4 has been qualitatively observed to be endothermic. Two overall reactions are possible for H_2O with excess N_2O_4.

	Heat of Reaction, Kcal/g-mole	Reaction
$H_2O + N_2O_4 \longrightarrow HNO_2 + HNO_3$	+ 5.51 ± 3.32	(I)
$H_2O + 2\ N_2O_4 \longrightarrow N_2O_3 + 2\ HNO_3$	+ 9.9 ± 4.0	(II)

Reaction II is preferred, since HNO_2 is rather unstable and since NO is stabilized in the form of N_2O_3. Therefore, 9.9 Kcal/g-mole is selected as the nominal heat of solution. The high value is 13.9 (9.9 + 4.0) and the low value is 2.19 (5.51-3.32). Combining these values with the heat of formation of H_2O yields the following values for H_2O dissolved in HDA.

Low	Nominal	High	
-66.1	-58.4	-54.5	Kcal/g-mole

The heat of solution of HF in HNO_3 was assumed to be between 0 (minimum) and that of HF in H_2O (maximum). The value of -65.14 ±0.2 Kcal/g-mole was taken for the heat of formation of $HF_{(g)}$ from Table 11, and heats of vaporization and solution in H_2O were derived from data in Ref. 26. Using these data

together with the uncertainty of 0.2 Kcal/g-mole for the heat of formation of HF(g), the following values for HF dissolved in HNO_3 are obtained.

Low	Nominal	High	
-76.7	-74.0	-71.8	Kcal/g-mole

The nominal value was selected approximately midway between the high and low values.

Use of Values for Other Mixtures. The nominal values that were derived for the heats of formation of N_2O_4, H_2O, and HF dissolved in HNO_3, are summarized in Table 13. They can be used to calculate the heats of formation of various HDA formulations, as well as IRFNA's, subject to the restriction that the H_2O and HF concentrations are small; i.e., a few percent or less. For compositions of the IRFNA type, the heat of solution of N_2O_4 is probably greater than the value incorporated into the heat of formation of N_2O_4 in Table 13. However, it is recommended that the values in Table 13 be used until more data become available.

TABLE 13. NOMINAL HEATS OF FORMATION OF COMPOUNDS DISSOLVED IN HNO_3

Compound	ΔH_f, Kcal/mole
N_2O_4	-6.24
H_2O	-58.4
HF	-74.0

Effect on Performance of Uncertainty in Heat of Formation. Performance calculations were made for HDA/UDMH at a mixture ratio of 2.8 and a chamber pressure of 500 psia, using low, nominal and high values for the heat of formation of HDA. The maximum uncertainty in the heat of formation corresponds to approximately ±5 K in chamber temperature, ±6 K in exit temperature at an area ratio of 45, and ±0.5 lbf-sec/lbm in vacuum specific impulse at an area ratio of 45.

Heat of Vaporization

An equation for the latent heat of vaporization of HDA was derived from the vapor pressure equation, using the Clapeyron equation:

$$\frac{d\ \ell n(P_{vp})}{d\ \ell n(\frac{1}{T})} = - \frac{\Delta H_v}{R(Z_v - Z_\ell)}$$

The term, Z_ℓ (the compressibility factor of the liquid) may be neglected since it is very small, about 0.004. The value for Z_v (the compressibility factor of the vapor) was obtained by assuming the vapor to be entirely NO_2. A value of 0.988 for Z_v was obtained from the generalized tables of Lydersen, Greenkorn, and Hougen (Ref. 10). Combining these components generated the following equations for the heat of vaporization of HDA:

$$\Delta H_v \left(\begin{matrix}\text{Kcal/g mole} \\ \text{vapor}\end{matrix}\right) = 21.251 - 0.12882\ N_{(w/o)} - \frac{2557.2}{T_{(K)}}$$

$$\Delta H_v \left(\begin{matrix}\text{Btu/lb mole} \\ \text{vapor}\end{matrix}\right) = 38{,}252 - 231.88 N_{(w/o)} - \frac{8{,}285{,}300.}{T_{(R)}}$$

which are valid for 43.2 to 45.6 w/o N_2O_4 and 256 to 397 K (461 to 714 R).

These equations were evaluated for the nominal composition (54.8 w/o HNO_3, 44.0 w/o N_2O_4, 0.5 w/o H_2O, 0.7 w/o HF) at the normal boiling point, 24.7 C (76.5 F), to give the following values: 7.00 Kcal/g-mole vapor or 12,600 Btu/lb mole vapor.

In order to put the heat of vaporization on a weight basis it is necessary to know the molecular weight and thus the composition of the vapor phase. This has not been determined for HDA. Attempts to estimate the composition, assuming ideal behavior, produced a poor estimate of the total pressure at the boiling point, 0.47 atm. Therefore, this assumption was discarded. Subsequently, molecular weight was estimated by two methods which represent extreme assumptions: (1) the vapor is pure NO_2, therefore MW = 46.005 (minimum); and (2) the partial pressure of HNO_3 is equal to the vapor pressure of pure nitric acid, therefore MW = 47.43 (maximum). Fortunately, the range of values is

small. Using these values, the following range is obtained for heat of vaporization of HDA on a weight basis: 148 to 152 cal/g (266 to 274 Btu/lb).

Viscosity

Modified Ostwald (Zhukov) capillary viscometers, fabricated from Pyrex, were used in viscosity determinations on HDA. The viscometers were fitted with a sealing valve consisting of a Pyrex body with a Teflon stem. Viscometer calibrations were accomplished using distilled water (degassed) and the following equation to develop viscometer constants:

$$\nu = ct$$

where

ν = kinematic viscosity
c = viscometer constant
t = efflux time

Viscosity measurements were made on three HDA formulations (described in the Propellant Formulation and Chemical Analyses section) over a temperature range of 1.1 to 54.4 C (34 to 130 F), using a Zhukov capillary viscometer. The resulting kinematic viscosity data (Table 14) were correlated as a function of temperature and composition through use of a least-squares curve-fit computer program. The correlation, which included the conversion to absolute viscosity using the density equation developed under this program, is represented by the following expressions:

$$\log \eta_{(cp)} = 0.27546 - \frac{470.89}{T_{(K)}} + \frac{216430}{T_{(K)}^2} - 1.7017 \times 10^{-2} N_{(w/o)} - 4.6580 \times 10^{-2} W_{(w/o)} \quad (7a)$$

TABLE 14. VISCOSITY DATA FOR SATURATED LIQUID HDA

Formulation	Temperature F	Temperature C	Kinematic (Measured), cs	Absolute (Calculated from equations 7a and 7b) cp	Absolute (Calculated from equations 7a and 7b) lbm/ft-sec x 10^3
HDA-N1	36.0	2.2	2.745	4.489	3.017
	49.6	9.8	2.110	3.528	2.371
	68.0	20.0	1.573	2.631	1.769
	89.8	32.1	1.224	1.941	1.305
	109.8	43.2	0.954	1.521	1.022
HDA-HN	36.0	2.2	2.528	4.217	2.834
	50.0	10.0	1.946	3.291	2.212
	68.0	20.0	1.559	2.472	1.661
	90.2	32.3	1.144	1.813	1.219
	109.8	43.2	0.890	1.429	0.950
	129.6	54.2	0.739	0.416	0.775
HDA-HW2	34.0	1.1	2.513	4.164	2.798
	50.0	10.0	1.926	3.130	2.103
	68.0	20.0	1.447	2.351	1.580
	90.0	32.2	1.088	1.730	1.162
	110.0	43.3	0.871	1.355	0.911
	110.6	43.7	0.867	1.346	0.904
	129.8	54.3	0.716	0.247	0.736

SAMPLE COMPOSITIONS:

Formulation	COMPOSITION, w/o HNO_3	NO_2	H_2O	HF	Fe_2O_3	Partic.
HDA-N1	55.0	44.0	0.4	0.4	0.03	0.2
HDA-HN	53.4	45.6	0.4	0.4	0.03	0.2
HDA-HW2	54.9	42.5	2.0	0.5	0.006	0.1

and

$$\log \eta_{(lbm/ft\text{-}sec)} = -2.89701 - \frac{847.874}{T_{(R)}} + \frac{701369}{T_{(R)}^2} - 1.7017 \times 10^{-2} N_{(w/o)} - 4.6580 \times 10^{-2} W_{(w/o)} \quad (7b)$$

where

η = absolute viscosity, centipoise or lbm/ft-sec
T = absolute temperature, Kelvin or Rankine
N = NO_2 concentration, weight percent
W = water concentration, weight percent

The standard error of estimate of these equations is 1.6 percent in η over a range of 42.5 to 45.6 w/o NO_2, 0.4 to 2.0 w/o water, and 1.1 to 54.4 C (34 to 130 F). The correlations are shown graphically in Appendix A.

Gas Solubility Measurements

Measurements were conducted to determine nitrogen gas solubility in hydrazine and in N_2H_4-UDMH (50-50) fuel blend as a function of temperature and pressure. As a check on the apparatus and techniques, measurements of nitrogen solubility in MMH were also conducted. Measurements of the solubilities were obtained over the temperature range from room temperature to 136 F and at inert gas pressures up to 1000 psia.

A special Rocketdyne-developed gas solubility apparatus was used to make the measurements. In principle, this apparatus (Fig. 6,7,8, and 9) designed and built under Rocketdyne funding, is a sophisticated piece of hardware that allows the operator to develop P-V-T data on the propellant system during pressure equilibration, in contrast to the more common technique involving chemical analysis on a (hopefully) representative propellant sample subsequent to equilibration.

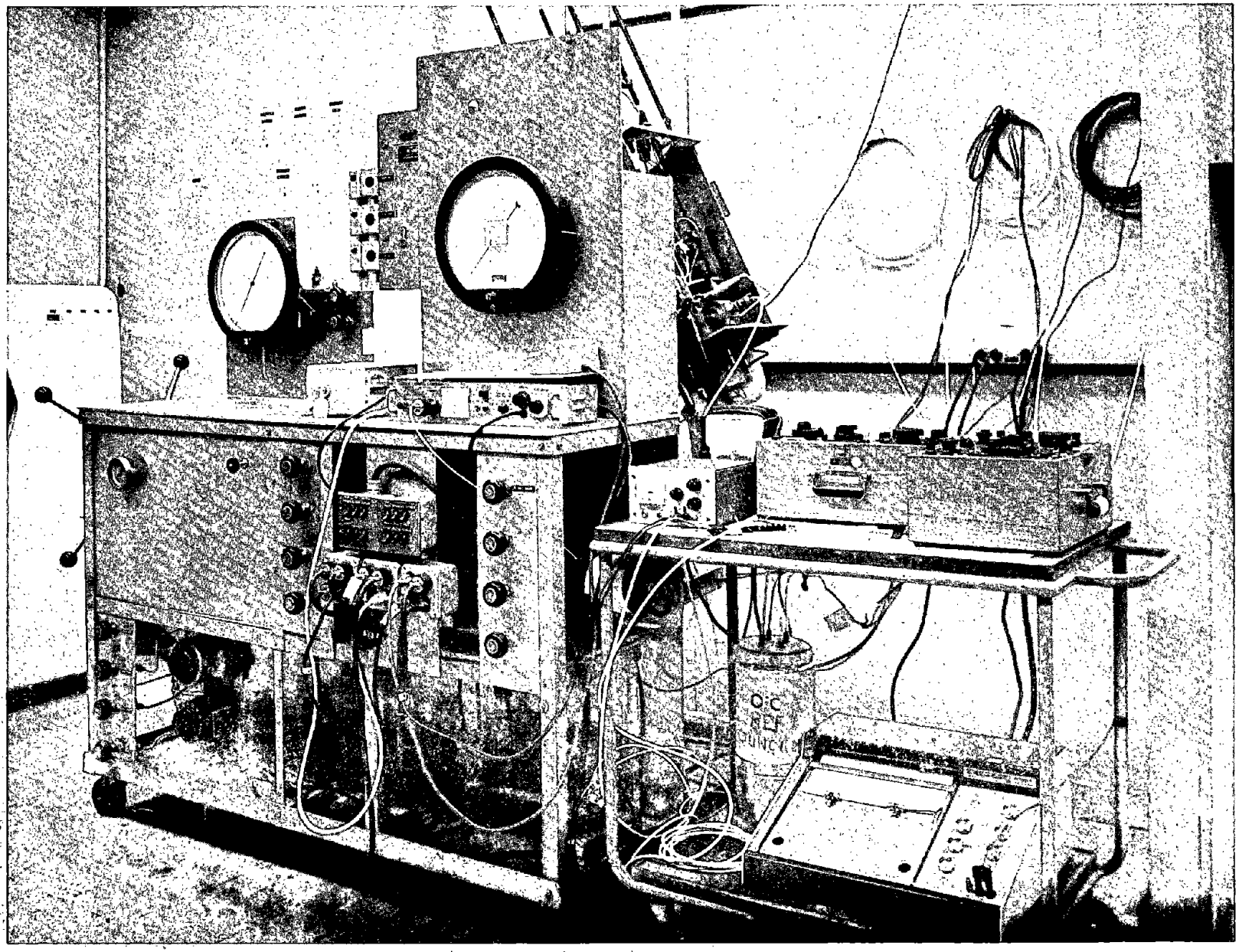

SAL31-6/18/73-C1A

Figure 6. Gas Solubility Apparatus and Readout Equipment

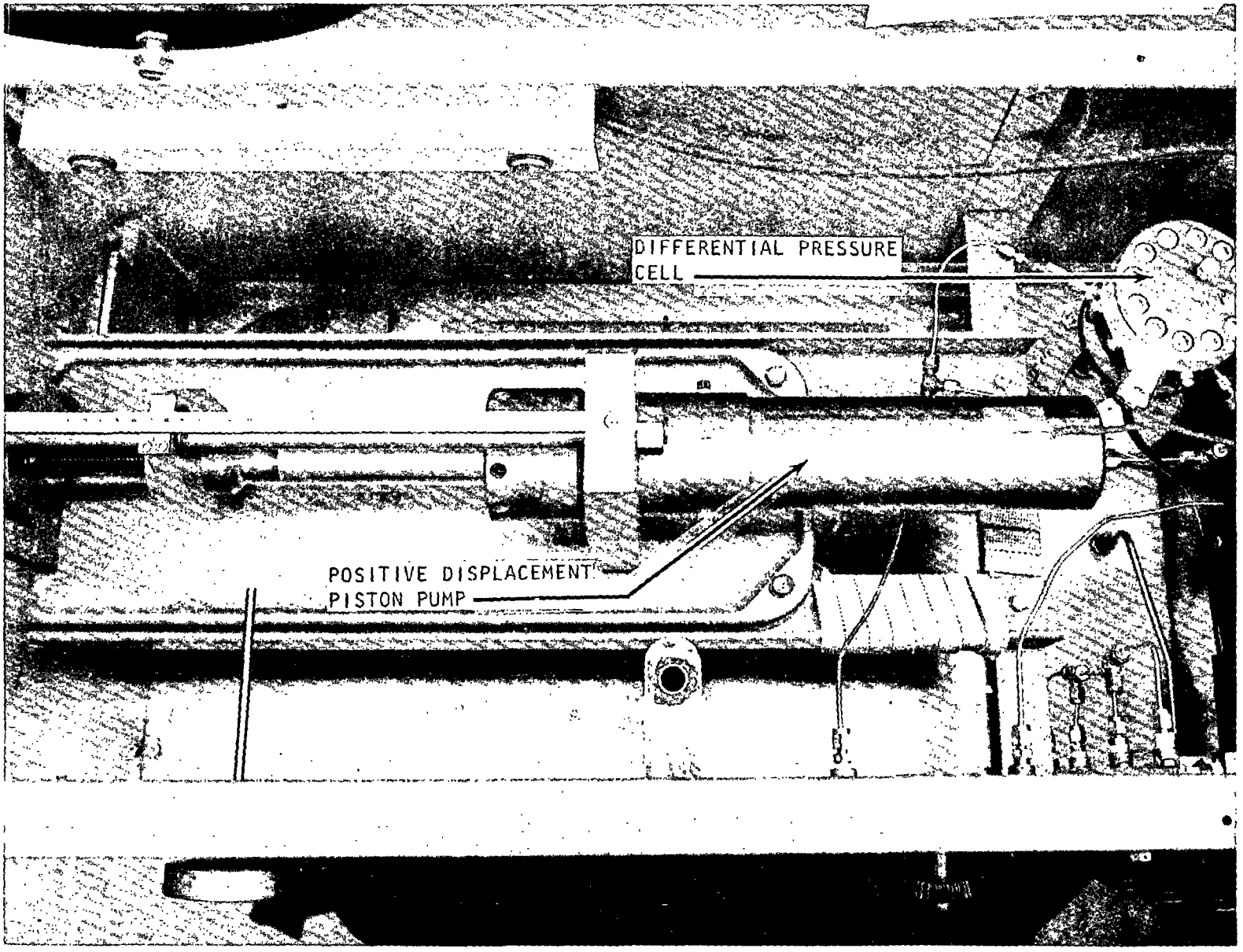

SAL31-6/18/73-C1D

Figure 7. Positive Displacement Piston Pump and Differential Pressure Cell

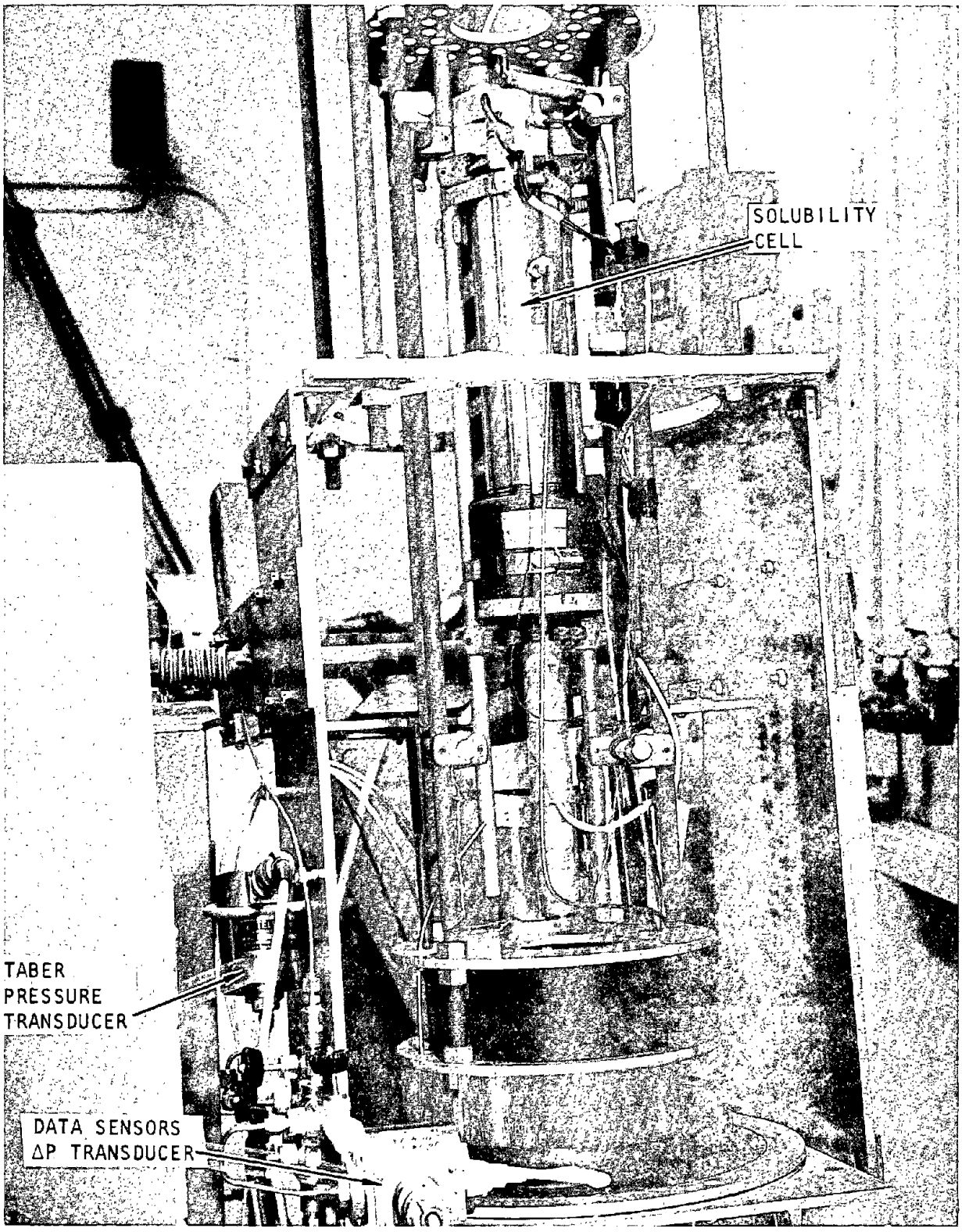

5AL31-6/19/73-C1

Figure 8. Gas Solubility Sample Cell in Bath Housing (Dewar Removed)

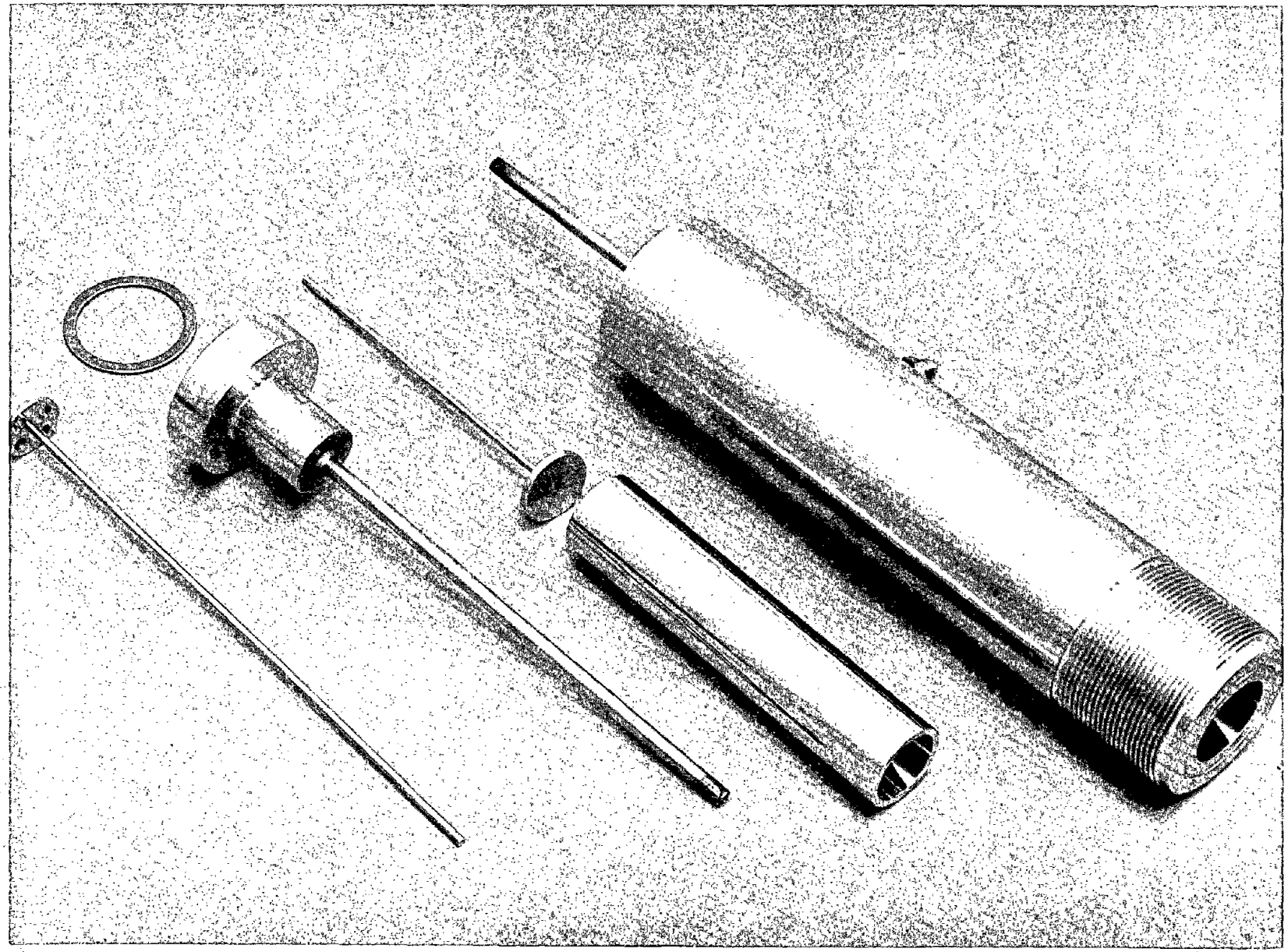

5AL31-6/18/73-C1B

Figure 9. Propellant-Wetted Parts of Disassembled Sample Cell

Measurement of the amount of gas injected into the system is obviously a critical measurement. To facilitate this measurement, a highly sensitive Ruska differential pressure (ΔP) cell is employed along with a null point indicator in the gas measuring system of the solubility apparatus (Fig. 7). The location of the ΔP cell in the solubility apparatus is shown in the overall schematic of the system (Fig. 10). The ΔP cell is used in conjunction with an accurate (±0.01 cubic centimeter) Ruska positive displacement piston pump (Fig. 7) to determine the quantity of gas injected into the solubility cell. A Data Sensors ΔP transducer (Fig. 8) is used in association with a highly stable power supply and a multi-range millivolt recorder to produce a permanent record of the pressure drop within the solubility cell during a run. A Taber pressure transducer (Fig. 8) is used to measure absolute pressure in the solubility cell and to set the reference pressures in both the ΔP transducer and the ΔP cell.

The thermocouple system employs a calibrated Honeywell galvanometer/potentiometer and two iron-constantan thermocouples with a constant-temperature ice-water bath as a reference junction. One thermocouple is attached to the outer skin of the solubility cell (Fig. 8), while the other is located on the positive displacement pump (Fig. 7). The cell-bath is essentially a large air-filled dewar bound on one end by the housing for a GN_2-operated blower. Temperature regulation is achieved by an accurate Bayley Instruments temperature controller in unison with the GN_2 blower. Housed within the cell bath enclosure are the solubility cell, two solenoids, the controlling heater, a base heater, associated wiring, and mechanical supports for the solubility cell (Fig. 8).

The apparatus to measure inert gas solubility in liquid propellants uses a unique design concept for the test cell (Fig. 9). Figures 11 and 12 illustrate inverse positions of the test cell showing the method of construction. The main cell body (1) is cylindrical. Externally operated solenoid agitators (2), (3) are provided at each end. A gas inlet port (4) is provided. The cell contains a cylindrical cup (5), of known internal volume, which is closely fitted to the inner cell wall, leaving only a narrow annular space (6).

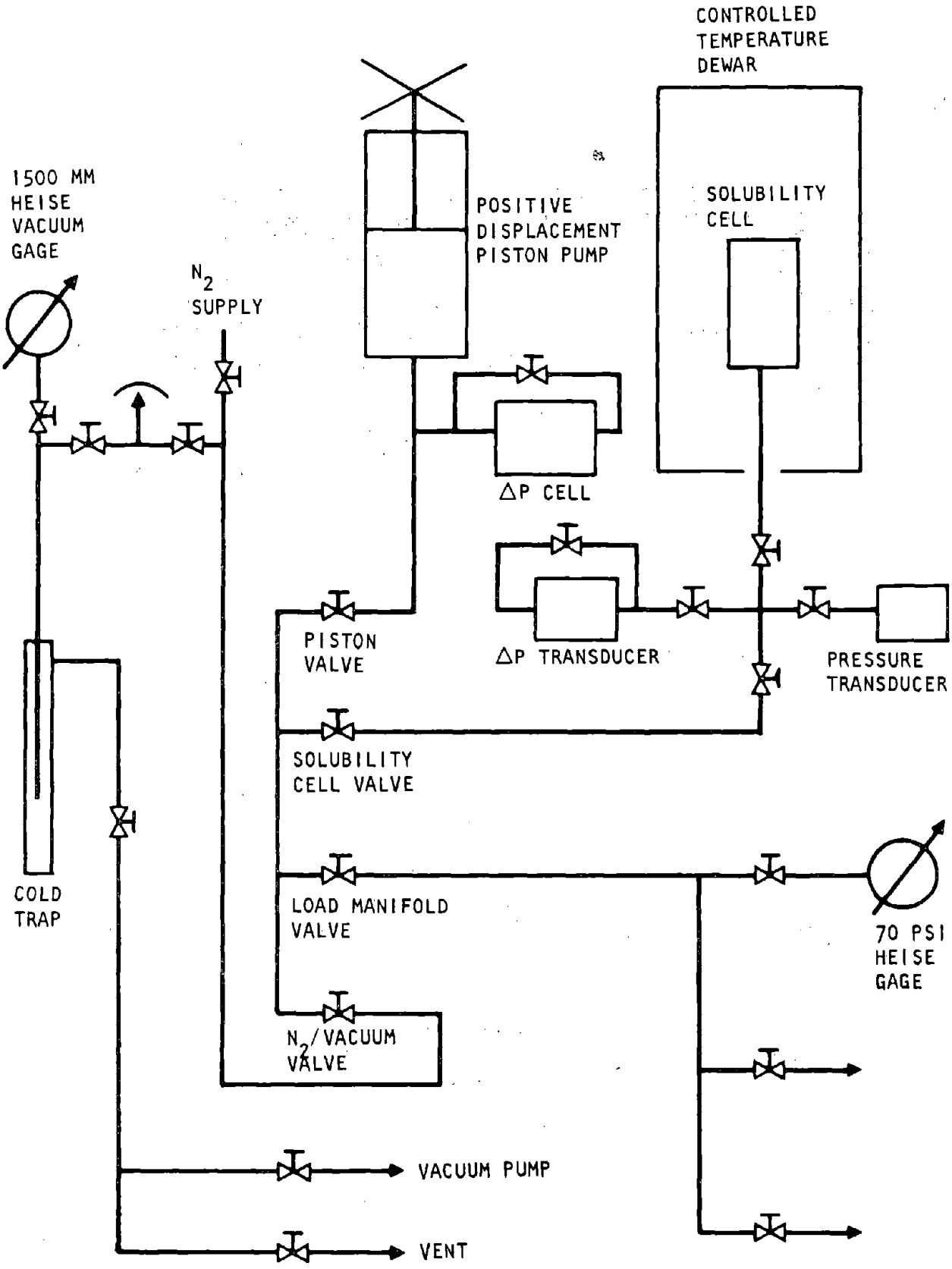

Figure 10. Solubility Apparatus Schematic Diagram

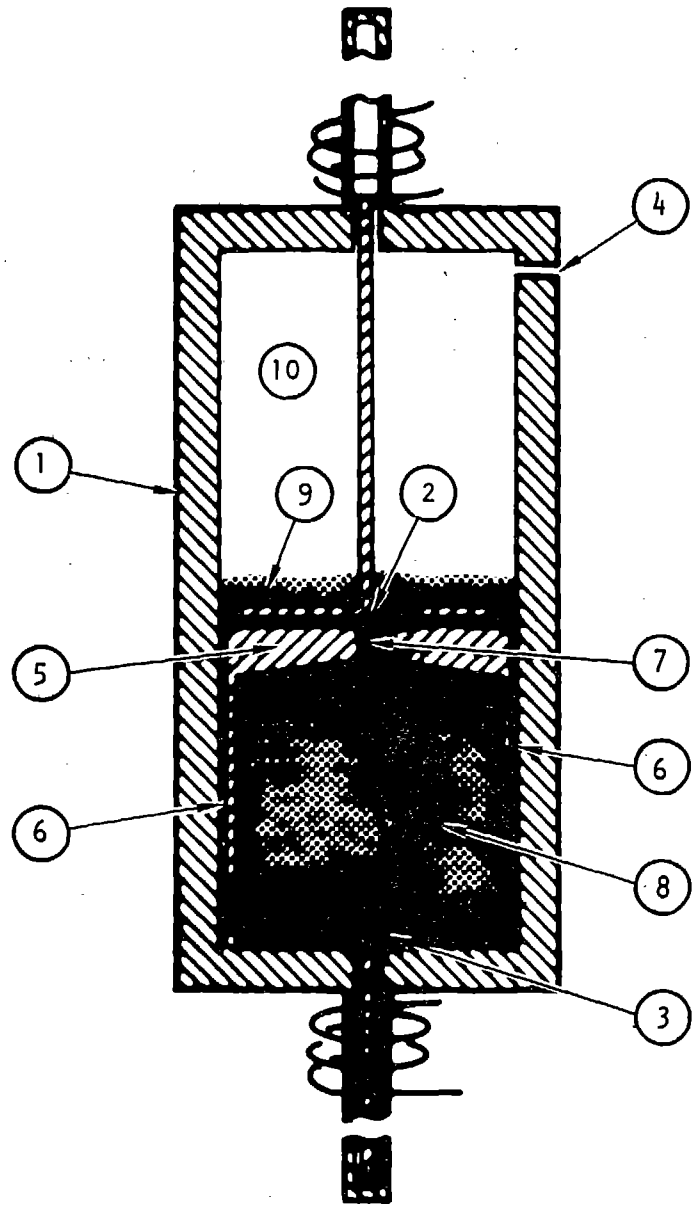

Figure 11. Gas Solubility Cell in Normal Position

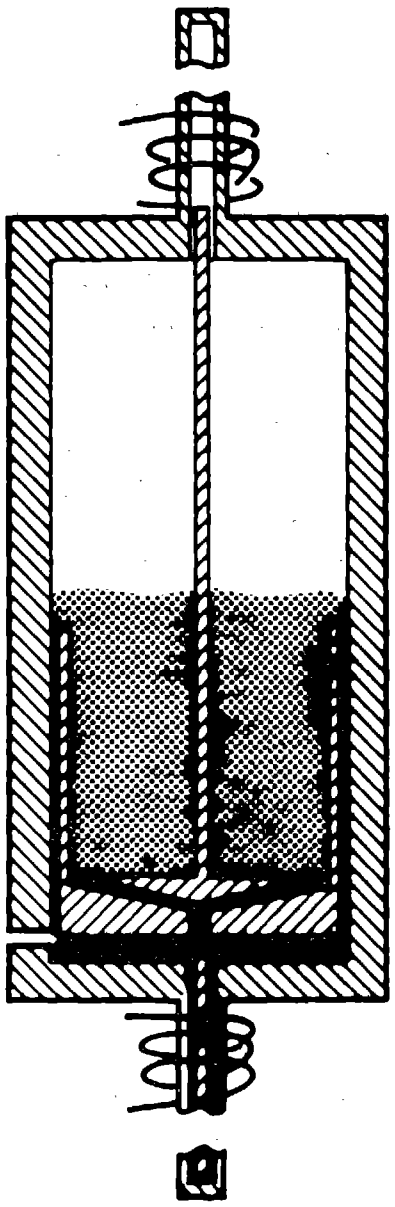

Figure 12. Gas Solubility Cell in Inverted Position

The closed end of the cup has one narrow hole (7). The internal configuration of this specially designed solubility test cell is such that, in one cell position (Fig. 11), a known portion of the liquid volume (8) in the cell can be excluded from the gas-liquid equilibrium in the remainder of the cell. This gas-liquid equilibrium is established between the vapor space (10) and a fixed portion of the cell liquid (9) by introducing gas through the port (4) and mixing by means of the agitator (2). Gas migration to the liquid inside the inverted cup can occur only by diffusion through the liquid in the annular space (6) and hole (7), which have small cross-sectional areas and represent neglibibly small volumes. This diffusion transport is relatively very slow and involves small (negligible) amounts of gas. Hence, the liquid portions outside and inside the cup are effectively separated and the liquid inside the cup is excluded from the solution process. Then by inverting the cell to the position shown in Fig. 12 , two-phase equilibrium at the same temperature and pressure can also be established with the entire liquid content (8,9) by means of the second agitator (3). The additional gas required in the latter case is, therefore, the gas dissolved in the excluded but known liquid volume (8). An accurate volume for the solubility cell cup is calculated from the known geometry of the cup, cup agitator, and other characteristics of the solubility cell.

The general nature of the experimental interpretation is illustrated in Fig. 13, which represents a graph of total cell equilibrium pressure against a quantity of gas introduced into the cell. All operations are carried out at some chosen temperature of interest. Line 11 represents the locus of successive equilibria obtained by adding gas and stirring with the cell in the position of Fig. 11. At some chosen point (12) the cell is inverted to the position of Fig. 12, and, after re-establishing equilibrium, the cell pressure corresponds to that of point 13. For this pressure (13), the amount of gas dissolved by the liquid inside the cup is the quantity N indicated in Fig. 13. Since the cup volume is known (and hence its liquid content), the specific solubility of the gas in the liquid is therefore established. The determination is repeated at different pressure levels in order of increasing pressure.

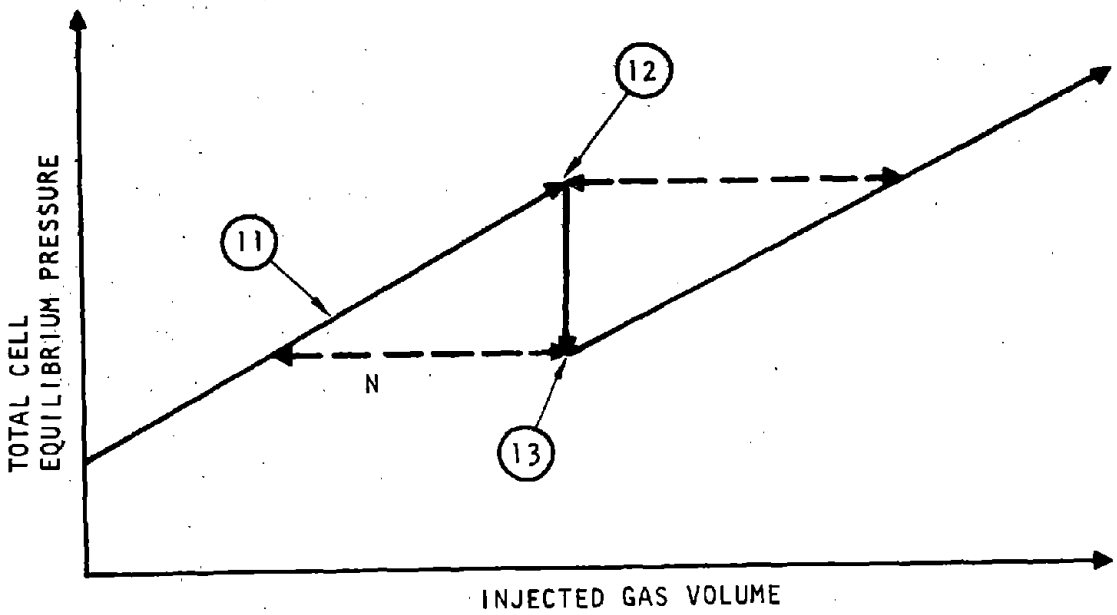

Figure 13. Typical Solubility Cell Data Interpretation

In addition, at the outset of the experimental effort on this task, a technique was developed to estimate the quantity of inert gas dissolved in the saturated propellant at the start of a set of measurements (at a particular temperature), thus eliminating the need for outgassing the liquid sample. This procedure involves gas-liquid equilibration of the total contents of the cell at the run temperature, by means of a cell inversion with agitation. A measurement of the initial total cell equilibrium pressure, P_o, is then taken. Later, in the data treatment phase, a plot of total equilibrium pressure versus quantity of dissolved gas, N, is developed for the set of measurements at that temperature. The smoothed curve includes the point P_o at zero dissolved gas volume. The absolute value of the difference between N at P_o and N at the point where the curve intersects the vapor pressure of the liquid (at the run temperature) is, therefore, the value of N_o, the quantity of dissolved gas at the start of the set of measurements. This technique is applied for each set of measurements following a gas pressure venting, regardless of whether the set is at a new temperature or not.

Nitrogen Gas Solubility in MMH. Measurements were conducted at a temperature of 95.4 F on a sample of neat MMH previously used in the apparatus. These results are in close agreement with those obtained two years ago by other Rocketdyne experimenters. The data, summarized in Table 15, were correlated by the equations:

$$\alpha_{(cc\ N_2\ (STP)/g\ MMH)} = 2.582 \times 10^{-3} P_{(psia)} + 1.30 \times 10^{-7} P^2_{(psia)} \quad (8a)$$

and

$$\alpha_{(cc\ N_2/lb\ MMH)} = 3.228 \times 10^{-6} P_{(psia)} + 1.63 \times 10^{-10} P^2_{(psia)} \quad (8b)$$

with standard errors of estimate of 0.019 cc N_2(STP)/g MMH and 2.4 x 10^{-5} lb N_2/lb MMH. This correlation is shown graphically in Fig. 14 .

TABLE 15. GAS SOLUBILITY OF NITROGEN IN LIQUID MONOMETHYLHYDRAZINE

Temperature		Nitrogen Partial Pressure		Experimental specific gas solubility, cc N_2(STP)/g MMH	Calculated Specific Gas Solubility, Eq. 8a, 8b	
F	C	psia	atm		cc N_2(STP)/ g MMH	10^{-4} lb N_2/ lb MMH
95.4	35.2	279	19.0	0.76	0.73	9.1
95.5	35.3	290	19.7	0.73	0.76	9.5
95.4	35.2	576	39.2	1.55	1.53	19.1
95.5	35.3	590	40.1	1.55	1.57	19.6
95.5	35.3	893	60.8	2.41	2.41	30.1

Also shown in Fig. 14 (dashed line) are the only other data found in the literature for higher pressures (procedure described in Ref. 29, data first reported in Ref. 30, later repeated in Ref. 31, which is more accessible). Reference 32 gives data for pressures of approximately one and two atm. Interpolation of the results of Ref. 30 to permit comparisons at equivalent conditions showed that the data were about 20-percent lower than the data measured during this program. The differences seem to be of a systematic

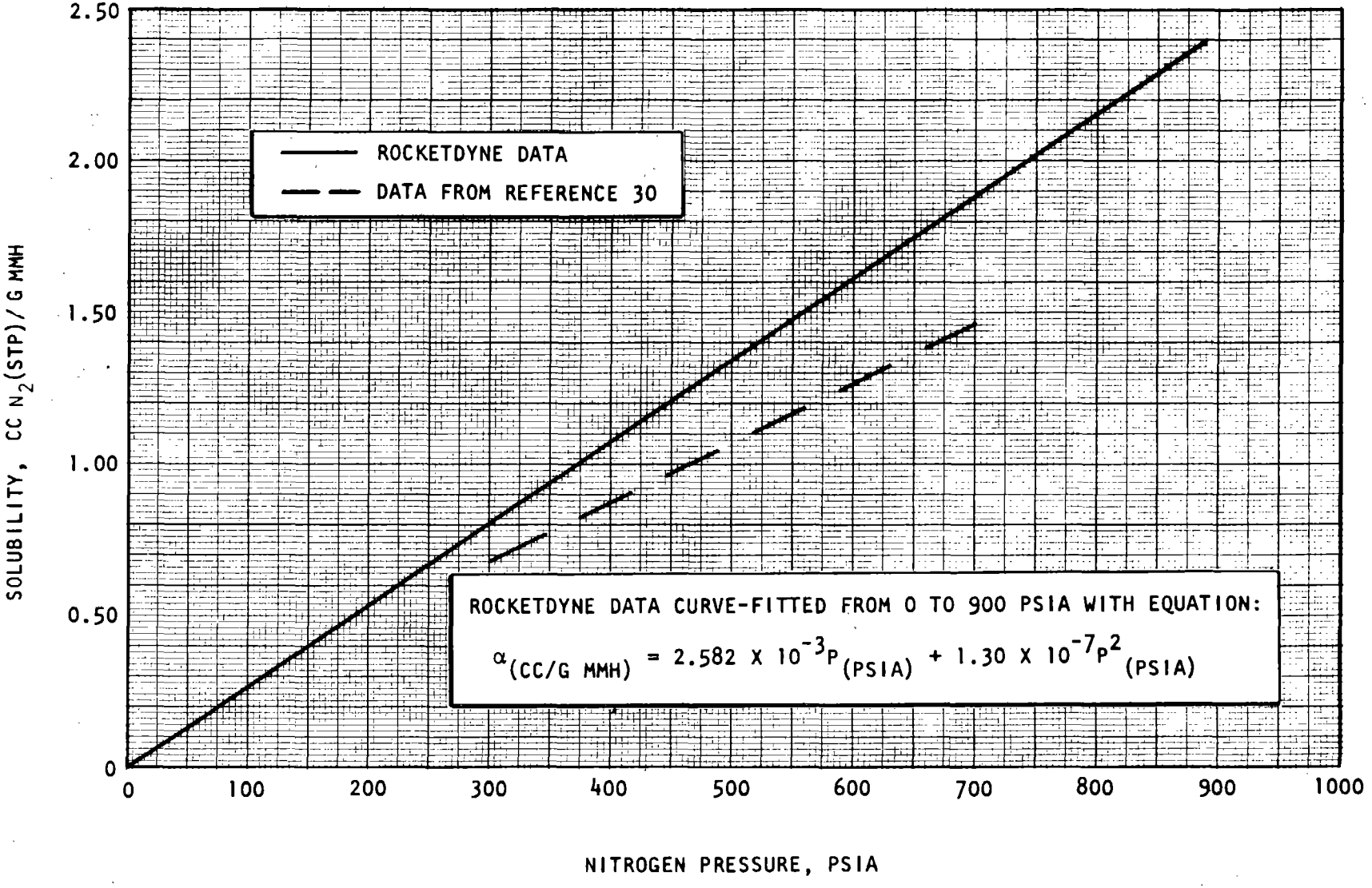

Figure 14. Nitrogen Solubility in Liquid Monomethylhydrazine (35.3 C Isotherm)

nature, rather than random differences. Since the method used during this project involves a direct measurement without potential errors during propellant sampling and analysis (especially dissolved gas loss), there appears to be no reason not to accept the new data.

Nitrogen Gas Solubility in N_2H_4. Nitrogen gas solubility measurements were conducted on neat hydrazine (99.0 w/o N_2H_4, 0.5 w/o H_2O, 0.5 w/o OSI) over the temperature range from 70.7 to 136.4 F (21.5 to 58.0 C). The reduced data are given in Table 16. A correlation of the resulting data by a computer curve-fit program resulted in the following expressions of gas solubility as a function of temperature and nitrogen partial pressure over the ranges measured:

$$\alpha_{(cc\ N_2(STP)/g\ N_2H_4)} = -5.799 \times 10^{-5} P_{(psia)} + 7.574 \times 10^{-6} T_{(C)} P_{(psia)} + 1.044 \times 10^{-3} P^{1/2}_{(psia)} - 4.020 \times 10^{-5} T_{(C)} P^{1/2}_{(psia)} - 6.43 \times 10^{-8} P^2_{(psia)} \quad (9a)$$

and

$$\alpha_{(lb\ N_2/lb\ N_2H_4)} = -2.408 \times 10^{-7} P_{(psia)} + 5.260 \times 10^{-9} T_{(F)} P_{(psia)} + 2.198 \times 10^{-6} P^{1/2}_{(psia)} - 2.792 \times 10^{-8} T_{(F)} P^{1/2}_{(psia)} - 8.04 \times 10^{-11} P^2_{(psia)} \quad (9b)$$

The standard errors of estimate are 0.009 cc N_2 (STP)/g N_2H_4 and 1.0×10^{-5} lb N_2/lb N_2H_4, respectively. Graphical representations of several isothermal gas solubility curves for this system appear in Fig. 15, while isobaric gas solubility curves are illustrated in Fig. 16.

TABLE 16. GAS SOLUBILITY OF NITROGEN IN LIQUID HYDRAZINE*

Temperature		Nitrogen Partial Pressure		Experimental specific gas solubility, cc N_2(STP)/g N_2H_4	Calculated Specific Gas Solubility, Eq. 9a, 9b	
					cc N_2(STP)/	10^{-4} lb N_2/
F	C	psia	atm		g N_2H_4	lb N_2H_4
70.7	21.5	300	20.4	0.031**	0.029	0.36
73.2	22.9	594	40.4	0.053**	0.049	0.61
74.7	23.7	1000	68.0	0.073**	0.060	0.75
77.7	25.4	300	20.4	0.029	0.035	0.44
79.7	26.5	592	40.3	0.048	0.061	0.77
81.0	27.2	999	68.0	0.076	0.082	1.03
96.1	35.6	299	20.3	0.057**	0.051	0.64
96.1	35.6	596	40.5	0.096**	0.094	1.17
95.9	35.5	1000	68.0	0.135**	0.134	1.68
95.2	35.1	301	20.5	0.055**	0.050	0.63
95.2	35.1	592	40.3	0.099**	0.092	1.14
114.6	45.9	297	20.2	0.065	0.067	0.83
114.6	45.9	594	40.4	0.122	0.130	1.62
114.6	45.9	1001	68.1	0.183	0.200	2.50
136.4	58.0	297	20.2	0.080	0.085	1.07
136.4	58.0	591	40.2	0.179	0.172	2.14
136.4	58.0	999	68.0	0.286	0.276	3.45

*SAMPLE COMPOSITION: 99.0 w/o N_2H_4, 0.5 w/o H_2O, 0.5 w/o other soluble impurities

**Measurements obtained with the original Data Sensors 0-20 psid differential pressure transducer.

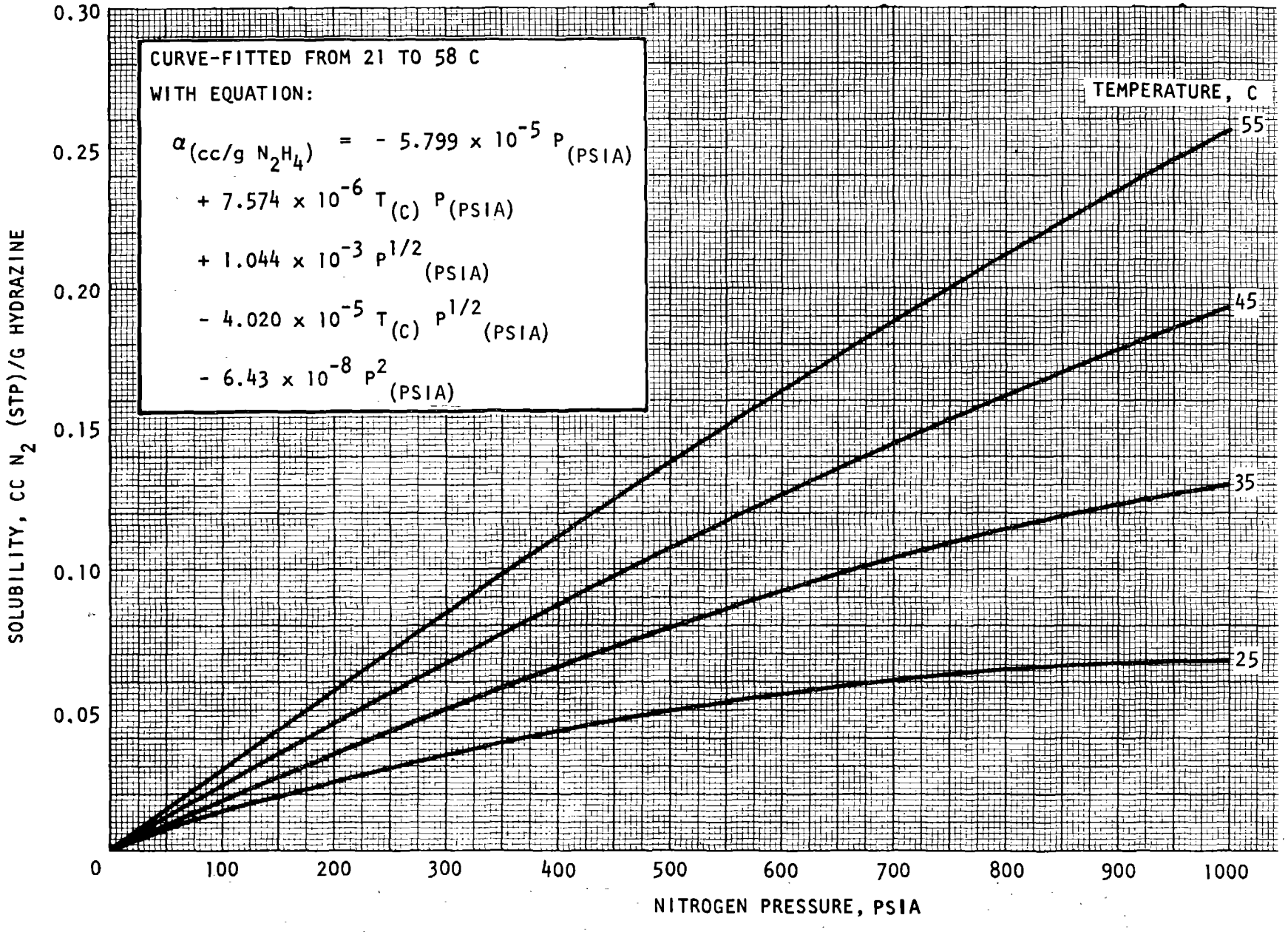

Figure 15. Solubility of Nitrogen in Liquid Hydrazine (Isothermal Solubility-Pressure Diagram)

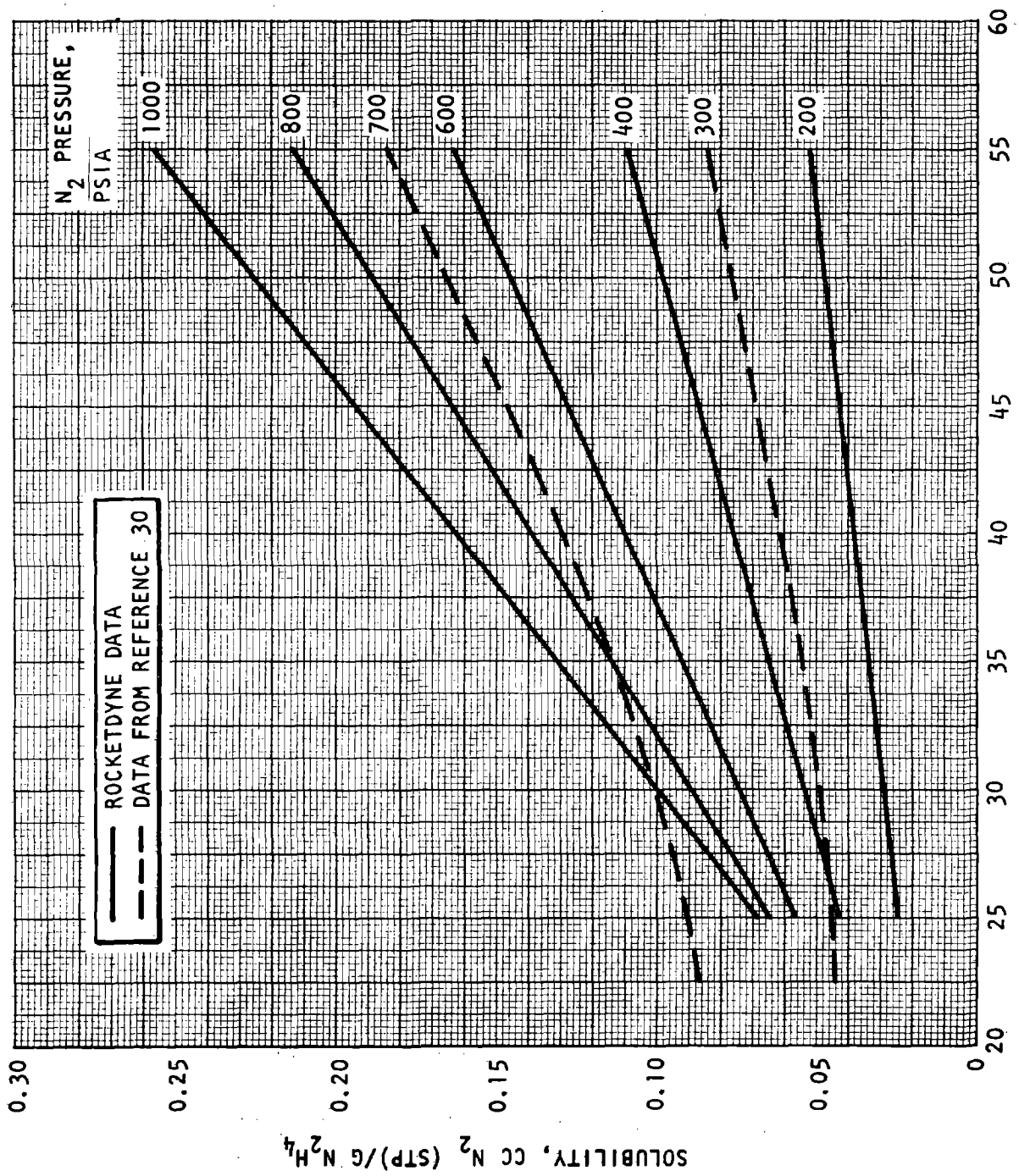

Figure 16. Solubility of Nitrogen in Liquid Hydrazine (Isobaric Solubility-Temperature Diagram)

Dashed curves have been drawn on the isobaric solubility plot, Fig. 16, to represent experimental solubility data obtained from Ref. 30 at 300 and 700 psia. The two sets of data agree very well at temperatures above about 90 F. At lower temperatures, the data of Ref. 30 show a less rapid decline in solubility (as temperature decreases) than the present results. It is concluded that the differences at low temperatures are of a systematic nature. There are some low pressure data (1 to 2 atm) in Ref. 32.

Experimentally, the gas solubility cell was removed from the apparatus and disassembled. During the unloading operation, extreme care was taken not to mar any of the highly-polished surfaces within the cell. After removal of the MMH the various parts of the cell were washed, rinsed, and then baked in a vacuum oven overnight at 70 C. The cell was then partially reassembled and, while under GN_2 pressure in a glove bag, was loaded with a sample of neat hydrazine. The cell was then completely reassembled and returned to the gas solubility apparatus.

Measurements of nitrogen gas solubility in hydrazine were then begun. However, a difficulty was encountered because of the low solubility of nitrogen in hydrazine (an order of magnitude lower than for MMH) which made it desirable to make further refinements of the apparatus to permit greater accuracy in measuring low gas solubilities. After these improvements, the apparatus performance was very satisfactory, even for such low values of gas solubility.

Nitrogen Gas Solubility in N_2H_4-UDMH (50-50) Fuel Blend. Gas solubility measurements were conducted on hydrazine-UDMH (50-50) fuel blend (composition A-5: 50.9 w/o N_2H_4, 48.6 w/o UDMH, 0.3 w/o H_2O, and 0.2 w/o OSI) over the temperature range 80.6 to 136.0 F (27.0 to 57.8 C). The reduced data are listed in Table 17. The following correlation was developed for the gas solubility as

TABLE 17. GAS SOLUBILITY OF NITROGEN IN LIQUID HYDRAZINE-UDMH (50-50) FUEL BLEND*

Temperature		Nitrogen Partial Pressure		Experimental specific gas solubility, cc N_2(STP)/g 50-50	Calculated specific gas solubility	
F	C	psia	atm		cc N_2(STP)/ g 50-50	10^{-4} lb N_2/ lb 50-50
80.6	27.0	284	19.3	0.551	0.552	6.9
82.0	27.8	585	39.8	1.042	1.032	12.9
83.1	28.4	983	66.9	1.609	1.607	20.1
95.4	35.2	286	19.5	0.612	0.616	7.7
95.0	35.0	586	39.9	1.122	1.132	14.1
95.0	35.0	986	67.1	1.753	1.754	21.9
113.2	45.1	237	16.1	0.589	0.587	7.3
113.4	45.2	483	32.9	1.083	1.077	13.5
113.5	45.3	741	50.4	1.550	1.554	19.4
113.5	45.3	989	67.3	1.977	1.981	24.8
135.7	57.6	279	19.0	0.765	0.765	9.6
136.0	57.8	578	39.3	1.425	1.426	17.8
136.0	57.8	975	66.3	2.230	2.225	27.8

*SAMPLE COMPOSITION A-5: 50.9 w/o N_2H_4, 48.6 w/o UDMH, 0.3 w/o H_2O, 0.2 w/o other soluble impurities.

a function of temperature and nitrogen partial pressure over the ranges measured:

$$\alpha_{(cc\ N_2(STP)/g\ 50\text{-}50)} = 1.0264 \times 10^{-3} P_{(psia)} + 1.7413 \times 10^{-5} T_{(C)} P_{(psia)} + 4.464 \times 10^{-3} P^{1/2}_{(psia)} + 1.416_{(C)} P^{1/2}_{(psia)} - 1.594\, P^2_{(psia)} \quad (10a)$$

and

$$\alpha_{(lb\ N_2/lb\ 50\text{-}50)} = 8.960 \times 10^{-7} P_{(psia)} + 1.2092 \times 10^{-8} T_{(F)} P_{(psia)} + 2.4338 \times 10^{-6} P^{1/2}_{(psia)} + 9.8339 T_{(F)} P^{1/2}_{(psia)} - 1.993 \times 10^{-10} P^2_{(psia)} \quad (10b)$$

The standard errors of estimate for these expressions are 0.007 cc N_2(STP)/g 50-50 HUDMH and 8.1×10^{-6} lb N_2/lb 50-50 HUDMH, respectively. Graphical representations of several isothermal gas solubility curves for this system appear in Fig. 17 ; isobaric gas solubility curves are shown in Fig. 18 .

Two dashed curves are shown on the isobaric plot of the present data (Fig. 18) to represent the data of Ref. 30 at 300 and 700 psia over a similar temperature range. It can be seen that the data of Ref. 30 are about 25 to 30 percent lower than the present results throughout the ranges of temperature and pressure. A third comparison is made on Fig. 18 with data from Ref. 33, measured at 75 and 95 F with pressures up to 240 psia. These data are represented at 200 psia by another dashed line on Fig. 18, showing them to be about 15 to 20 percent lower than the present data. A triple comparison can be made at 240 psia, by extrapolating the Ref. 30 data down to 240 psia from 300 psia. This shows the TRW point (Ref. 33) and the Aerojet point (Ref. 30) to lie about 17 and 33 percent, respectively, below the present data under these conditions. The two very approximate low pressure points of Ref. 34 (also cited in Ref. 31) were not useful for comparison.

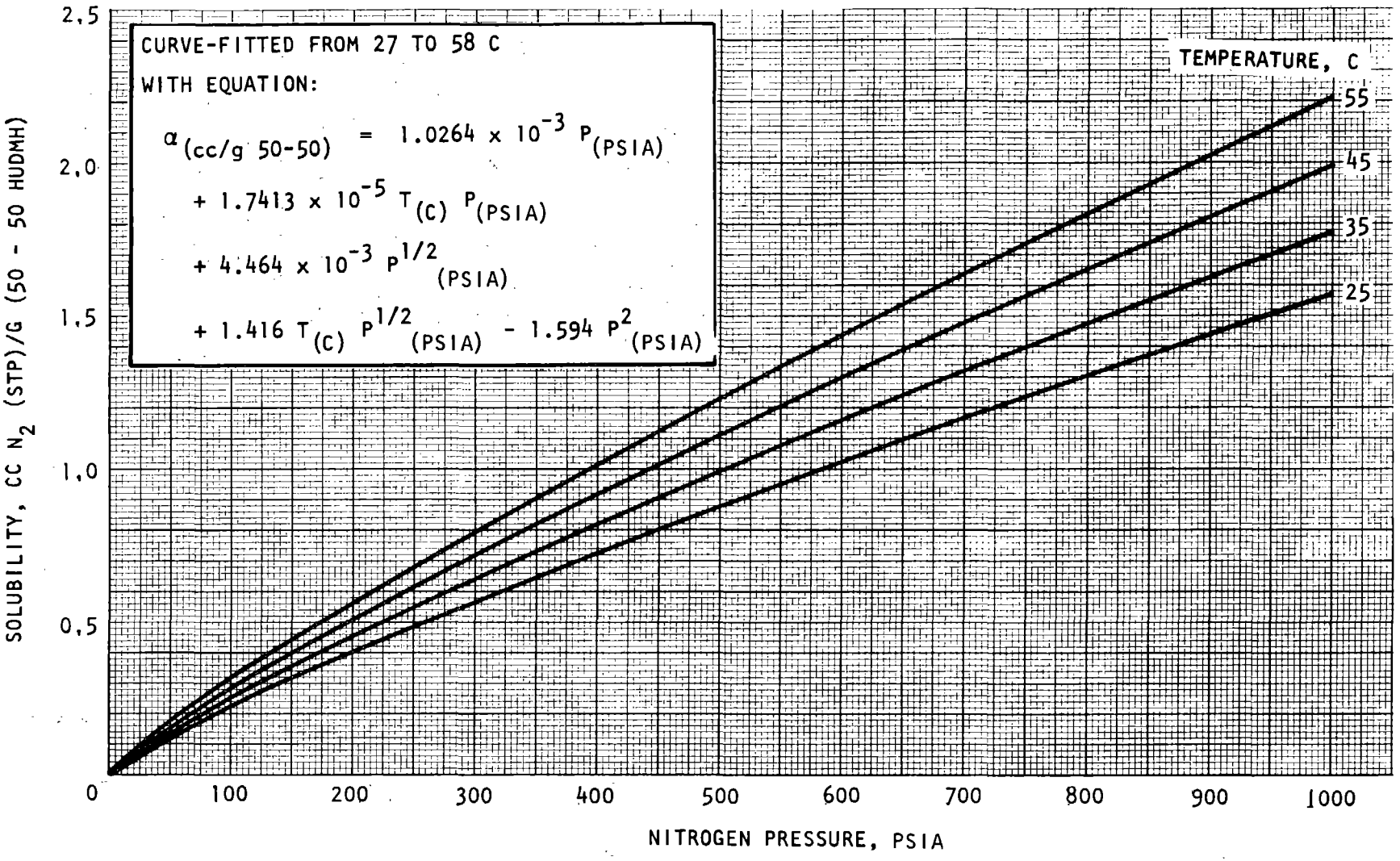

Figure 17. Solubility of Nitrogen in Liquid [50 w/o N_2H_4 - 50 w/o UDMH] (Isothermal Solubility--Pressure Diagram)

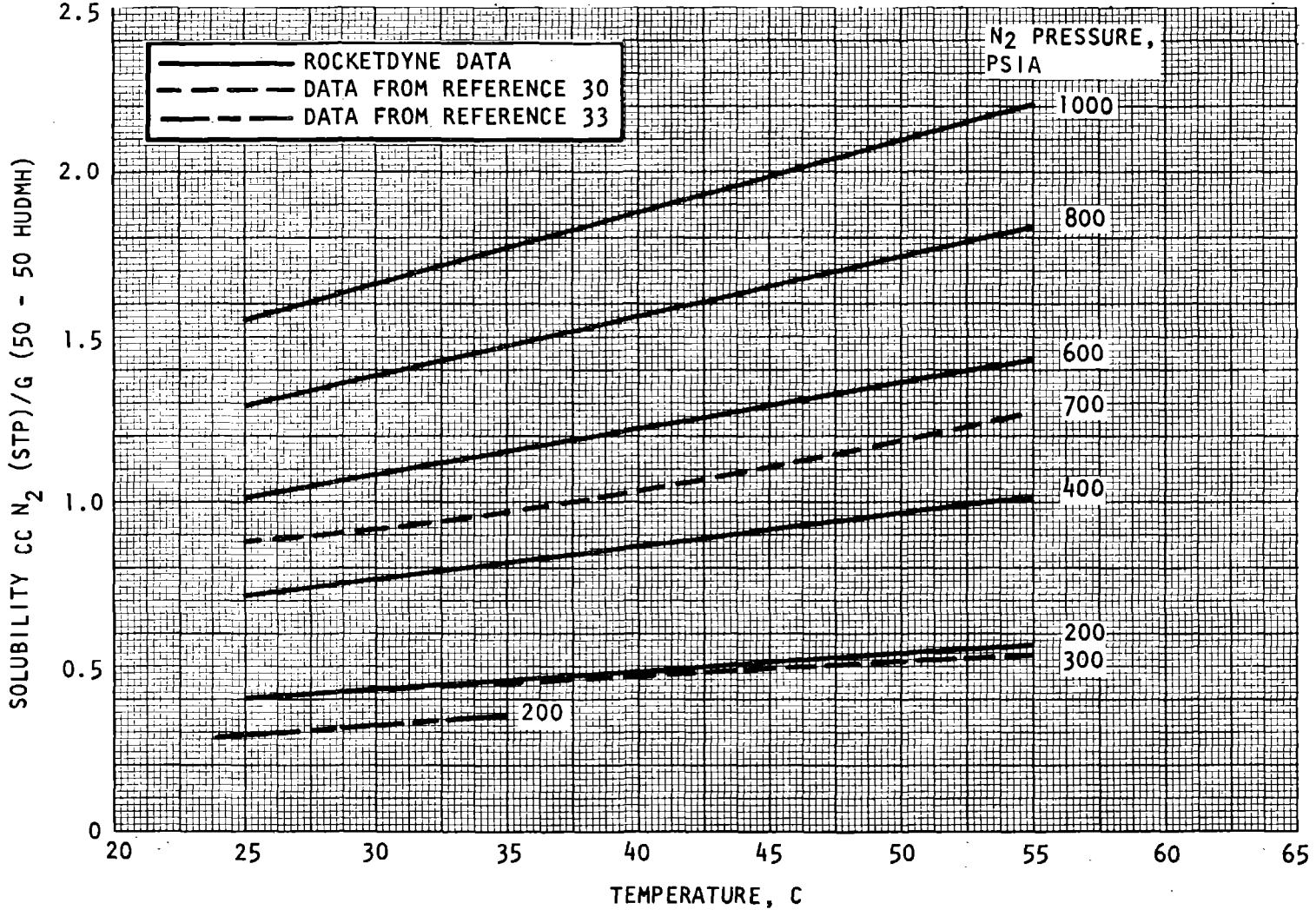

Figure 18. Solubility of Nitrogen in Liquid [50 w/o N_2H_4 - 50 w/o UDMH] (Isobaric Solubility--Temperature Diagram)

Experimentally, the gas solubility sample cell was removed from the apparatus and the liquid propellant was unloaded following the last measurements on the N_2-N_2H_4 system. The disassembled propellant-wetted parts of the cell were then thoroughly washed, rinsed, and vacuum-dried before being reassembled. A 50-50 mixture of N_2H_4-UDMH fuel blend was formulated and then loaded under dry GN_2 into the solubility sample cell. The solubility cell was relocated in the gas solubility apparatus. A new ΔP transducer of greater range was obtained from Rocketdyne stocks, thoroughly cleaned, calibrated at a series of line pressures, and installed in the gas solubility apparatus. Following leak-checking and volume calibration of the gas lines, the measurements of nitrogen gas solubility in N_2H_4-UDMH (50-50) fuel blend were conducted.

Propellant Stability and Hazards

A variety of tests were made on selected propellants to determine detonation propagation characteristics, detonation sensitivity, flash point, and thermal stability. The propellants were carbonyl diisocyanate (CDI), dicyanofuroxan (DCFO), DCFO bottoms, malonitrile (MN), and various mixtures of DCFO, MN, and DCFO bottoms. These tests and their results are discussed in the following subsections.

Carbonyl Diisocyanate. Detonation propagation tests were conducted on a sample (~40 g) of CDI (carbonyl diisocyanate) received from AFRPL. The sample was packed in dry ice until its transfer into the test tubing under an inert dry atmosphere. Because of the limited quantity of test sample, it was not possible to make duplicate tests; also, short (6-inch) lengths of tubing were used with the detonation generated by a 50 g Composition C booster charge initiated by a duPont E-83 blasting cap. Three tests were conducted at ambient temperature (~20 C) and in 3/8-, 1/2-, and 1-inch tubing. The results were negative, with no evidence of propagation, indicating that carbonyl diisocyanate will not propagate a detonation in 3/8-, 1/2-, and 1-inch tubing.

Two runs were made on CDI with the standard JANNAF thermal stability apparatus. The point of adiabatic self-heating was reached at 650 F on one run and 675 F

on the other. In both cases, the exotherm was very mild and slow, resulting in the release of only a small amount of energy when the diaphragm ruptured. The amount of energy released is judged qualitatively from the loudness of the rupture and the magnitude of the temperature spike shown by the sample temperature recorder.

The modified Cleveland open cup flash point apparatus was used in an attempt to determine the flash point of CDI. At a temperature of approximately 220 F the sample began to boil and continued until the liquid was completely evaporated, without ever igniting. The evaporating vapors caused the test flame to flare very slightly, indicating some reaction with the flame, but never enough to initiate a self-propagating flame. At the conclusion of the test, there was a heavy rime or crust of white solids on the top rim of the test cup. The sample evidently polymerized in the vapor phase and condensed on the cooler top edge of the cup.

By all the tests conducted, it is concluded that carbonyl diisocyanate appears to be an extremely stable material and is insensitive to impact, temperature, and open flame.

DCFO Detonation Propagation and Sensitivity. A series of tests were made to determine the detonation propagation characteristics of dicyanofuroxan (DCFO). It was found that a detonation could be propagated through tubing as small as 2.5-mm (0.098-in.) ID. Propagation was found to occur both in the solid state at ambient temperature and in the liquid state at 74 to 77 C (165 to 170 F). It should be noted that detonation propagation tests do not measure detonation sensitivity, but whether a detonation, once initiated, would be self-propagating. One detonation sensitivity (pseudo card-gap) test was made, indicating that neat DCFO would be classified as a Class A explosive. More than 75 cards were required to prevent detonation of neat DCFO; 70 cards or more designates a Class A explosive.

A list of the tests conducted is given in Table 18. A "Yes" in the "Detonation propagated?" column indicates that a detonation was propagated through the

TABLE 18. RESULTS OF DETONATION PROPAGATION TESTING WITH DCFO AND DCFO/MALONITRILE MIXTURES

Sample Composition, w/o malononitrile in DCFO	Tube OD, inches	Tube ID, inches	Temperature, C	Detonation propagated?
0	0.125	0.098	Ambient	Yes
0	0.187	0.149	74 - 77 (liquid)	Yes
0	0.187	0.120	Ambient	Yes
0	0.187	0.149	Ambient	Yes
0	0.187	0.149	Ambient	Yes
0	0.187	0.149	Ambient	Yes
0	0.250	0.180	74 - 77 (liquid)	Yes
0	0.250	0.154	Ambient	Yes
0	0.250	0.180	Ambient	Yes
0	0.250	0.180	Ambient	Yes
0	0.375	0.305	Ambient	Yes
0	0.750	0.654	Ambient	Yes
0	1.0	0.75-in. card gap	Ambient	Yes
19.2	0.125	0.098	Ambient	Yes
19.2	0.125	0.098	Ambient	Yes
25	0.250	0.063	Ambient	Yes
29.2	0.125	0.082	Ambient	Yes
29.2	0.125	0.082	Ambient	No*
29.2	0.125	0.082	Ambient	No*
29.2	0.125	0.082	Ambient	No*
29.2	0.125	0.082	Ambient	No*
40	0.125	0.098	Ambient	No
40	0.125	0.098	Ambient	No
40	0.187	0.149	Ambient	No
40	0.250	0.180	Ambient	No
40	0.250	0.180	Ambient	No
40	0.375	0.305	Ambient	Yes
40	0.500	0.260	Ambient	No*
40	0.500	0.260	Ambient	No*
40	0.500	0.260	Ambient	No*
44.3	0.500	0.430	Ambient	No
44.3	0.500	0.430	Ambient	No
44.3	0.750	0.652	Ambient	Yes
44.3	1.0	0.06-in. card gap	Ambient	Yes
44.3	1.0	0.25-in. card gap	Ambient	No
50	0.50	0.430	Ambient	No
50	0.750	0.652	Ambient	No
50	0.750	0.652	Ambient	No
50	1.0	0.90	Ambient	No
50	1.0	0.90	Ambient	No
100	0.125	0.098	Ambient	No

A result listed as No means that only a part of the test tube was recovered. This indicates that a detonation was initiated by the booster charge, but that it damped out within a few inches. These combinations of tubing and liquid composition are therefore very close to the critical diameters.

tubing and punctured the witness plate. A "No" indicates no detonation, with the plate intact and most of the test tube undamaged.

DCFO was supplied by AFRPL and was labeled "Vacuum Distilled," with a melting point of 40 to 41 C. The detonation propagation experiments were carried out in an underground blast cell. All tests used a booster charge of 50 grams of Composition "C" and were initiated with a duPont Number E-83 blasting cap. For the pseudo card-gap test, plates of Lucite were placed between the tubing and the booster charge.

For the first test in 3/4-inch tubing, solid crystals of DCFO were scraped out of the sample bottle into the tubing and gently tamped with a wood dowel. All succeeding tests used a melt-loading technique, wherein liquid DCFO was sucked up into a length of tubing and then allowed to freeze in place. For the elevated temperature tests, the ends of the loaded tube were sealed with a thin sheet of polyethylene, and the tube was then placed inside a 12-inch length of 3/4-inch steel tubing and sealed to it by means of rubber stoppers. The annular space between the two tubes was filled with water and a thermocouple was inserted. A heating tape was wrapped around the outside of the large tube. After setting in place the witness plate, booster charge, and blasting cap, the heating tape was turned on and the temperature was monitored remotely. About 10 minutes were required to heat up to 165 to 170 F, and the temperature was then held constant for 15 minutes before firing.

All of the tests showed positive evidence of a high-order detonation being self-propagated through the tubing. In no case was any of the tubing recovered, and in every case the witness plate had a hole partially or completely burned through it. In some tests where the witness plate thickness was greater than half the ID of the tube, the plate was not completely perforated, but the appearance of the plate was such as to leave no doubt that a detonation had occurred.

Since propellant systems using tubing smaller than 1/8-inch are not likely to be considered, there would have been little value in running further tests at smaller diameters in hope of locating the actual critical diameter.

Detonation Propagation and Sensitivity of DCFO-MN Mixtures. The series of detonation propagation tests with neat DCFO led to the conclusion that the critical diameter for detonation of pure dicyanofuroxan was so small that detonation could not be prevented by the use of small diameter tubing in a practical system. Subsequent tests were made with mixtures of DCFO and malononitrile.

DCFO from the lot supplied by AFRPL was used. The malononitrile was obtained from Matheson, Coleman and Bell, and was labeled, "Practical Grade" (melting point 30 to 32 C). All mixtures tested were dark brown liquids at ambient temperature. All tests were conducted at ambient temperature. The experiments were carried out in an underground test cell. All tests used a booster charge of 50 grams of Composition "C" and were initiated with a Number E-83 blasting cap. For the pseudo card-gap tests, plates of Lucite were placed between the test tube and the booster charge. Liquid was sealed within the test tube by a thin polyethylene sheet stretched over the tube ends.

The results are included (together with the results, previously discussed, for neat DCO) in Table 18. Figure 19 is a graph of critical diameter as a function of composition. It is seen that a mixture must contain at least 37-percent MN to be safe even in quarter-inch tubing. A 50-50 DCFO-MN mixture, however, can be used in tubing as large as one inch.

The curve through the open circles in Fig. 19 represents the upper boundary of the safe operating region. True critical diameter as a function of composition must lie somewhere between the two lines. Standard stainless-steel tubing sizes and the corresponding safe compositions determined from Fig. 19 are:

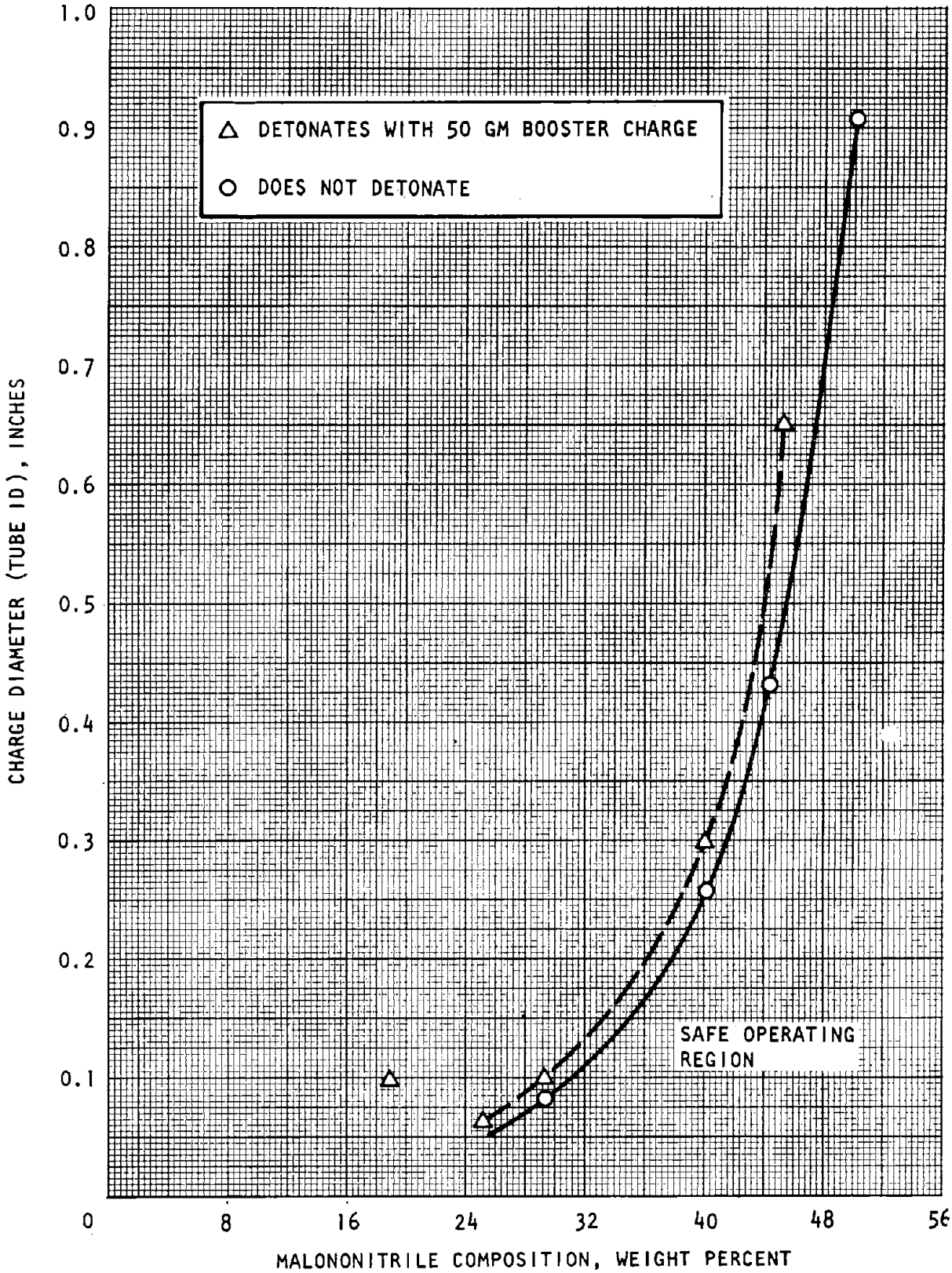

Figure 19. Critical Diameter for Detonation Propagation of DCFO-Malonitrile Mixtures

1/4 in. x 0.035 wall - 37-percent MN
3/8 in. x 0.035 wall - 42-percent MN
1/2 in. x 0.035 wall - 44-percent MN
3/4 in. x 0.049 wall - 48-percent MN
1 in. x 0.049 wall - 50-percent MN

The above numbers represent limits for which a detonation will not be propagated through the tubing more than a few inches, regardless of the magnitude of the stimulus involved.

In plotting the results of the critical tests (those bracketing the critical diameter) in Fig. 19, it is assumed that only the inside diameter of the tube is significant. This is not always completely true, and Table 18 shows that a wide variety of tube wall thicknesses was used to obtain the desired range of inside diameter. Wall thickness effects, however, are definitely secondary and will be averaged out over a number of tests such as those presented here.

It is also desirable to know something of the sensitivity, that is the ease of initiating a detonation, in diameters larger than the critical diameter. This type of information is revealed by the pseudo card-gap tests, also listed in Table 18. Although neat DCFO would be rated as a Class "A" explosive (detonates at 70 cards or more), the 50-50 mixture is probably not detonable. Even the 44.3-percent MN composition is relatively insensitive, with a rating of between 6 and 25 cards.

Detonation Propagation of DCFO Bottoms and its Mixtures. One-half pound of DCFO Bottoms was received from AFRPL for evaluation of detonation potential. This material is a low melting point (100 C) white crystalline solid. It was obtained by recrystallization from the pot residue left after distilling DCFO from the crude reaction product. The pure material was melt-loaded into lengths of stainless-steel tubing for detonation propagation tests. As with pure DCFO, this material was found to propagate detonations even in the smallest tubing

used (0.125-inch OD x 0.082-inch ID). The results of these tests should be used to conclude only that the potential detonation hazard with neat DCFO Bottoms is of the same order of magnitude as that for neat DCFO.

Because the critical diameter for detonation is quite sensitive to composition, it was desired to have a relative comparison of DCFO Bottoms vs DCFO in mixtures of malononitrile. This would make it possible to evaluate the effect of substituting one material for the other in a propellant mixture. A mixture of 19-percent malonontrile in DCFO will propagate a detonation in 0.125-inch OD x 0.098-inch ID tubing. Therefore, a mixture of 19-percent malonitrile in DCFO Bottoms was tested for comparison. Negative results were obtained with both 0.082 and 0.111-inch ID tubing. This would appear to indicate a lower hazard than with DCFO. However, the DCFO-malononitrile mixtures were homogeneous liquids at ambient temperature, while the DCFO Bottoms malononitrile mixture did not appear to form a solution. As the mixture cooled down it seemed that a high-melting phase was freezing out, leaving behind most or all of the malononitrile as a liquid interspersed among the solid crystals. Test results with such a non-homogeneous mixture must be viewed with some caution.

Detonation propagation tests were also conducted on a mixture of 34 w/o DCFO - 40 w/o DCFO Bottoms - 26 w/o malonitrile. The tests were conducted at ambient temperature (~25 C) where the mixture is a liquid. Testing indicated that the mixture would propagate a detonation in 1/4-inch tubing but not in 3/16-inch tubing.

It is tentatively concluded that DCFO Bottoms can be substituted for DCFO at no increase in detonation hazard; however any proposed mixture of DCFO, DCFO Bottoms, and malononitrile must be tested at the specific composition of interest in order to determine critical diameter.

Flash Point of DCFO. A Cleveland open-cup flash test apparatus was modified for remote operation and used to determine the flash point of DCFO. The standard Cleveland open-cup flash test (ASTM D-92) apparatus was installed in Cell 1 at ECL. The thermometer was replaced by a thermocouple for remote

readout and a variable-speed electric motor was attached to the flame wand for remote operation. The entire apparatus was encased in a black box for protection from both wind and light. One side of the black box was open and placed against the cell window. Thus the cup could be observed and operation controlled from inside the lab. Checkout runs were made with acetic anhydride and ethylene glycol. Literature values for the flash points are 65.5 C (150 F) and 115.5 C (240 F), respectively. Using the standard quantity of material per test, results of 60 C (140 F) and 129.5 C (265 F) were obtained. Because of the hazards associated with DCFO, it was desired to minimize the quantity of sample used. Therefore, repeat runs were made using only 10 cc of sample confined in a small aluminum cup. This yielded flash points of 71.2 C (160 F) and 126.7 C (260 F), again for acetic anhydride and ethylene glycol, respectively. It was concluded that test data was not significantly biased by the use of the smaller sample size. Identical procedures were used in testing DCFO.

Two runs were made with DCFO, giving flash points of 131.5 C (269 F) and 134 C (273 F). The calibration materials, when ignited, continued to burn with a quiet diffusion-type flame which was easily quenched. On the other hand, DCFO, being a monopropellant, quickly progressed to a vigorous pyrotechnic flame that destroyed thermocouple wiring and plastic parts of the apparatus.

Adiabatic Compression Sensitivity. U-tube adiabatic compression sensitivity tests were conducted on malononitrile at 75 C (167 F) following a functional check of the apparatus with nitromethane. Three tests were conducted using a gaseous nitrogen bubble at the closed end of the tube at driving pressure ratios of 128, 130, and 130, respectively; and three tests were conducted using an air bubble at a driving pressure ratio of 130. All tests indicated no sensitivity of the malononitrile to adiabatic compression.

O-Ring Compatibility

Elastomeric O-ring compatibility was evaluated using ASTM methods D1414 and D471 as guidelines. These test procedures comprise determining changes in weight, volume, hardness, 100-percent modulus and compression set up to 50-percent compression.

The AF-E-124D O-rings (perfluorovinyl ether elastomer) were supplied by AFRPL and were subjected to static immersion testing in IRFNA (MIL-P-7254F, Type III B) for a period of 32 days at ambient temperature. O-ring exposure was as follows: three samples under free immersion, three samples immersed in fixtures that provided 25-percent compression of the O-ring, and one control sample.

Data resulting from these tests, presented in Table 19 and Fig. 20 , show a significant decrease in tensile characteristics; however, all other properties were essentially unaffected by the test exposure. Compressed samples were essentially exposed to IRFNA from the outside diameter only, as the O-rings sealed off the inner portion of the fixture. Visually this was evident when the seals were examined upon removal from the IRFNA. The outer portion of the compressed seals was whitened and opaque, while the inner portion was still translucent. All surfaces of the free immersion samples were opaque. This condition is observed in Fig. 21 . However, when examined after tensile testing, it was observed that the opaque zone extended only about one-quarter of the ring cross-sectional diameter. As expected, the tensile properties of the compressed samples were less affected than those of the free immersion samples.

TABLE 19. EFFECTS ON AF-E-124D O-RINGS OF 32-DAY EXPOSURE TO IRFNA

Property	Test Environment		
	Control	Free Immersion	25 Percent Compression and Immersion
Hardness, Shore "A"	74	71	76
Weight Change, percent	0	+4.7	+2.3
Volume Change, percent	0	+6.0	+3.4
Compression Set, percent (30 minutes)	--	--	48.2
Compression-Deflection	See Fig. 20	See Fig. 20	See Fig. 20
Tensile Properties:			
100-percent Modulus, psi	850	650	725
Tensile Strength, psi	2200	1170	1700
Elongation, percent	170	120	150

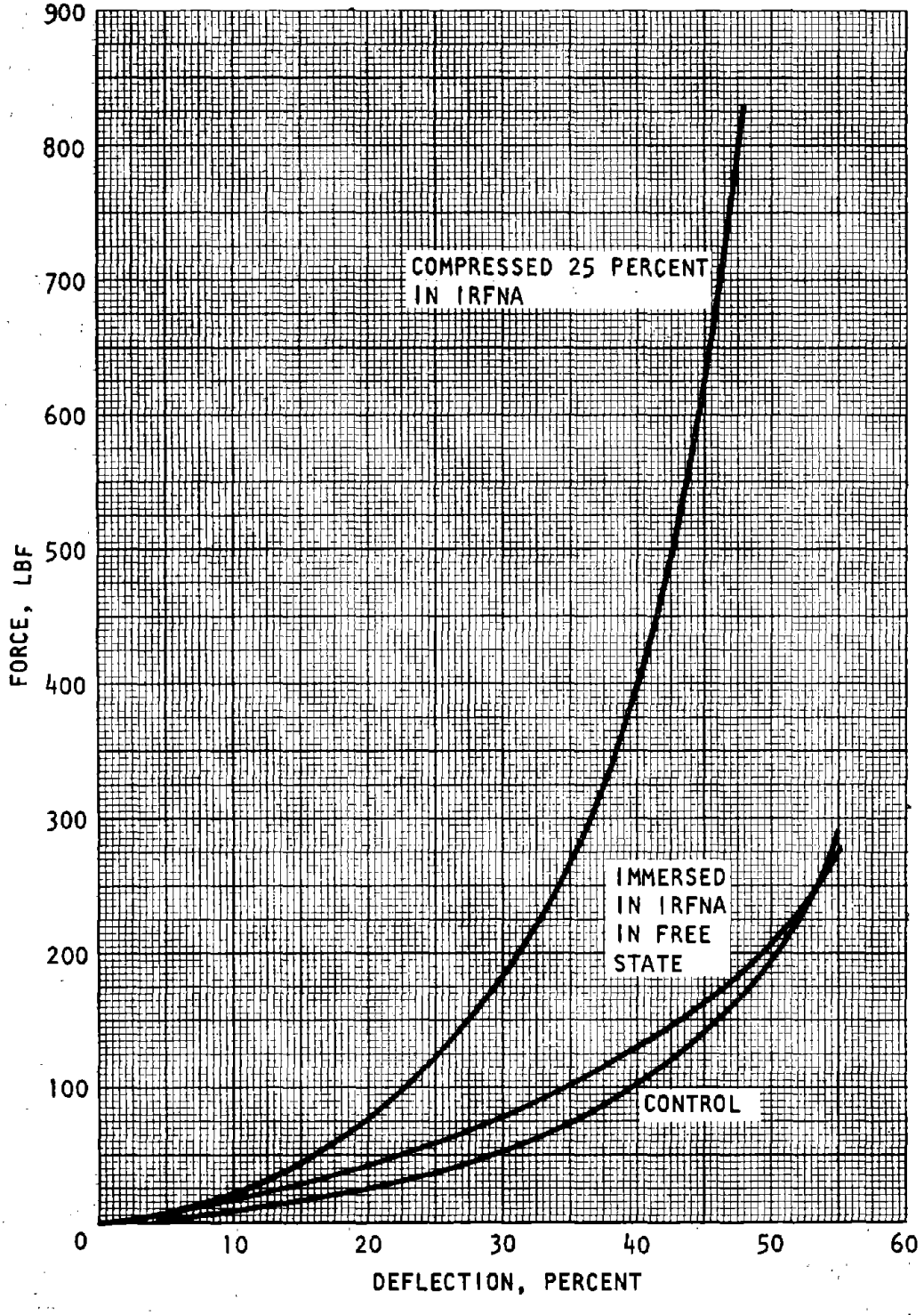

Figure 20. Compression-Deflection of AFE-124D O-Rings

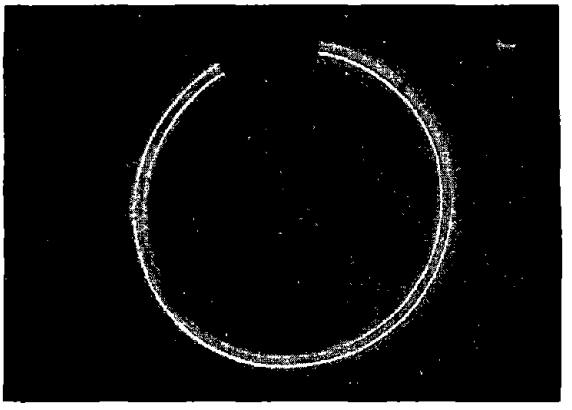

TRANSLUCENT CONTROL SEAL

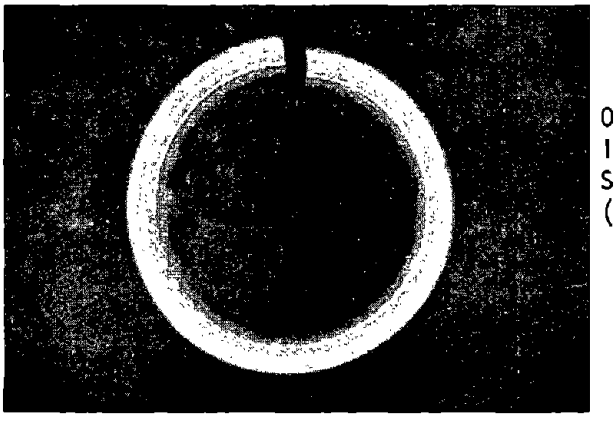

O-RING AFTER 32 DAYS IN IRFNA IN COMPRESSION FIXTURE (NOTE OPAQUE HALO)

O-RING AFTER 32 DAYS FREE IMMERSION IN IRFNA

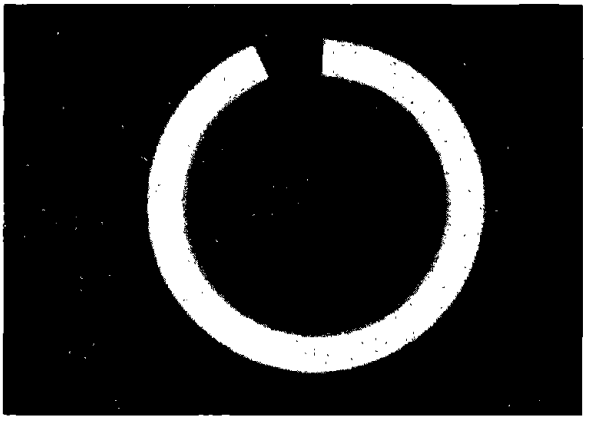

Figure 21. Photomacrographs (2X) of AFE-124D O-Rings

HDA-Materials Interactions

During this physical characterization program, HDA was handled in various materials under various conditions. Several qualitative observations were made on HDA interactions with corrosion resistant steels:

1. The 17-7 PH steel diaphragm of the pressure transducer used in the Poole-Nyberg densimeter showed signs of etching after use in HDA at temperatures of 0 to 200 F.

2. Solid material was visible in the propellant stream when the 304 stainless-steel equilibrium pressure cylinders were emptied after tests with HDA at 140 F over a period of three weeks. Visual inspection of the cylinder inner walls indicated a thin light blue-green solid coating that would flake off with vibration. A section of 321 stainless-steel tubing located between the cylinder body and the pressure transducer showed signs of etching and some particulate matter on the inner walls.

3. HDA flow from a 304 stainless-steel cylinder being used as a storage vessel for the nominal formulation showed no evidence of particulate matter with minimum flowrates; however, particulate matter was observed when the flowrates were increased slightly. These observations were made through a Teflon sight tube.

4. A 304 stainless-steel cylinder, which was used as a HDA storage bomb during the previous program under Contract F04611-68-C-0087, was emptied after 10 months of storage at ambient temperatures ($\sim$72 F). The HDA flow characteristics were similar to those reported in paragraph 3. After the cylinder was emptied, evacuated, filled with dry gaseous N_2, and the fittings were removed, a large quantity of light blue-green solid matter was vibrated loose and collected for qualitative analysis. The cylinder was then sectioned lengthwise and inspected. Photographs of the sectioned bomb are in Fig. 22 and 23. The inner walls of the cylinder, which was stored in a vertical position, indicated a definitive liquid-vapor interface. An appreciable

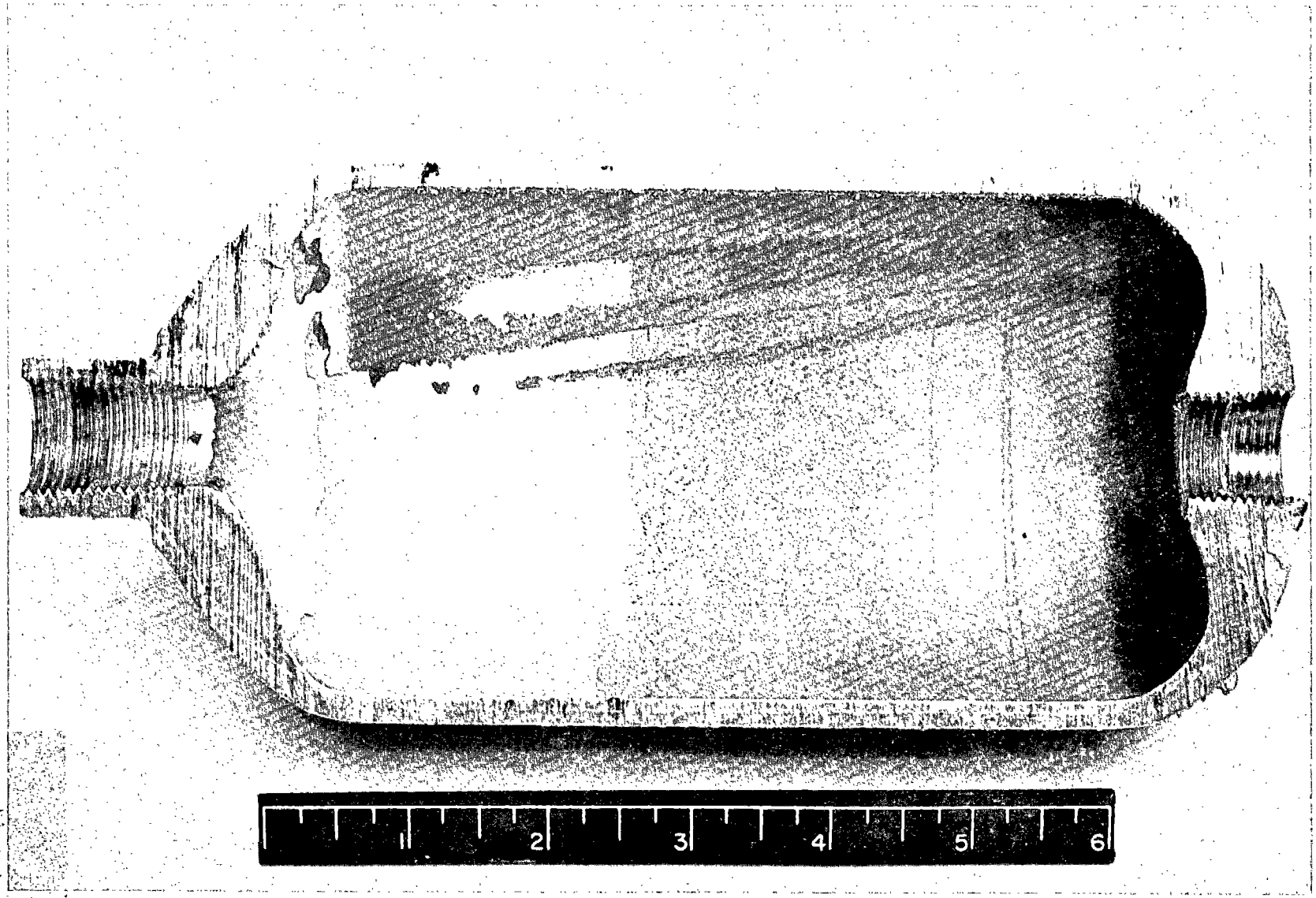

5AA12-6/9/71-C1A

Figure 22. Section of 304 Stainless-Steel Bomb After 10-Month Exposure to HDA at Ambient Temperature

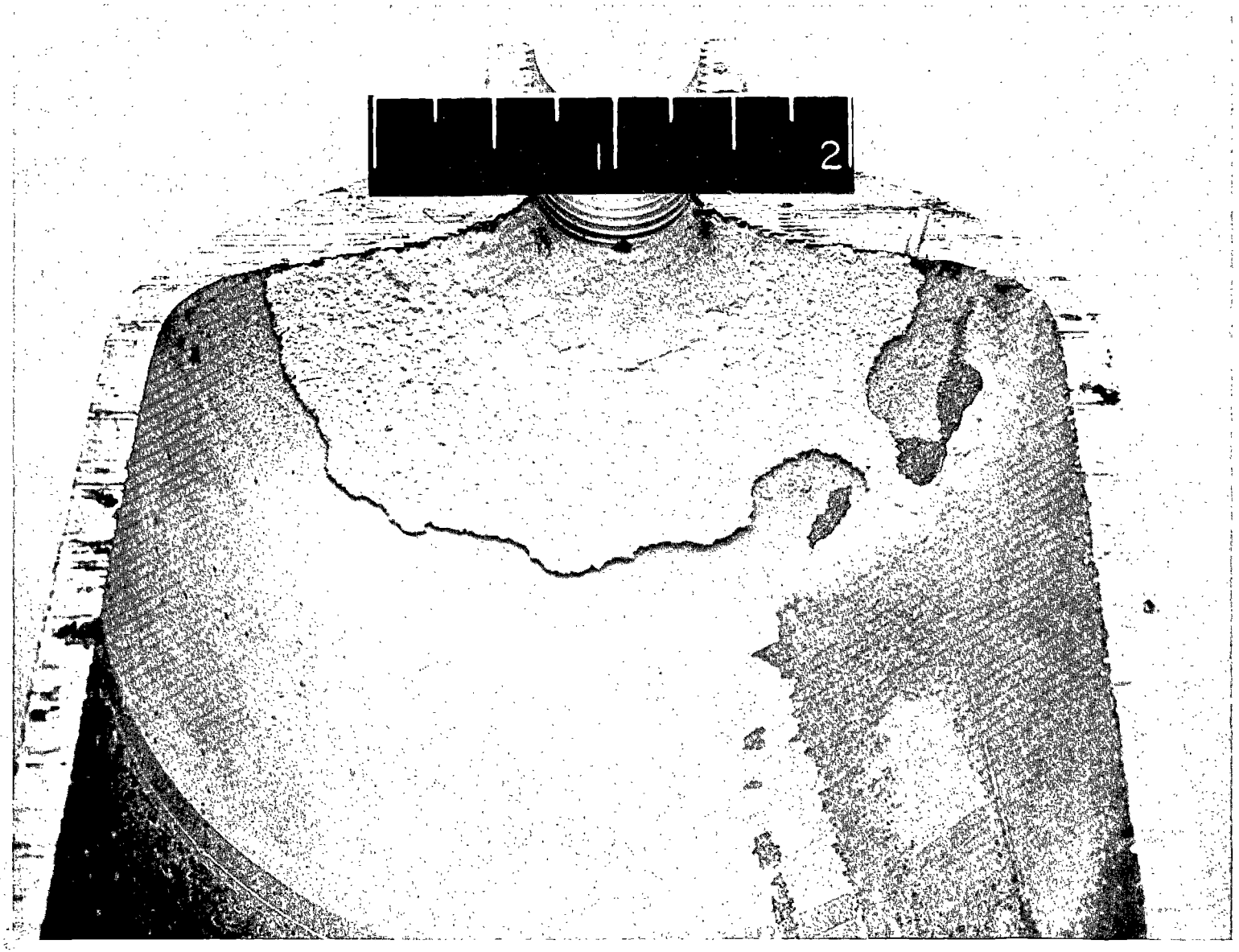

5AA12-6/9/71-C1B

Figure 23. Section of HDA Storage Bomb Showing Light Blue-Green Solid Material Collected at Bottom of Bomb (Top of Photo)

amount of the light blue-green solid material was deposited at the bottom of the cylinder (to the left in Fig. 22 , and to the top in Fig. 23); the portion of the cylinder wall in contact with liquid was bright with a general etch. In the section stored in contact with the vapor, the metal was darker with random and severe pitting; no general coating was observed, but coating "spots" were evident. This section was photographed and the solid material was analyzed.

In the corrosion product analysis, the Cr, Ni, and Fe determinations were made by dissolving a portion of the sample in HNO_3 and using an x-ray fluorescence spectrometric solution method for the determination. The F content was determined by first distilling the sample with a 1:1 $HClO_4$ solution using standard techniques and then by titrating with 0.1 M $La(NO_3)_3$, using a fluoride specific ion electrode as an indicator. The NO_3^- concentration was found by dissolving a portion of the sample in a small amount of H_2SO_4 and diluting to a known volume, neutralizing the acid to pH of 5.0 and determining the NO_3^- by a standard addition method.

Analytical results obtained for the corrosion products are as follows:

iron 28.4 w/o
chromium 7.64 w/o
nickel 2.02 w/o
fluoride 56.7 w/o
nitrate 2.32 w/o

The analysis of the propellant sample removed from the 304 stainless-steel cylinder indicated substantial decreases in the NO_2 and HF contents and increases in the HNO_3 and H_2O content. Although the decrease in NO_2 content may be attributed to slight vapor leakage, the magnitude of its decrease and the HF decrease appear significant.

CDI Reaction Study

The viscosity of CDI (carbonyl diisocyanate) has been observed to increase with time. The reaction that causes this may be a polymerization; however, the reaction path has not been established. The effects and rates of the CDI reaction were investigated by conducting non-volatile residue (NVR) determinations on freshly distilled CDI as a function of time, temperature, and materials of construction. The sample materials specified by AFRPL were: Pyrex glass, 347 stainless-steel, soft copper, Apiezon-L grease, and chrome-plated 304 stainless steel.

Since moisture has a deleterious effect on CDI, a vacuum system for distilling CDI and for conducting NVR determinations on CDI was designed and fabricated. It was essentially an all-glass system and included an isolatable and removable distillate trap, a distillation vessel, and provision for six ampoule connections. Nine reusable compatibility ampoules were also fabricated. All valves in contact with CDI were Fischer-Porter Teflon needle valves. All connections were made by O-ring joints using Viton O-rings. A constant temperature bath and the associated stirrer, heater, and thermotrol unit were set up in a fume hood. A modified Burrel wrist-action shaker was used to agitate the loaded compatibility ampoules while they were immersed at temperature in the bath. For the test series at -10 C, however, the freezer compartment of a refrigerator was used, and no agitation of the samples was provided. All non-vacuum-line transfers of CDI were performed in a GN_2-filled glove bag.

The most comprehensive set of NVR data was produced with the CDI/Pyrex glass system. Twenty-two individual NVR determinations were made at temperatures of -10, 20, 30, and 40 C. The reduced data from those measurements are given in Table 20. The initial rates of NVR production at each temperature were correlated with a least-squares curve-fit program, assuming an Arrhenius relation for temperature dependence, and were fitted remarkably well (Fig. 24) by the equation:

$$r = 9.19 \times 10^{11} \exp(-8524/T)$$

TABLE 20. EFFECT OF CDI REACTION ON NON-VOLATILE RESIDUE PRODUCTION

Material	Bath Temperature, C	Actual Time in Bath, Min	Estimated Total at Equivalent Time Bath Temperature, Min	Total NVR, Weight Percent Original CDI	CDI Appearance
Pyrex Glass	-10	14,400	14,400*	2.2*	2,5
	-10	24,500	24,500*	3.1*	2,5
	-10	34,500	34,500*	4.5*	2,5
	-10	53,000	53,000*	7.0*	4,5
	-10	83,300	83,300*	11.7*	4,5
	20	60	200	0.66	1,5
	20	120	300	1.06	1,5
	20	180	330	1.27	1,6
	20	240	380	1.38	1,5
	20	300	460	2.31	1,7
	20	300	460	2.42	1,7
	30	50	90	0.75	1,5
	30	95	130	1.14	1,5
	30	140	180	1.56	1,5
	30	185	220	2.53	1,8
	30	230	270	2.93	1,8
	40	50	70	1.39	1,5
	40	95	110	3.40	1,8
	40	140	160	5.11	1,8
	40	185	200	7.56	1,8
	40	230	240	7.90	1,7
	40	300	320	11.08	1,6
347 Stainless Steel	30	50	108	1.22	
	30	95	153	1.74	
	30	140	198	1.71	3
	30	185	243	2.17	3
	30	230	288	2.51	3
Copper	30	50	110	0.85	1,5
	30	95	155	1.21	3,5
	30	140	200	1.58	3,8
	30	185	245	1.92	3,8
	30	230	290	2.31	3,5
Apiezon-L Grease	30	50	104	1.55	1,5
	30	95	148	1.72	1,5
	30	140	194	2.21	1,5
	30	185	239	2.58	1,5
	30	230	284	3.09	1,5
Chrome-Plated 304 Stainless Steel	30	50	103	2.19	1,8
	30	95	148	2.87	1,8
	30	140	193	3.32	1,8
	30	185	241	3.66	1,8
	30	230	289	4.57	1,8

CDI Appearance Notes:

(1) CDI in bath was clear
(2) CDI in bath was clear with white crystal growth
(3) CDI in bath was cloudy
(4) CDI in bath was cloudy with white crystal growth
(5) CDI-NVR was white crystalline solid
(6) CDI-NVR was clear glass
(7) CDI-NVR was milky glass
(8) CDI-NVR was mixture of glass and white residue

(*) The NVR value for this sample was reduced by a quantity equivalent to the average NVR value produced from two control samples, which were loaded with CDI at the same time as the other samples in this series. For this reason, the estimated total equivalent time listed is identical to actual time.

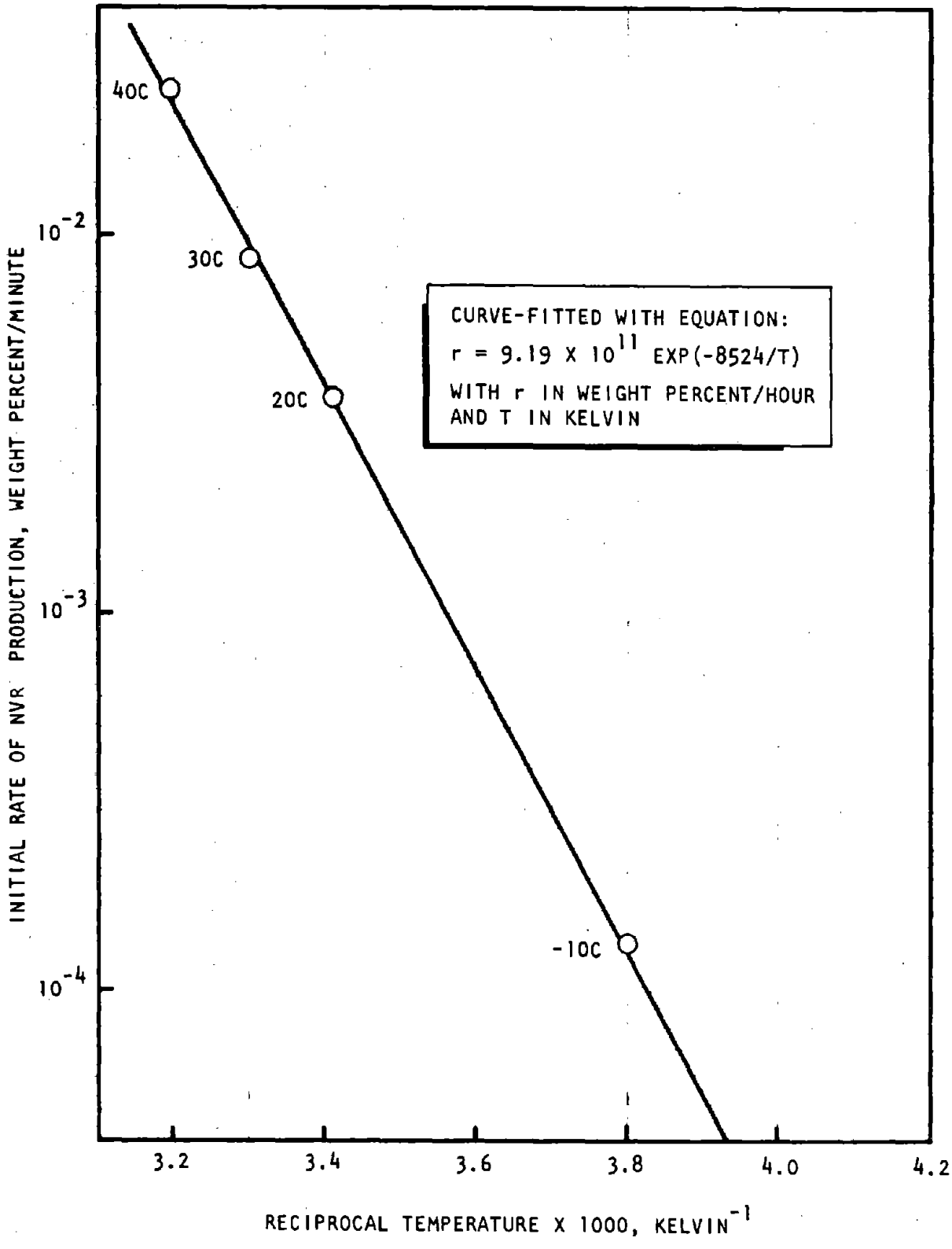

Figure 24. Correlation of NVR Production Rates of CDI in Pyrex

where r is the initial rate of NVR buildup in weight percent per hour, and T is temperature in degrees Kelvin.

A detailed analysis of the data generated during the various Pyrex test series was performed. In addition to the time during which the CDI in an ampoule was under the controlled (test) temperature, there was also, unavoidably, some time during which it was at room temperature during the loading operations and later during the nonvolatile residue (NVR) determination. The measured NVR was in each case the sum of that produced during the loading, test time at controlled temperature, and NVR determination.

The first data analysis effort, therefore, was to separate the amount of NVR produced during the test period from that produced during the room temperature operations, using all available information to make the best estimate possible. For the test series in Pyrex glass at -10 C, two control ampoules were loaded at the same time and under the same conditions as the other ampoules, but were then attached immediately to the CDI vacuum system and an NVR determination was performed on each. The NVR's obtained (their values agreed to within 5 percent) served as blanks for that test series. The average value for the control NVR's was subtracted from the measured NVR's for each ampoule run at -10 C.

Other data analysis efforts were performed for the data in Pyrex glass at 20, 30, and 40 C. The efforts were more difficult, however, since it was not practical to run blank determinations to help account for the NVR production during room temperature operations. The NVR produced while each ampoule was at room temperature, both before and after immersion in the constant-temperature bath, was accounted for in terms of additional equivalent time at the test temperature. A number of iterations were necessary in the data treatment to produce the final results. The additional times were then added to the respective bath times and the resultant values are represented in Tables 20 under the heading Estimated Total Equivalent Time at Bath Temperature.

It should be noted that, in the case of the 20 C run, two ampoules were withdrawn from the bath at 300 minutes, thereby providing a check on the reproducibility of the NVR determinations. The duplicate values agree to within 5

percent. In addition, it should be mentioned that the original Pyrex glass NVR results at 30 C do not appear in Table 20. Since these results appeared high, generally, in comparison with all others, a second test series was conducted with the Pyrex glass at 30 C, and the values listed were actually generated from this second test series. The unusually high values of the original test series could have been due to some type of passivation reaction, since it was the first test series conducted with the new glass ampoules.

The final evaluation of the CDI/Pyrex glass system shows that the five data points at -10 C, which were curve-fitted (forcing the curve through zero NVR at zero time), agree closely with a straight line (i.e., constant rate of NVR production) with slope 0.0079 weight-percent/hour. The standard error of estimate in NVR was only 0.1 weight-percent (in comparison with measured values from 2 to 12 weight-percent/hour). For the other temperatures, the final reduced data indicate that the NVR production rate was fairly constant, but with a moderate increase in rate with time.

Test series were also conducted for CDI in contact with the other specified materials of interest: soft copper, 347 stainless steel, chrome plated 304 stainless steel, and Apiezon-L grease. These tests were all conducted at 30 C; the results of the NVR determinations for them appear in Table 20. In addition, curves depicting NVR buildup for these materials, including Pyrex glass at 30 C, as a function of estimated equivalent bath time are illustrated in Fig. 25. Despite the fact that the sample-surface-area-to-CDI-volume ratio was intentionally kept at approximately 13.5 in^{-1} for both the wetted surface of the glass ampoule and for the test material immersed in the CDI, it would be incorrect to assume that the NVR results, therefore, should be strictly additive. A review of the data listed in Table 20 would appear to confirm the validity of this statement. In fact, it could possibly be argued that certain materials in CDI may even have an inhibiting effect on NVR production in the presence of Pyrex glass.

Data treatment of the non-Pyrex glass systems involved development of a method for estimating equivalent bath time when NVR data at more than one temperature were not available for each system. A reasonable assumption is made that the temperature dependence of the NVR rates is the same for the non-Pyrex materials

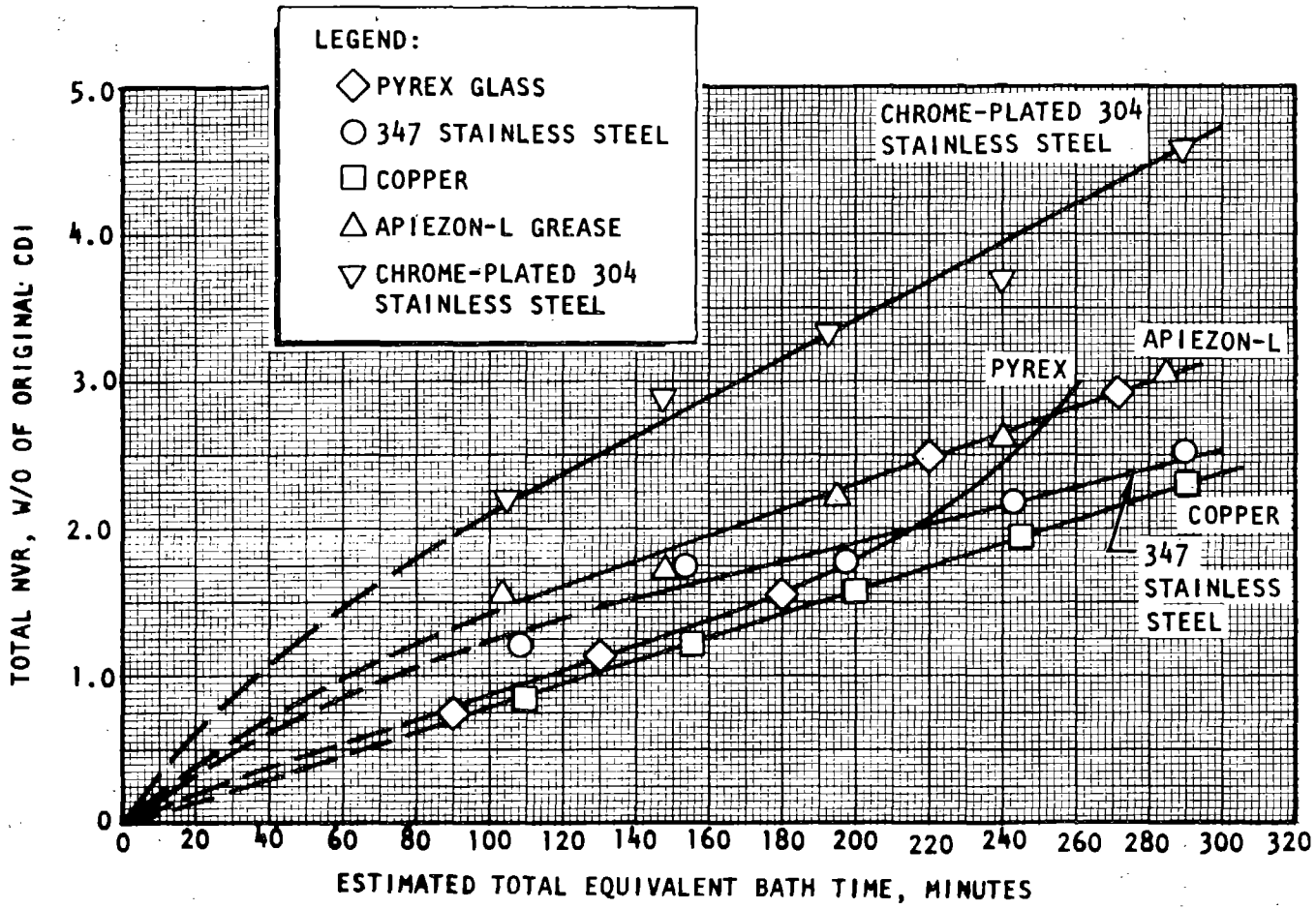

Figure 25. NVR Production vs Time for CDI in Contact With Selected Materials at 30 C (86 F)

as for the Pyrex, i.e., a plot of log r vs 1/T, where r is the NVR buildup rate and T is degrees Kelvin, would exhibit essentially the same slope for each system studied. Therefore, with $r \propto \exp(-8524/T)$ (from the Pyrex glass runs) and $t = NVR/r$, the following equation can be developed:

$$t_b = t_r \exp\left[-8524\left(\frac{1}{T_r} - \frac{1}{T_b}\right)\right],$$

where t_b is the time at T_b (bath temperature in degrees Kelvin) and t_r is the time at T_r (room temperature in degrees Kelvin). The total equivalent time (at T_b), therefore, is the actual bath time plus t_b.

The experimental technique employed in each of the test series involved cleaning five or six identical compatibility ampoules (approximately 10 cc volume), placing them in a vacuum oven, weighing them with the sample material inside, and then loading them (in a GN_2-filled glove bag) with 5 cc of freshly distilled CDI. The CDI was distilled usually on the same day that the ampoules were loaded. In all cases, the distilled CDI was kept under dry-ice until used. (Approximately 70 gms of CDI had been received from AFRPL for the study.) The ampoules were then weighed and placed in a constant-temperature bath with mild agitation or in the freezer compartment without agitation. After various periods of time over the time range of interest, each ampoule was withdrawn and attached to the special vacuum line for removal of volatile material. Each ampoule, with any NVR remaining, was then removed and weighed.

In general, the sample surface area to CDI volume ratio was approximately 13.5 $in.^{-1}$ (for both the wetted surface of the glass ampoule and for the test material immersed in the CDI). This was maintained to facilitate evaluation of the NVR data. Achieving a specific sample surface area to CDI volume ratio was accomplished by calculating: (1) the wetted surface area of the glass ampoule, (2) the volume of a sample of test material having that same surface area, (3) the new wetted surface area of the glass ampoule with the test specimen immersed in the CDI, and then reiterating until the two surface areas involved in the calculation were essentially equivalent. Knowing the surface area desired, the test specimens were then selected in the shape of rods, as in the case of the Pyrex glass, or wire, as with the metals, and then cut to the proper total

lengths. In the case of Apiezon-L grease, several Pyrex glass rods with the proper surface area were coated with a fine layer of the grease.

AFRPL Propellant Storability Tests

Propellant samples from long-term storability tests at AFRPL were analyzed by methods consistent with the analysis procedures outlined in the appropriate military procurement specifications. In all, ten MHF-5, five N_2O_4, and two ClF_5 samples were received from AFRPL. Although no quantitative results exist from the chemical analyses made by AFRPL before the tests were begun, all propellants had been analyzed and found to fall within the appropriate MIL specifications.

Nitrogen Tetroxide Analyses. Analysis of the nitrogen tetroxide samples (received in glass bottles with Teflon caps) from AFRPL long-term storability tests was accomplished using analytical methods consistent with MIL-P-26539C (the water equivalents were determined by AFRPL before shipment of the samples to Rocketdyne). Two of the samples (labeled UNK and TANK IV M7039 LONG TYPE LOADED 8 DEC 66 SAMPLE 14 SEPT 72) contained insufficient material for analysis when received at Rocketdyne. One of these (labeled UNK) had a leaking valve and contained no propellant when received by the Chemistry Laboratory at AFRPL. The remaining three samples had insufficient material for replicate nitric oxide and chloride analysis. The three analyzed samples all had a greenish color with particulate matter present. The results of the analyses are summarized in Table 21, along with MIL-P-26539C composition limits.

It is not known whether the samples were originally red-brown NTO or green NTO (MON-1). In either case, none of the analyzed samples met all of the chemical composition and physical properties required in MIL-P-26539C. However, none of the samples had appeared to suffer major degradation during the 5.5- to 6-year storage period.

Rocket performance calculations were made with Rocketdyne's Propellant Performance Program to assess the potential impact of the observed changes in composition during storage. The comparisons were made for theoretical shifting (ODE) specific impulse for optimum expansion from a chamber pressure of 1000 psia to an exit pressure of 14.7 psia, at mixture ratios chosen to give maximum

TABLE 21. CHEMICAL ANALYSIS OF NITROGEN TETROXIDE FROM AFRPL STORABILITY TESTS

AFRPL Sample Identification	Rocketdyne Log Number D/589-199	Composition, weight percent			
		Nitrogen Tetroxide	Nitric Oxide	Chloride	Water Equivalent
SN14 SPGG Test 16 May 1967- 22 September 1972	8-7-73	99.6	Trace, less than 0.1 (e)	Less than 0.001	0.11
UNK	8-8-73	(c)	(c)	(c)	(c)
Tank IV M7039 Long Type Loaded 8 December 1966- Sample 9-14-72	8-9-73	(c)	(c)	(c)	0.14
Tank No. 2 M2014 (d) Long Type Loaded 8 December 1966- 14 September 1972	8-10-73	99.2	0.2 (e)	Less than 0.001	0.11
SPGG SN009 in Test 16 May 1967- 20 September 1972	8-11-73	99.3	0.3 (e)	Less than 0.001	0.11
MIL-SPEC Red-Brown	--	99.5 minimum	(a)	0.040 maximum	0.17 maximum
MIL-SPEC Green (MON-1)	--	99.5 minimum (b)	0.8 ±0.20	0.040 maximum	0.17 maximum

(a) The NO content shall be limited to that which does not change the specified red-brown color of the propellant
(b) Minimum weight percent N_2O_4 + NO
(c) Insufficient sample for analysis
(d) Composition used for performance calculations
(e) Propellant had definite green color; therefore, did not meet red-brown specification requirement

specific impulse for the nominal (in-specification) propellants. The worst of the final compositions in Table 21 (Tank No. 2 M2014) is compared with nominal in-specification propellant (99.6 w/o N_2O_4, 0.1 w/o H_2O), in terms of its performance with two typical rocket fuels, in the table below:

Propellants	Mixture Ratio	Specific Impulse, lbf-sec/lbm	
		Nominal In-Spec	Tank No. 2 M2014
N_2O_4/N_2H_4-UDMH(50-50)	2.0	288.8	288.6
N_2O_4/MMH	2.15	288.3	288.1

A performance loss of only about 0.07 percent would be expected from the small changes in propellant composition observed during these storage tests. This would be undetectable in an actual rocket engine system.

Chlorine Pentafluoride (ClF_5) Analyses. Two ClF_5 propellant samples (received in metal containers) from AFRPL long-term (approximately 5-year) storage tests were analyzed by gas chromatography and infrared spectrophotometry as outlined in MIL-P-27413 and Ref. 35.

The chromatographic column did not adequately separate ClF_3 from ClF_5 at the low ClF_3 concentrations found in these two samples. The ClF_3 values obtained were confirmed by infrared spectrophotometry. The analytical results, shown in Table 22 , indicate that the propellant is within the specification limits established in Military Procurement Specification 27413 with respect to ClF_5, HF, and other impurities. A gas chromatographic analysis of the ullage gas in both samples was also performed. The results, also shown in Table 22 , were nearly the same as for the liquid phase: essentially all ClF_5.

MHF-5 Analyses. MHF-5 propellant samples from long-term storability tests at AFRPL were analyzed using analytical methods consistent with the procedure outlined in MIL-P-81507(AS). In order to improve the accuracy and reproducibility of the analysis set forth in this specification, upgraded gas chromatograph materials were used. These include the use of Teflon support material

TABLE 22. CHEMICAL ANALYSIS OF CHLORINE PENTAFLUORIDE FROM AFRPL STORABILITY TESTS

Sample Identification			Composition, weight percent							
AFRPL	Rocketdyne	Phase	ClF_5	HF	ClF_3	ClF	F_2	Cl_2	$FClO_3$	$FClO_2$
11[b]	3-8-29	Liquid	99.4	0.08	0.5	Trace	Trace	0.0	0.0	0.0
		Vapor	Remainder	(a)	(a)	Trace	0.005	--	--	--
19[b]	3-8-30	Liquid	99.6	0.04	0.4	0.0	Trace	0.0	0.0	0.0
		Vapor	Remainder	(a)	(a)	Trace	0.006	--	--	--
MIL-P-27413		Liquid	99.0 Minimum	0.4 Maximum	1.0 Maximum Other Impurities					

(a) Infrared determination was not performed to determine ClF_3 and HF.

(b) Tank filled on 23 August 1967; sampled 18 September 1972

(as required in the current military specifications for other hydrazine-type propellants) and special injection port inserts that were designed to remove nitrate deposits that affect subsequent runs and would eventually destroy the column.

Evaluation of the analytical results, shown in Table 23 , indicates that none of the samples were within specification limits. The concentrations of other soluble impurities (predominantly ammonia) were between 3.5 and 6.5 w/o for all samples, indicating propellant decomposition.

Rocket performance calculations were made to assess the potential effects of the observed changes in MHF-5 composition during long-term storage. The comparisons were made for theoretical shifting (ODE) specific impulse for optimum expansion from a chamber pressure of 1000 psia to an exit pressure of 14.7 psia, at mixture ratios chosen to give maximum specific impulse for the nominal (in-specification) propellant. The worst of the final compositions in Table 23 (SEA-15 N_2H_4) is compared with nominal in-specification propellant (55.0 w/o MMH, 26.0 w/o N_2H_4, 19.0 w/o $N_2H_5NO_3$, 1.0 w/o H_2O, 1.0 w/o OSI (i.e., NH_3) in terms of its performance as a monopropellant and with a typical oxidizer, ClF_5, in the table below.

Propellants	Mixture Ratio	Specific Impulse, lbf-sec/lbm	
		Nominal In-Spec	Tank SEA-15 N_2H_4
MHF-5 (monopropellant)	--	217.8	200.7
ClF_5/MHF-5	2.5	305.0	303.7

These performance losses from the changes in MHF-5 composition observed during storage are about 0.4 percent under typical bipropellant conditions and 7.8 percent as a monopropellant. The reduction for bipropellants would be modest. However, the potential degradation in monopropellant performance could be serious, and should be considered in any future design studies.

TABLE 23. CHEMICAL ANALYSIS OF MHF-5 FROM AFRPL STORABILITY TESTS

Sample Identification		Composition, Weight Percent				
AFRPL	Rocketdyne	$CH_3N_2H_3$	N_2H_4	$N_2H_5NO_3$	H_2O	OSI [a]
005 N_2H_4	6-86	50.6	24.3	17.1	1.4	6.5
SEA-15N_2H_4 [b]	6-87	49.2	23.5	16.3	7.5	3.5
006 NOH_4(S.I.C.)	6-88	51.1	24.6	17.3	1.9	5.2
001 N_2H_4 SN D3743	6-89	52.9	26.5	16.4	0.7	3.5
S/N 003	6-147	52.6	24.8	16.3	1.1	5.2
S/N 011	6-148	53.8	23.6	16.7	1.0	4.9
S/N 17	6-149	52.3	22.7	17.8	1.5	5.7
S/N 22	6-150	52.7	23.5	18.4	0.9	4.5
S/N 23	6-151	51.2	22.3	19.2	1.9	5.4
S/N 19	6-152	52.3	22.7	18.2	2.2	4.6
MIL-P-81507 (AS)		55.0 ±2.0	26.0 ±2.0	19.0 ±2.0	2.0 MAX H_2O+OSI	

(a) OSI = other soluble impurities

(b) Composition used for performance calculations

NOTES:

(1) Samples 6-86 to 6-89 were received in metal cylinders. All showed gas pressure when opened and all samples were clear with a pinkish cast common to partially decomposed hydrazine-type fuels.

(2) Samples 6-147 to 6-152 were received in glass containers. All samples had a yellow tinge and black particles were observed on the bottom of the containers.

Propellant Storability and Compatibility

Long-term, ambient-temperature storability tests of ClF_3, ClF_5, Florox, MHF-5, and MHF-7 are continuing in potentially applicable metals of construction. Each of the storage containers used in these tests was fabricated entirely from the selected material following the design shown in Fig. 26 . This construction eliminated bimetallic junctions and nonmetallic sealants. Pressure transducers, fabricated from the same materials, are being used to monitor progress of the tests by measuring pressure rises caused by propellant reactions and/or decomposition. Readout of the pressure transducers is being accomplished by 500-microampere panel meters driven by operational amplifiers.

In fabrication of the storability containers, the two halves of each container (Fig. 26) were machined from bar stock of the indicated materials. The halves were joined by electron beam welding with 100-percent penetration (some weld drop-through was observed on the inside surface). Tungsten-inert gas welding was used to attach the fill tubes and transducers. The transducers, fill tubes, and Swagelok plugs were fabricated from the same materials as the container, with one exception. The pressure transducers for the 2219 Al containers were fabricated from 2024 Al.

Immediately before loading, the oxidizer containers were propellant passivated. The procedure involved an evacuation to ~5 microns, exposure to propellant vapors at 200 mm Hg pressure for 10 minutes, a re-evacuation to ~5 microns, re-exposure to propellant vapors at 600 mm Hg pressure for 4 hours, and a third evacuation to ~5 microns followed by loading. The fuel containers were not propellant passivated.

All containers were loaded by vacuum transfer from a transfer bomb containing the required quantity of propellant to give a 2 v/o ullage at 200 F. As noted in Fig. 26 , the internal volume of all containers, except for those fabricated from 1100 Al, is 595 cc. The 1100 Al bombs have an internal volume of 550 cc. The amount of propellant loaded was determined gravimetrically during the loading and verified by weight measurements before and after the loading. An argon pad of ~1 atm was placed in the containers before sealing (under flowing argon gas) with the Swagelok plugs.

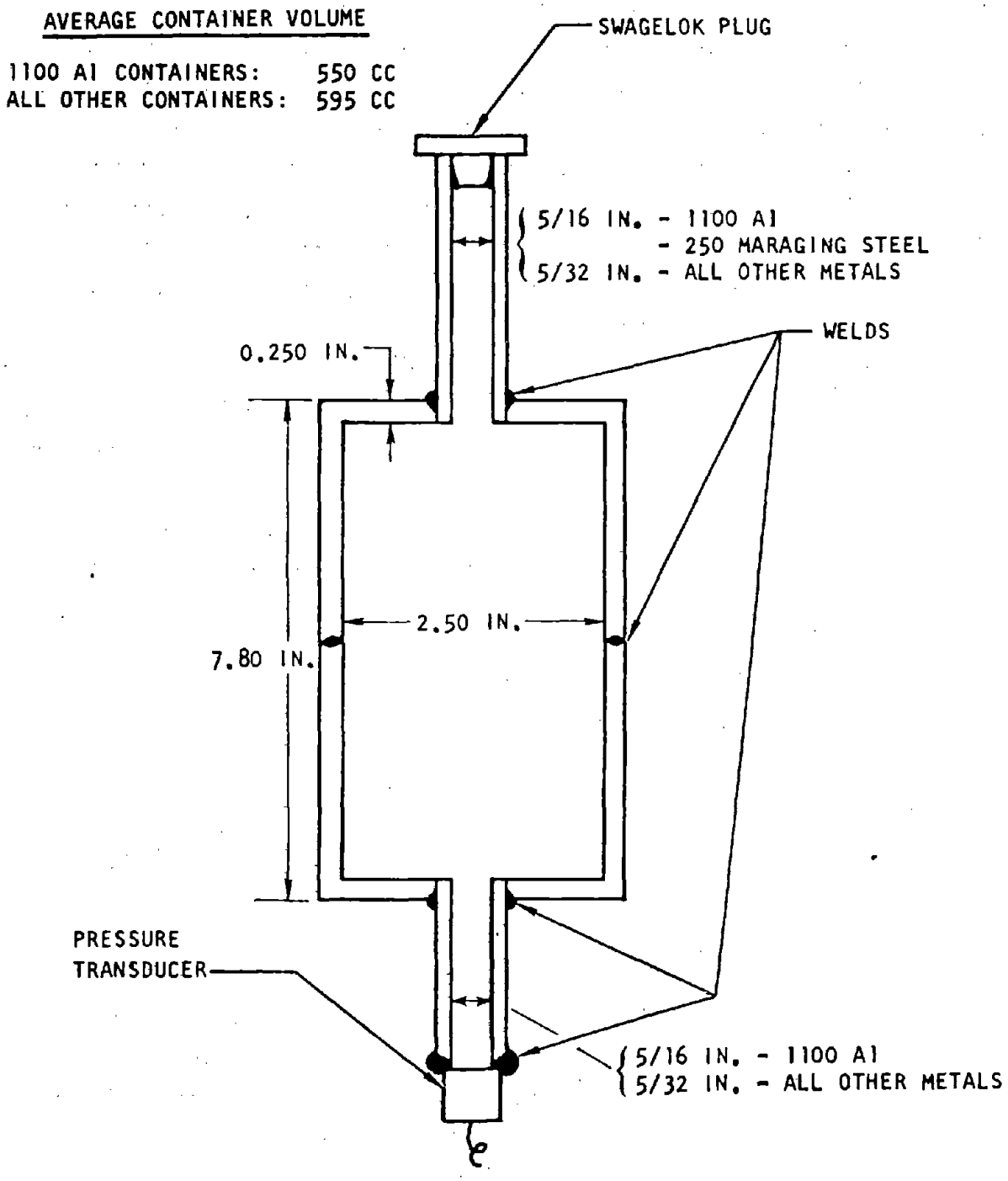

Figure 26. Storability Test Container

The MHF-5 and MHF-7 containers were loaded on 11 February 1970 and the oxidizer tests were initiated on 23 March 1970. The temperature of the bombs, which are stored in a horizontal position inside an open wooden building (fuels) and a metal warehouse (oxidizers), is allowed to fluctuate with the ambient temperatures (which are recorded) at Rocketdyne's Santa Susana Field Laboratory. During the storage period to date, these temperatures have varied from ~40 to 110 F. The tests are being continuously monitored by internal pressure and environmental temperature measurements.

At future termination of the tests, the container contents (both liquid and vapor phases) will be chemicahly analyzed and compared with the initial contents shown in Table 24. The following procedures were used for analysis: MHF-5, Rocketdyne Material Specification STO147RBO008, 10 October 1968; MHF-7, MIL-P-81342 (WP), 10 December 1965; ClF_3, ClF_5, and ClF_3O, gas chromatography and infrared spectrophotometry as described in Ref. 35.

To date, most of the containers show little pressure variation. Although the pressure transducers and associated electronics were calibrated before test initiation, it will be necessary to perform post-test calibrations on both the pressure measurement systems and the total liquid and ullage volumes present in each tank. This information will make it possible to derive final pressure versus time data (reduced to a common equivalent temperature) from the raw data that have been recorded. Until these post-test calibrations are made, caution should be used in drawing conclusions from the pressure readings.

A summary of the raw data obtained to date is presented in Table 25. Twenty-four of the 26 tanks are still under test, and appear to have developed no appreciable pressure changes during approximately 3-1/2 years. However, the magnitude of these pressure changes is such that it is difficult to conclude whether there are actual pressure changes or pressure measuring system zero shifts. The 1100 aluminum pressure transducers have shown very erratic performance, which is attributed to zero shifts resulting from temperature effects on the material. In this case, the only pressure data obtainable will be final pressures resulting from post-run calibrations.

TABLE 24. PRE-TEST CHEMICAL ANALYSES OF ROCKETDYNE STORABILITY SAMPLES

Chlorine Trifluoride	
ClF_3, w/o	99.4
HF, w/o	0.3
$FClO_2$, w/o	0.1
ClO_2, w/o	0.1
Cl_2, w/o	0.1

Chlorine Pentafluoride	
ClF_5, w/o	98.6
ClF_3, w/o	1.3
HF, w/o	0.1

Florox	
ClF_3O, w/o	98.7
ClF_3, w/o	0.7
FNO_2, w/o	0.3
$FClO_2$, w/o	0.1
Cl_2, w/o	0.1
HF, w/o	0.1

MHF-5	
$CH_3N_2H_3$, w/o	54.7
N_2H_4, w/o	26.2
$N_2H_5NO_3$, w/o	18.6
H_2O + OSI, w/o	0.5

MHF-7	
$CH_3N_2H_3$, w/o	80.0
N_2H_4, w/o	13.5
H_2O, w/o	5.9
OSI, w/o	0.6

TABLE 25. CURRENT RESULTS OF ROCKETDYNE PROPELLANT STORABILITY TESTS

Propellant	Material	Date of of Test Initiation	Initial Conditions		Conditions on 9/27/73		Test Period, Days	Summary Analyses
			Pressure, psia	Temperature, F	Pressure, psia	Temperature, F		
MHF-5	1100 Al	2/11/70	*	55	*	82	2050	Instrumentation anomalies
	2219 AL	2/11/70	16.5	55	20	82	2050	
	321 SS	2/11/70	19.3	55	--	82	594	Terminated-pressure 360 psia at 80 F
	Ti-6Al-4V	2/11/70	13.5	55	40	82	2050	
MHF-7	1100 Al	2/11/70	*	55	*	82	2050	Instrumentation anomalies
	2219 Al	2/11/70	11.5	55	20	82	2050	
	321 SS	2/11/70	14.5	55	18	82	2050	
	Ti-6Al-4V	2/11/70	18.0	55	10	82	2050	
ClF_3	1100 Al	4/16/70	20	62	*	93	1010	Terminated-leakage
	2219 Al	3/23/70	27	76	26	93	1285	
	321 SS	3/23/70	30	76	27	93	1285	
	Hastelloy C	3/23/70	27	76	26	93	1285	
	Maraging Steel 250	3/23/70	31	76	30	93	1285	
	Inconel 718	3/23/70	29	76	7	93	1285	
ClF_5	1100 Al	4/16/70	55	62	*	93	1261	
	2219 Al	3/23/70	64	76	70	93	1285	
	321 SS	3/23/70	60	76	60	93	1285	
	Hastelloy C	3/23/70	63	76	55	93	1285	
	Maraging Steel 250	3/23/70	65	76	60	93	1285	
	Inconel 718	3/23/70	73	76	80	93	1285	
ClF_3O	1100 Al	4/16/70	15	62	*	93	1261	Instrumentation anomalies
	2219 Al	3/23/70	22.5	76	16	93	1285	
	321 SS	3/23/70	17	76	40	93	1285	
	Hastelloy C	3/23/70	21	76	12	93	1285	
	Maraging Steel 250	3/23/70	19.5	76	5	93	1285	
	Inconel 718	3/23/70	18	76	11	93	1285	

*Shifting zero on pressure transducer prevented accurate measurement of pressure.

The test of MHF-5 in 321 stainless steel was terminated on 28 September 1971 after 594 days of storage. During this time, a peak pressure of about 430 psia was achieved during high (about 110 F) ambient temperature excursions. At test termination, the pressure of the storage bomb was 360 psia at 80 F. Chemical analyses of liquid and ullage samples from the bomb gave the following compositions:

Liquid		Ullage	
N_2H_4	- 24.1 w/o	N_2	~ 90 v/o
$CH_3N_2H_3$	- 55.8 w/o	H_2	~ 6 v/o
$N_2H_5NO_3$	- 18.7 w/o	NH_3	~ 3 v/o
H_2O	- 0.5 w/o	Remainder includes fuel vapors, O_2, and Ar	
OSI	- 0.9 w/o		

The test of ClF_3 in 1100 aluminum was terminated during January 1973, after approximately 1010 days at ambient temperatures, when the container developed a leak around the fill tube plug. The entire contents of the cylinder leaked out, thereby precluding post-run chemical analysis.

Propellant Formulation and Chemical Analysis

All propellants used during the physical and engineering property measurements were of propellant-grade quality obtained from commercial manufacturers or were formulated to specified compositions using standard procedures. The techniques applied in chemical analyses of the propellant samples used in the measurements followed military specification procedures, are equivalent to the specified procedures, or are standard Rocketdyne procedures that have been developed in the absence of specified procedures. During all handling and transfer operations, all required precautions were taken to prevent contamination or chemical deterioration of the propellant sample.

Brief summaries of the procedures used in the formulation of the propellant mixtures and in the chemical analyses of the propellant samples are presented in the following paragraphs. The results of the chemical analyses are presented here and also with the data from the measurements in the appropriate sections.

HDA. Early in this program, two liters of propellant-grade High Density Acid (HDA-N1) were obtained from Vandenberg AFB for use in selected physical property determinations. The HDA was stored under its own vapor pressure in two stainless-steel cylinders. Samples of the HDA (required for the property measurements described in other sections of this report) were withdrawn from the storage cylinders as needed by a gravimetric volume and vacuum transfer procedure. In order to correlate the measured physical properties with small variations in composition from the nominal, it was necessary to prepare and study several high-water HDA formulations (HDA-HW1 and HDA-HW2) and a high-NO_2 HDA formulation (HDA-HN). Subsequently, it became necessary to obtain an additional quantity (approximately two liters) of propellant-grade acid (HDA-N2) from Vandenberg AFB in order to complete the studies. The chemical analyses of these five propellants appear in Table 26.

TABLE 26. COMPOSITIONS OF HDA SAMPLES

Formulation	Composition, w/o					
	HNO_3	NO_2	H_2O	HF	Fe_2O_3	Particulates
HDA-N1	55.0	44.0	0.4	0.4	0.03	0.2
HDA-N2	55.7	43.2	0.46	0.54	0.006	0.1
HDA-HN	53.4	45.6	0.4	0.4	0.03	0.2
HDA-HW1	54.3	43.4	1.7	0.4	0.03	0.2
HDA-HW2	54.9	42.5	2.0	0.5	0.006	0.1

The as-received propellant-grade samples of HDA were chemically analyzed for total acid, HF, and NO_2 concentrations using the procedures of MIL-P-7254E, and for H_2O concentration and particulate matter (total solids) concentration using a modified procedure of MIL-P-7254F. The formulated compositions were determined mathematically from calculations of the ingredient quantities and experimental confirmation (by chemical analyses) of the added ingredients.

Nitrogen Tetroxide. The nitrogen tetroxide (red-brown N_2O_4) was obtained commercially and then was chemically analyzed for N_2O_4, 99.9 w/o, and H_2O equivalent, 0.01 w/o, using the procedures specified in MIL-P-26539C.

NO-Rich MON-1. The NO-rich MON-1 (Nominal MON-1 composition: 99 w/o N_2O_4-1 w/o NO) sample used in the density measurements was formulated by loading N_2O_4 through a vacuum line into a chilled cylinder, adding NO by volume expansions through the vacuum line into the same cylinder, and then warming the cylinder. The oxidizer blend was then chemically analyzed using procedures described in MIL-P-26539C. The sample contained: 98.5 w/o N_2O_4, 1.17 w/o NO, <0.01 w/o Cl^-, and 0.07 w/o H_2O.

Hydrazine. The hydrazine (N_2H_4) used in the gas solubility measurements, and as a component in a fuel blend used in the density measurements, was obtained commercially. Its composition was determined by chemical analysis to be 99.0 w/o N_2H_4, 0.5 w/o H_2O, and 0.5 w/o other soluble impurities. The analysis was conducted by gas chromatography techniques consistent with that specified in MIL-P-26536C.

Hydrazine-UDMH(50-50). The hydrazine (see above) and the UDMH, $(CH_3)_2N_2H_2$, used in this fuel blend were obtained commercially. Five formulations were prepared (four under inert atmosphere in a dry box and one under GN_2 in a glove bag). Their respective compositions appear in Table 27.

TABLE 27. COMPOSITIONS OF HYDRAZINE-UDMH (50-50) SAMPLES

Formulation	Composition, w/o			
	UDMH	N_2H_4	H_2O	OSI
A-1	46.9	52.6	0.3	0.2
A-2	50.3	49.1	0.3	0.3
A-3	46.6	51.3	1.9	0.2
A-4	48.3	49.6	1.9	0.2
A-5	48.6	50.9	0.3	0.2

Chemical analyses of the samples were conducted using gas chromatography techniques equivalent to those specified in MIL-P-27402B.

PHASE III: EVALUATION AND COMPILATION OF DATA

OBJECTIVE

During the entire period of the contracted program, efforts under Phase III were directed toward the assembly of all data generated by Phases I and II, unification of the data sources, critical comparison of conflicting data, and tabulation of the results.

RESULTS AND ACCOMPLISHMENTS

Phase III effort during the program included the compilation and evaluation of physical properties data from the literature for selected propellants. The principal work in the phase was devoted to the reduction, evaluation, and correlation of all data generated from the Phase II experimental efforts. However, to maintain continuity in this text, the latter results are reported under the pertinent Phase II headings. A brief summary of some of the other major efforts under Phase III is given in the following paragraphs.

Melting Point Lowering of Nitrogen Tetroxide

An evaluation was made of potentially useful propellant additives to nitrogen tetroxide which might result in a sufficiently low melting point to be attractive for a wider range of applications than neat nitrogen tetroxide. A survey of physical properties and handling characteristics was also made for the two additives selected for tests, FTM and TNM.

Critical Properties

The critical properties of HDA were needed. It would not be practical to measure them because of the decomposition of its components at high temperatures. A literature survey indicated that no useful data exist for pure nitric acid or its other mixtures; however, no data were expected because of decomposition (no data were found). Subsequently, pseudocritical properties were estimated for HDA, as described in the Critical Properties section under Phase II.

HDA Heat of Formation

A careful estimate was made of the heat of formation of HDA, the maximum uncertainty in this estimate, and the potential impact of this uncertainty on rocket performance calculations. These are described in detail under Phase II.

Inert Gas Solubility

The data obtained from a literature survey on solubility of nitrogen and helium in hydrazine, MMH, UDMH, N_2H_4-UDMH (50-50), and N_2O_4 were critically evaluated, reduced to common bases, and used in comparisons with experimental gas solubility data measured during this program.

REFERENCES

1. AFRPL-TR-66-122, Final Report, Engineering Properties of Rocket Propellants, Rocketdyne Division, Rockwell International, Canoga Park, California, Contract AF04(611)-10546, July 1966.

2. Final Report, Contract AF04(611)-11407. Rocketdyne Division, Rockwell International, Canoga Park, California.

3. Annual Summary Report, Contract F04611-68-C-0087, Rocketdyne Division, Rockwell International, Canoga Park, California.

4. Final Report, Contract F04611-68-C-0087, Rocketdyne Division, Rockwell International, Canoga Park, California.

5. Handbook of Chemistry and Physics, 53rd Edition, 1972-1973, CRC Press, a Division of Chemical Rubber Co.

6. Rocketdyne data, Personal Communication from R. Wagner, Rocketdyne Division, Rockwell International, Canoga Park, California, September 1973.

7. Kay, W. B., Ind. Eng. Chem., 28, 1014 (1936).

8. Leland, T. W., Jr., and W. H. Mueller, Ind. Eng. Chem., 51, 597 (1959).

9. Lydersen, A. L., Estimation of Critical Properties of Organic Compounds, Engineering Experiment Station Report No. 3, University of Wisconsin, Madison, Wisconsin, April 1955.

10. Lydersen, A. L., R. A. Greenhorn, and O. A. Hougen, Generalized Thermodynamic Properties of Pure Liquids, Engineering Experiment Station Report No. 4, University of Wisconsin, Madison, Wisconsin, October 1955.

11. Gates, D. S. and G. Thodos, AIChE J, 6, 50 (1960).

12. Reidel, L., Z. Elektrochem., 53, 222 (1949).

13. García-Bárcena, G. J., unpublished S.B. Thesis in Chemical Engineering, Massachusetts Institute of Technology, 1958. (as given in Ref. 14)

14. Reid, R. C. and T. K. Sherwood, The Properties of Gases and Liquids (2nd edition), McGraw-Hill Book Company, New York, New York, 1966, p.42.

15. Poole, D. R. and D. G. Nyberg, "High Pressure Densimeter," J. Sci. Instru., 30, 576 (1962).

16. Selleck, F. T., H. H. Reamer, and B. H. Sage, "Volumetric and Phase Behavior of Mixtures of Nitric Oxide and Nitrogen Dioxide," Ind. Eng. Chem., 45, 814-819 (1953).

17. Reamer, H. H. and B. H. Sage, "Volumetric Behavior of Nitrogen Dioxide in the Liquid Phase," Ind. Eng. Chem., 44, 185-87 (1952).

18. WADC Technical Report 54-380, Preparation of Nitric Oxide--Nitrogen Dioxide Mixtures from the FMC Nitrogen Fixation Furnace by Chilling, FMC Corporation, Contract AF18(600)-34, October 1954.

19. Pascal and Garnier, "Relations entre le peroxyde d'azote et l'acide nitrique," Bull. Soc. Chem., 24, 309 (1919).

20. Mittasch, Von A., E. Kuss, and H. Schlueter, "Dichten and Dampfdrucke von Wassrigen Ammoniaklosungen und von flussigen Stickstofftetroxide fur das Temperaturgebiet 0° bis 60°," Z. Anorg. Allgem. Chem., 159, 1 (1926).

21. LRP 198, Storable Liquid Propellants--Nitrogen Tetroxide/Aerozine 50, 2nd Edition, Aerojet-General Corp., June 1962.

22. McGonigle, T. J., "Mixed Oxides of Nitrogen-Properties and Handling," Nitrogen Division of Allied Chemical Corporation, Hopewell, Virginia.

23. Greenspan, M. and C. E. Tschiegg, "Tables of the Speed of Sound in Water," J. Acoust. Soc. Am., 31, 75 (1959).

24. Wilson, W. D. and D. Bradley, "Speed of Sound in Four Primary Alcohols as a Function of Temperature and Pressure," J. Acoust. Soc. Am., 36, 333 (1964).

25. AFTPL-TR-67-311, The Heat of Formation of Propellant Ingredients, Special Report, The Dow Chemical Company, Midland, Michigan, December 1967.

26. Rossini, F. D. et al, Selected Values of Chemical Thermodynamic Properties, NBS Circular 500, Government Printing Office, Washington, D.C., 1952.

27. Interoffice Memo, 914:70:0311-1: GJ, Bell Aerospace Company, Buffalo, New York, March 1970.

28. Interoffice Memo, 914:70:0424-1: GJ, Bell Aerospace Company, Buffalo, New York, April 1970.

29. Beegle, R. L. Jr., D. L. Quick, and W. J. Flaherty, Measurement of Helium and Nitrogen Solubility in Nitrogen Tetroxide, Monomethylhydrazine and Aerozine-50, Aerojet-General Corp., Appendix to Report LM 0696-03-7, May 2, 1966. (See also, succeeding Report No. LM 0696-03-08, June 1966).

30. Report No. 2736, Pressurization Systems Design Guide, Volume IIB, Aerojet-General Corp., Azusa, California, Contract NAS7-169, Revised, July 1966.

31. Report DAC-60510-F1, Pressurization Systems Design Guide, Volume III Pressurant Gas Solubility in Liquid Propellants, McDonnell Douglas, Newport Beach, California, Contract NAS7-548, July 1968.

32. Chang, E. T., N. A. Gokcen, and T. M. Posten, J. Phys. Chem., 72, 638 (1968). Originally in Chang, Gokcen, and Posten, Thermodynamic Properties of Gases in Propellants, Air Force Report No. SAMSO-TR-68-23 [Aerospace Report No. TR-0158(3210-10)-2], Aerospace Corporation, Los Angeles, October 1967.

33. Gardner, M. P., D. Wells, and J. Buehner, Study of Pressurant Gas Solubility in Nitrogen Tetroxide and Aerozine 50, TRW Report 01827-6205-RO-00, TRW, Los Angeles, California, 10 December 1968.

34. AFBSD-TR-62-2, Titan II Storable Propellant Handbook, Final Handbook, Revision B, Bell Aerosystems Company, Buffalo, New York, Contract AF04(694)-72, March 1963. (Bell Report No. 8182-933004)

35. R-7034, Final Report, Verification of a New Liquid Oxidizer, Rocketdyne, A Division of North American Aviation, Inc., Canoga Park, California, Contract NOw66-0639-d, May 1967,

APPENDIX A

PHYSICAL PROPERTIES OF HDA

The physical and thermodynamic properties of HDA are presented in Table A-1 and Fig. A-1 through A-6a.

All of the data given in this section (with the exception of melting point and surface tension) were developed during this program, either from experimental measurements and subsequent correlations, or from theoretical estimates (where indicated as such). All properties were curvefitted as functions of N_2O_4 and H_2O composition, as well as temperature, since data were obtained for several compositions. Although this leads to lengthier expressions, it does permit interpolation for any particular composition, within the limits given. Variations in HF content were too small to produce any correlation; therefore, this variable was not included in the equations. Points for the table and the figures were obtained by evaluating curvefitted expressions for the nominal HDA composition (54.8 w/o HNO_3, 44.0 w/o N_2O_4, 0.5 w/o H_2O, and 0.7 w/o HF).

TABLE A-1. PHYSICAL PROPERTIES OF HDA AT 25 C (77 F)

Property	Value		Figure Number	Reference Number
	Metric	English		
General Identification				
Identification	HDA (High Density Acid) or Maximum Density Inhibited Fuming Nitric Acid			
Nominal Composition	54.8 w/o HNO_3, 44.0 w/o N_2O_4, 0.5 w/o H_2O, 0.7 w/o HF			
Empirical Formula, g atoms/100 g	$H_{0.9602}\ N_{1.8261}\ O_{4.5495}\ F_{0.0350}$			
Melting Point	-37.2 C	-35 F		A-1
Triple Point	approx.-37.2 C	approx.-35 F		
Normal Boiling Point	24.7 C	76.5 F		
Critical Properties				
Temperature	540 K*	512 F*		
Pressure	97.2 atm*	1428 psia*		
Density	0.00935 g-mole/cc*	0.584 lb-mole/cu ft*		
Volume	107 cc/g-mole*	1.71 cu ft/lb-mole*		
Compressibility Factor	0.235*	0.235*		
Phase Properties				
Density				
Solid	--	--		
Liquid	1.624 g/cc	101.4 lb/cu ft	A-1,-1a	
Gas	--	--		

*Estimated values

TABLE A-1. (Concluded)

Property	Value		Figure Number	Reference Number
	Metric	English		
Phase Properties (Cont.)				
Compressibility				
Adiabatic	3.157×10^{-5} atm^{-1}	2.148×10^{-6} $psia^{-1}$	A-2,-2a	
Isothermal (liquid)	--	--		
Vapor Pressure	1.01 atm	14.9 psia	A-3,-3a	
Surface Tension	29.8 dynes/cm	2.04×10^{-3} lbf/ft	A-4,-4a	A-2
Thermodynamic Properties				
Heats of				
Formation (liquid)	-43.4 ±0.8 Kcal/100 g	-779 ±14 Btu/lb		
Fusion	--	--		
Vaporization (at NBP)	7.0 Kcal/g-mole vapor**	270 Btu/lb**		
Heat Capacity	--	--		
Transport Properties				
Viscosity (liquid)	2.28 cp	1.54×10^{-3} lbm/ft-sec	A-5,-5a	
Thermal Conductivity	--	--		
Sonic Velocity (liquid)	1404 m/sec	4605 ft/sec	A-6,-6a	

**Calculated from vapor pressure equation

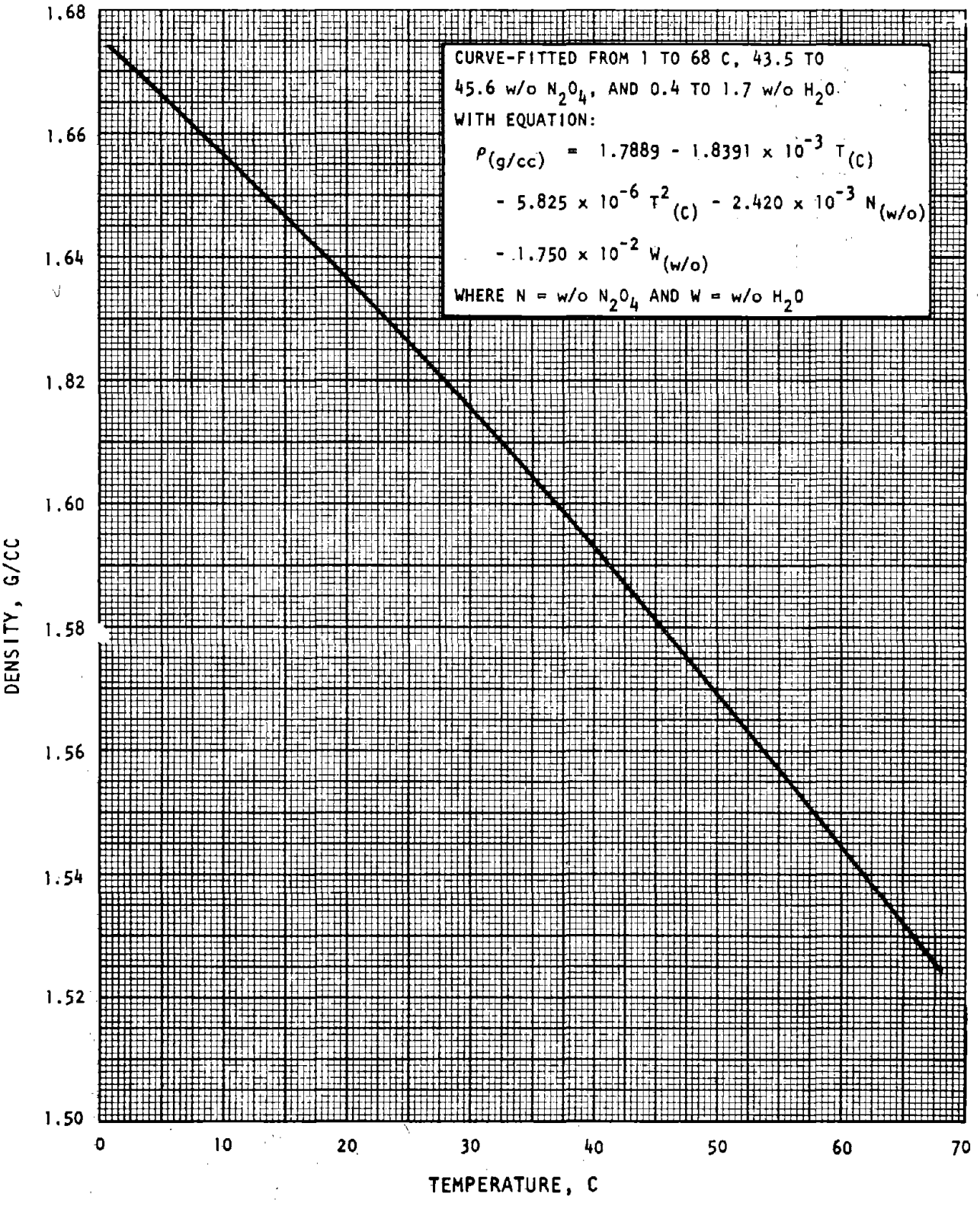

Figure A-1. Density of Saturated Liquid HDA

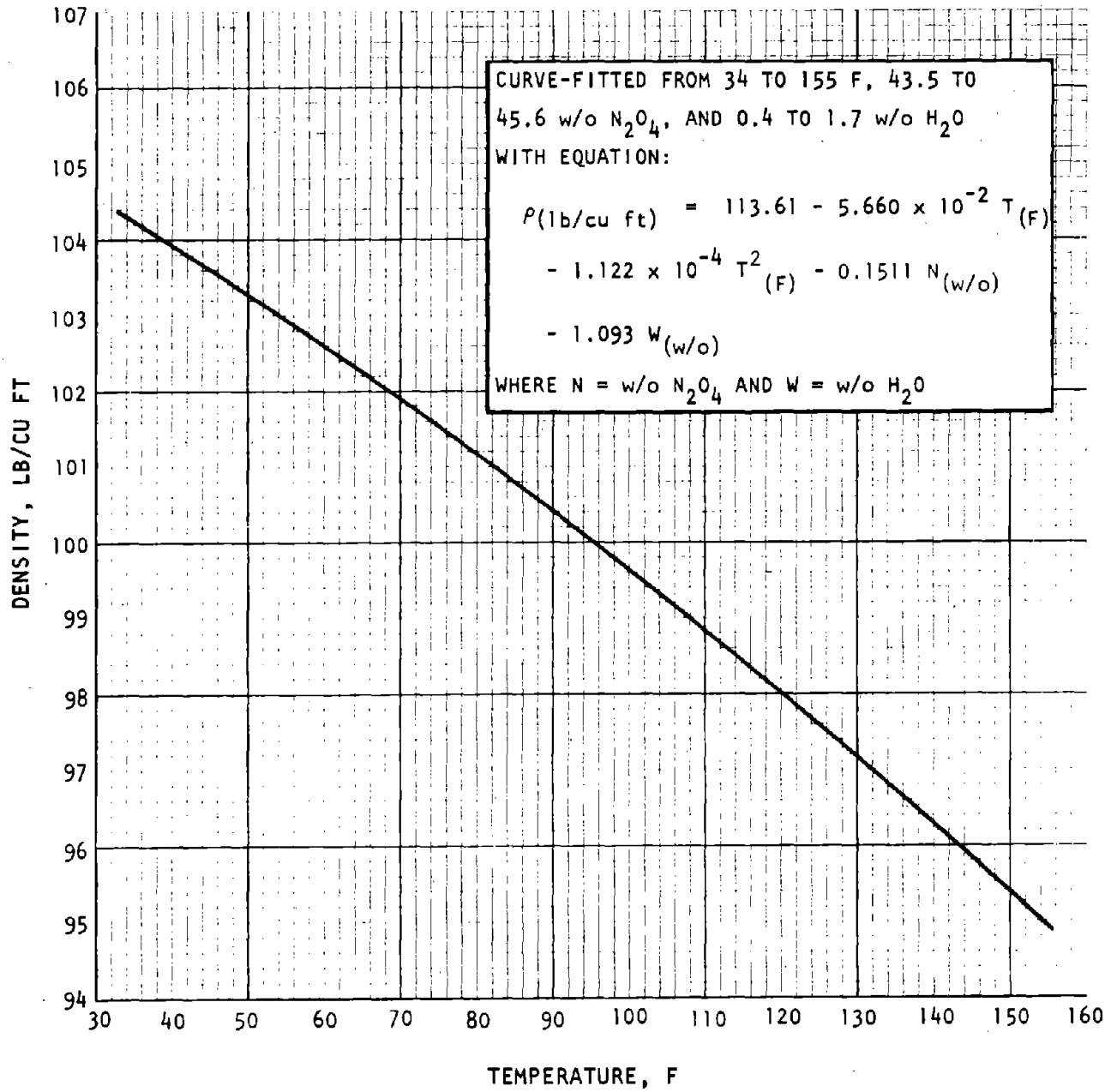

Figure A-1a. Density of Saturated Liquid HDA

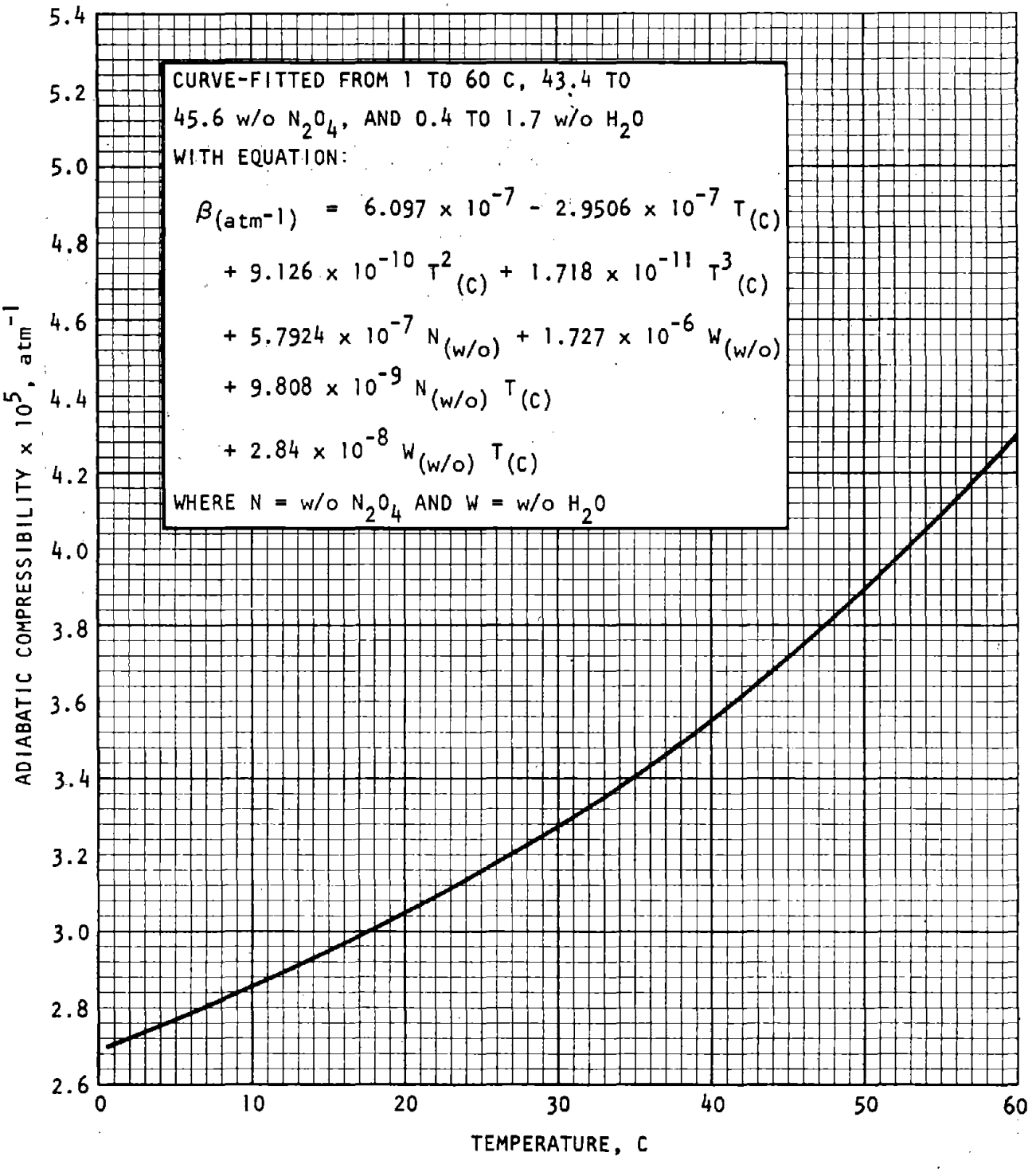

Figure A-2. Adiabatic Compressibility of Saturated Liquid HDA

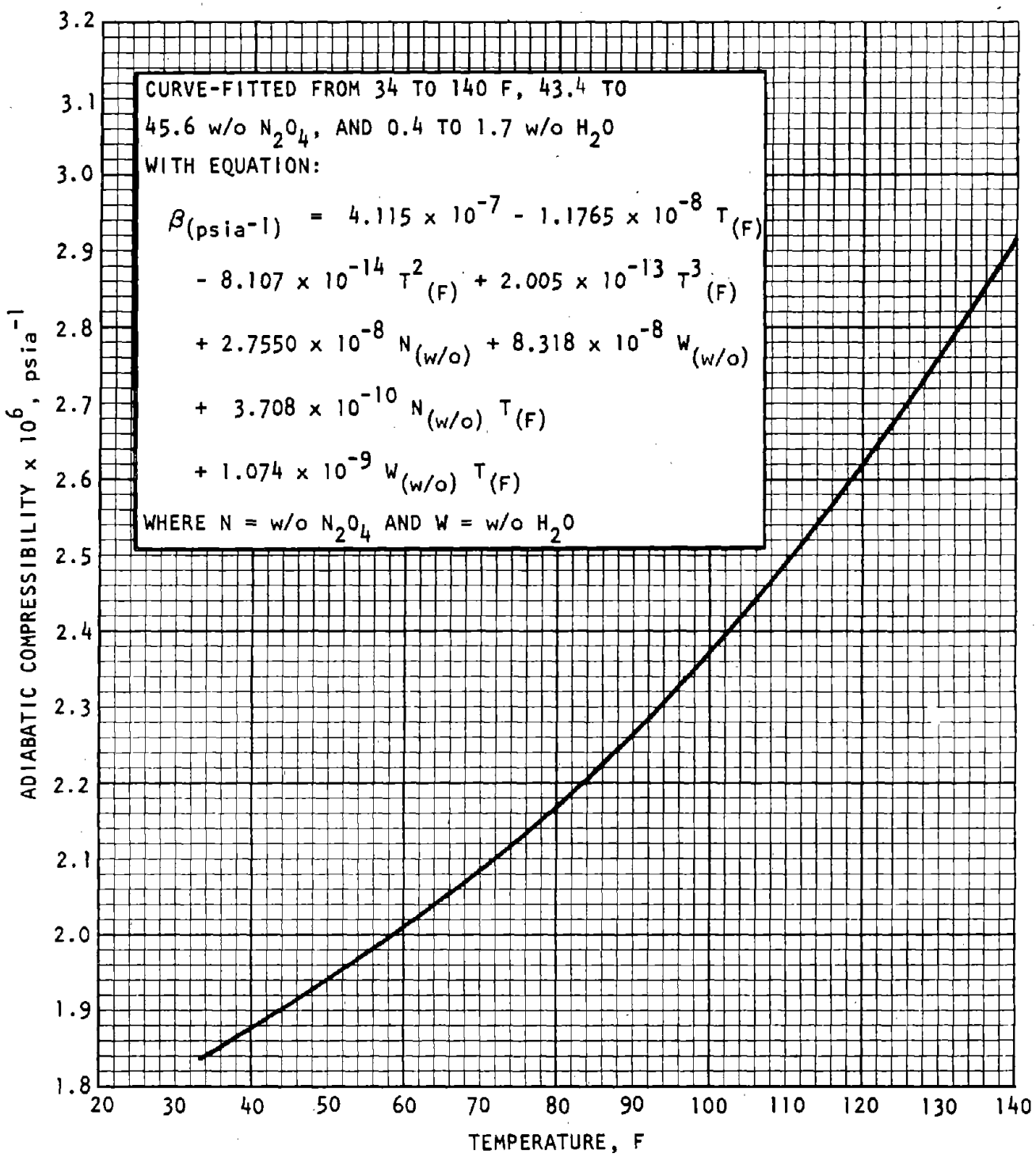

Figure A-2a. Adiabatic Compressibility of Saturated Liquid HDA

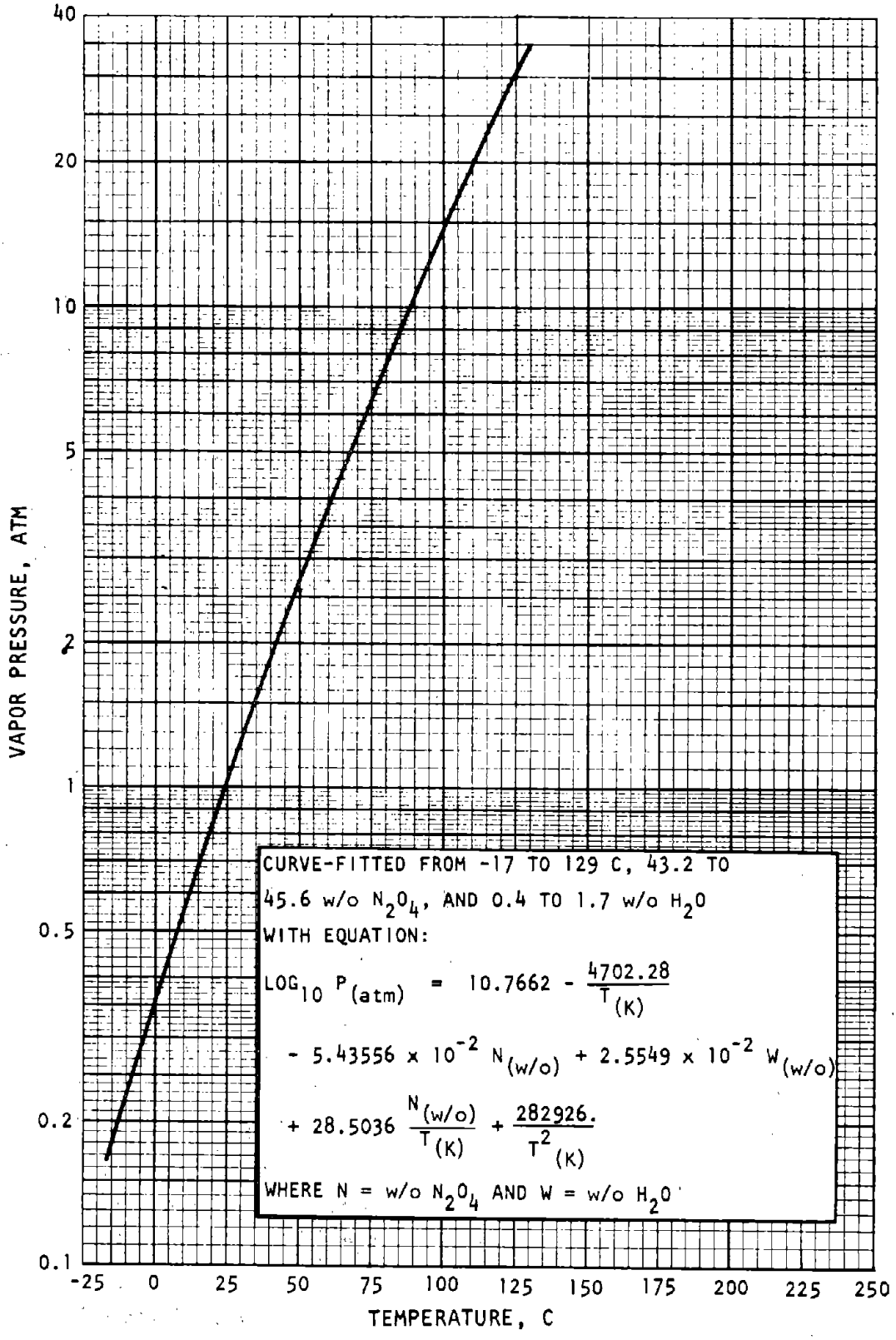

Figure A-3. Vapor Pressure of HDA

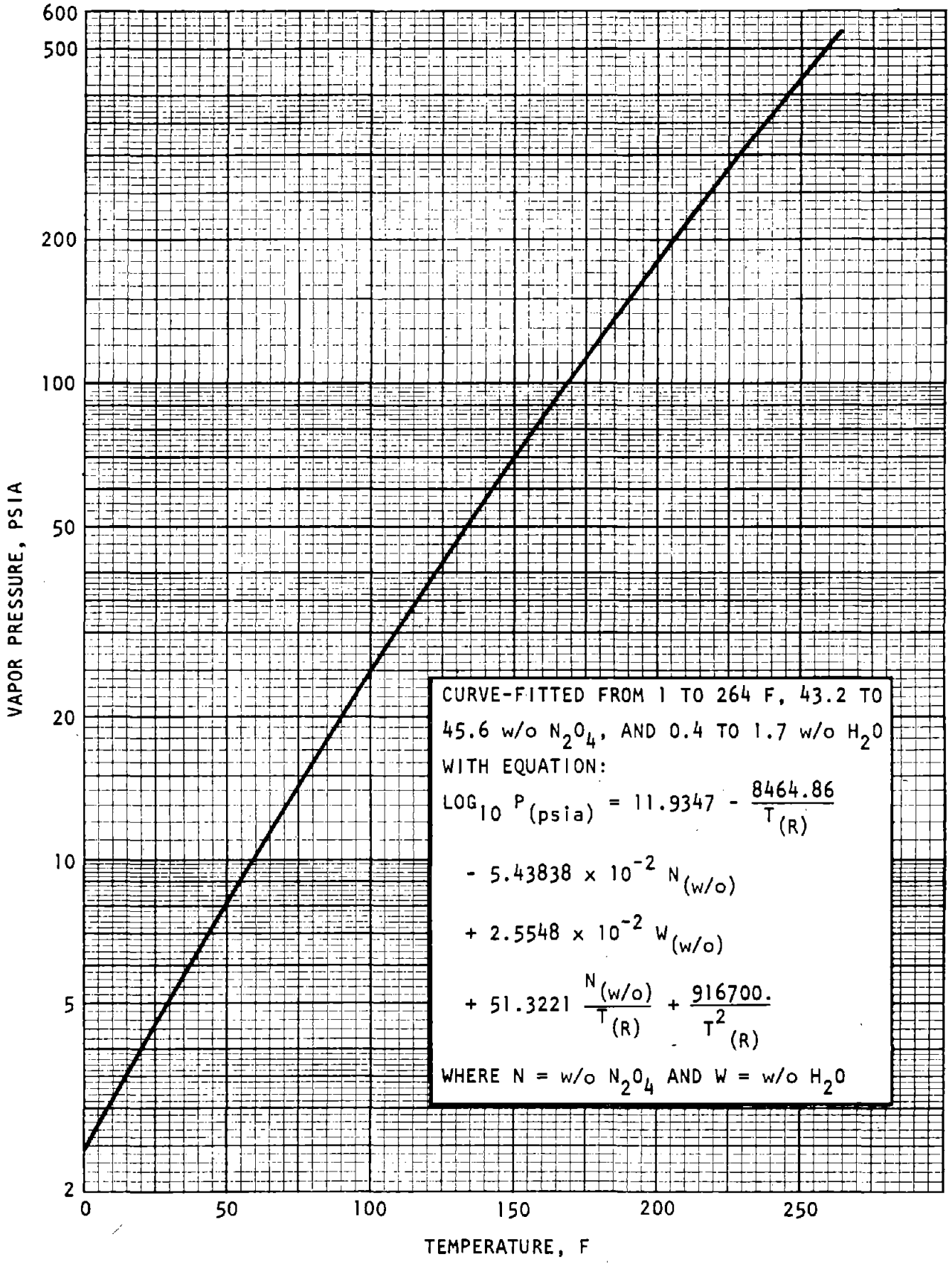

Figure A-3a. Vapor Pressure of HDA

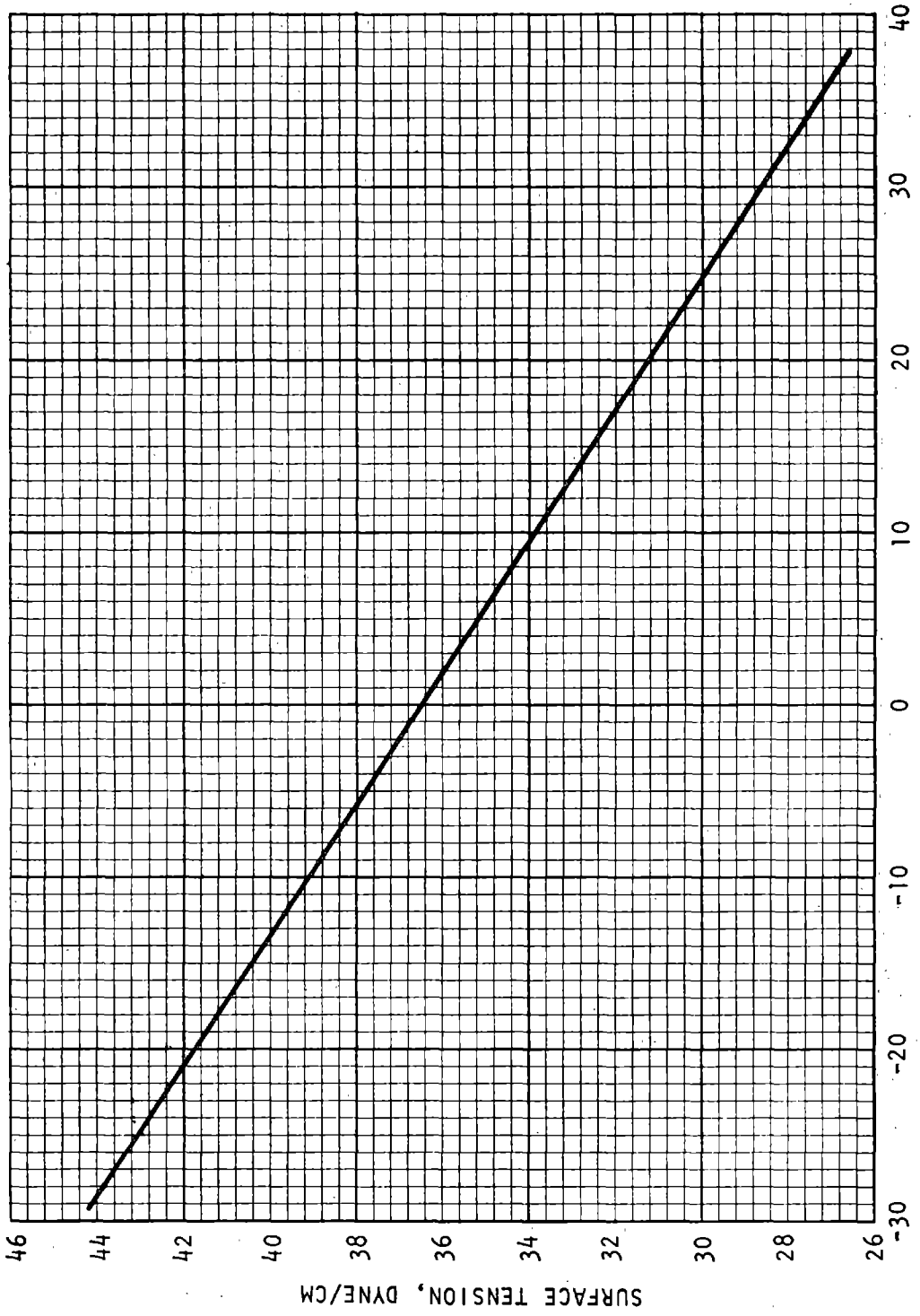

Figure A-4. Surface Tension of Saturated Liquid HDA (Ref. A-2)

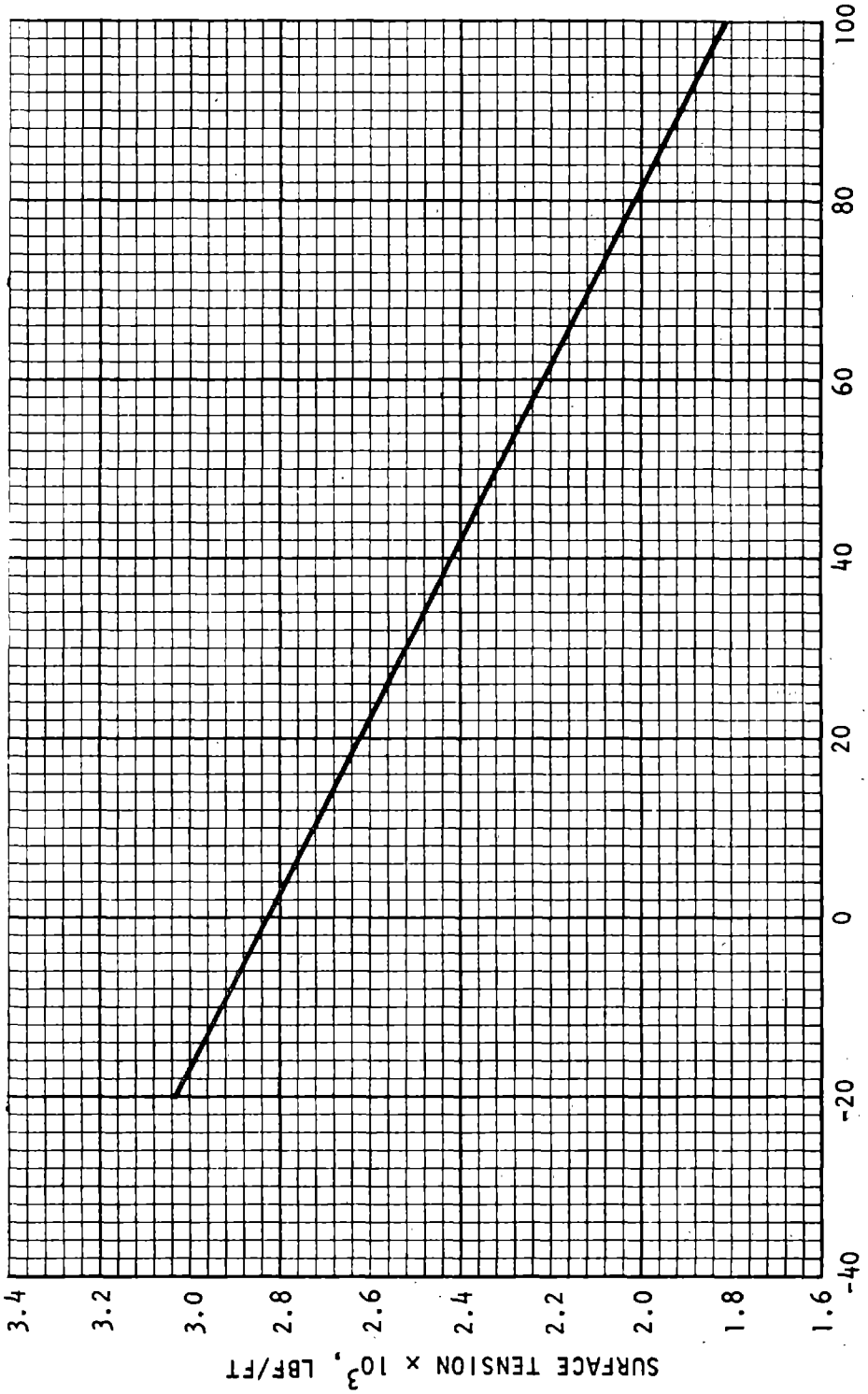

Figure A-4a. Surface Tension of Saturated Liquid HDA (Ref. A-2)

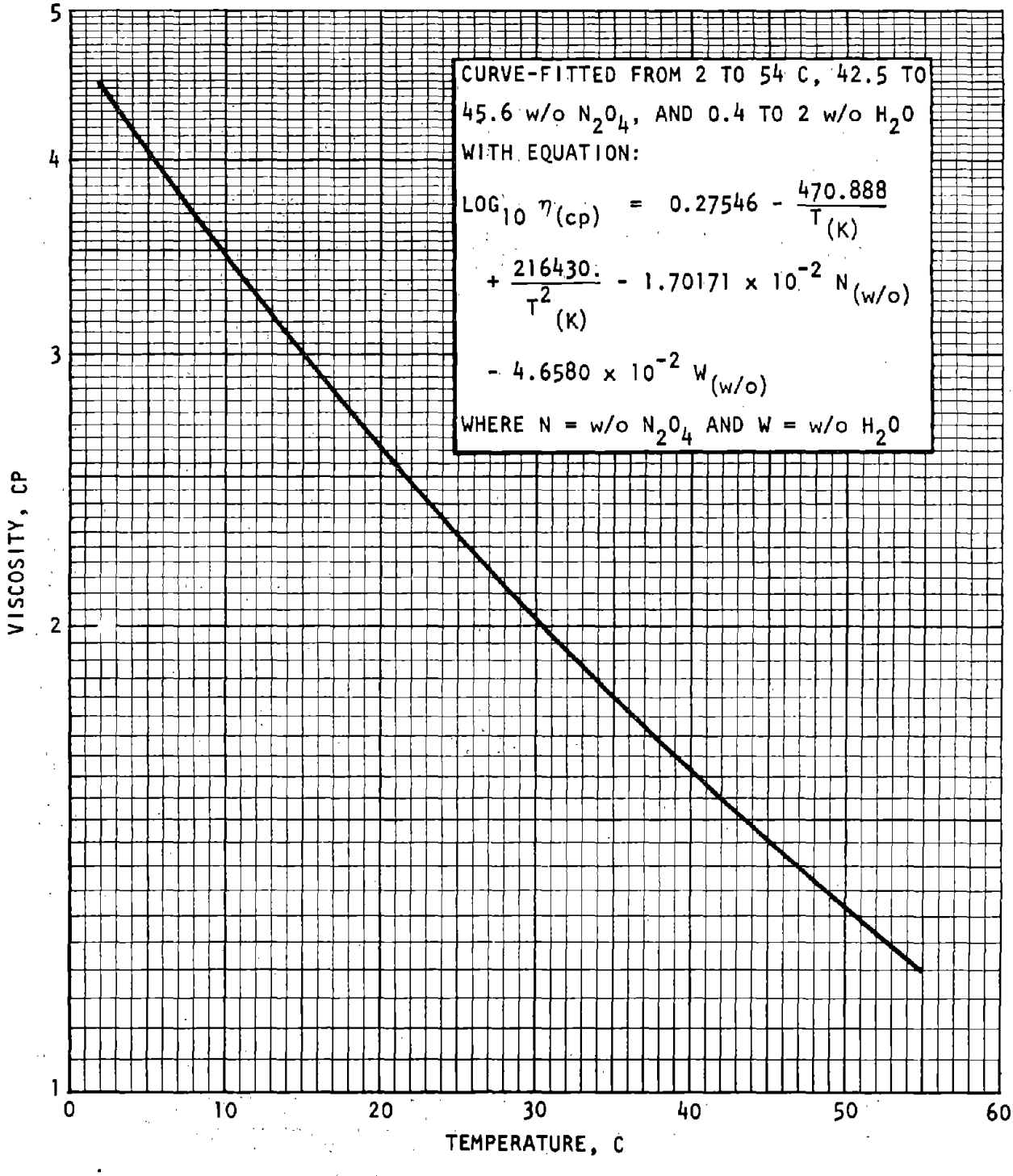

Figure A-5. Viscosity of Saturated Liquid HDA

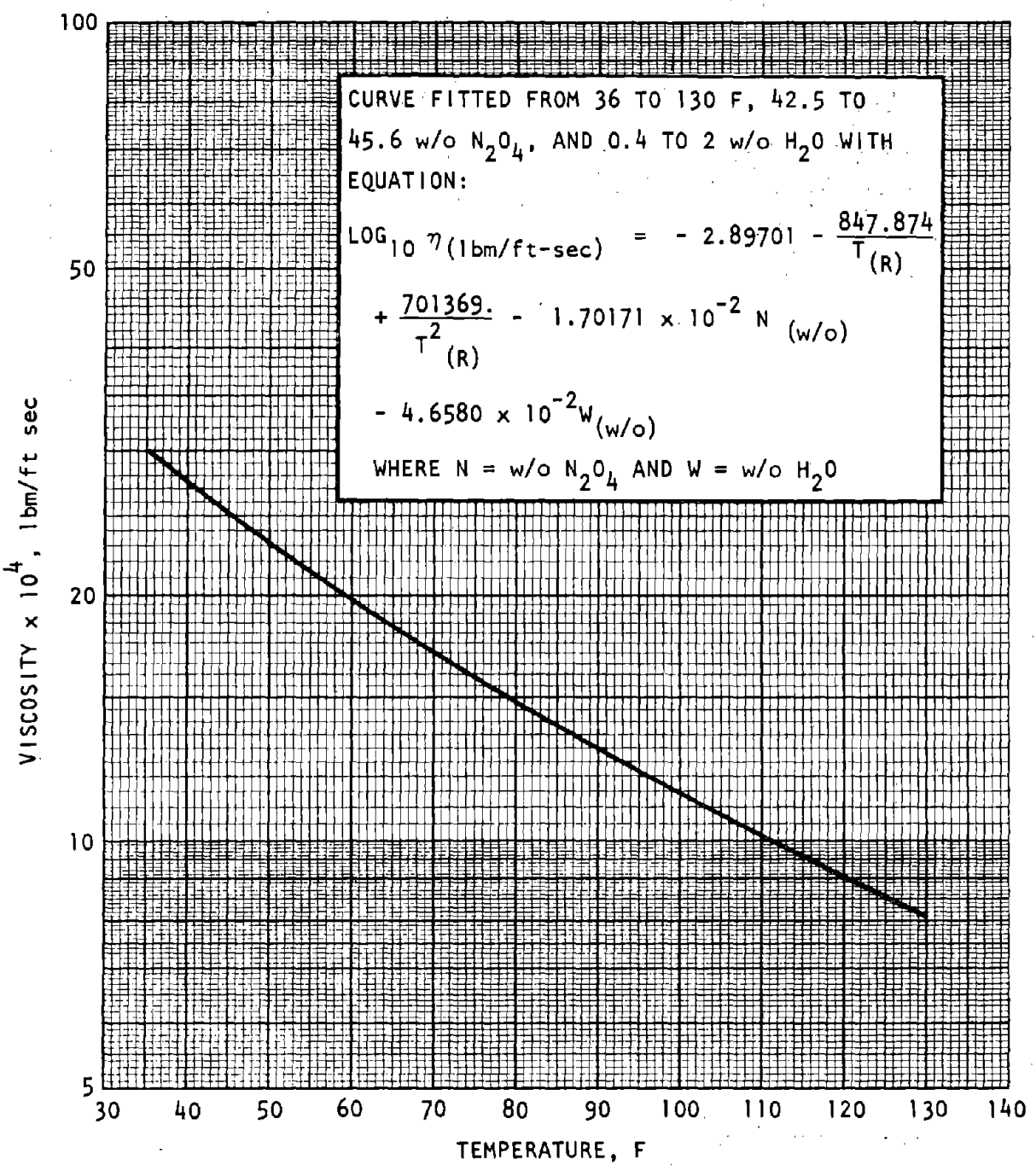

Figure A-5a. Viscosity of Saturated Liquid HDA

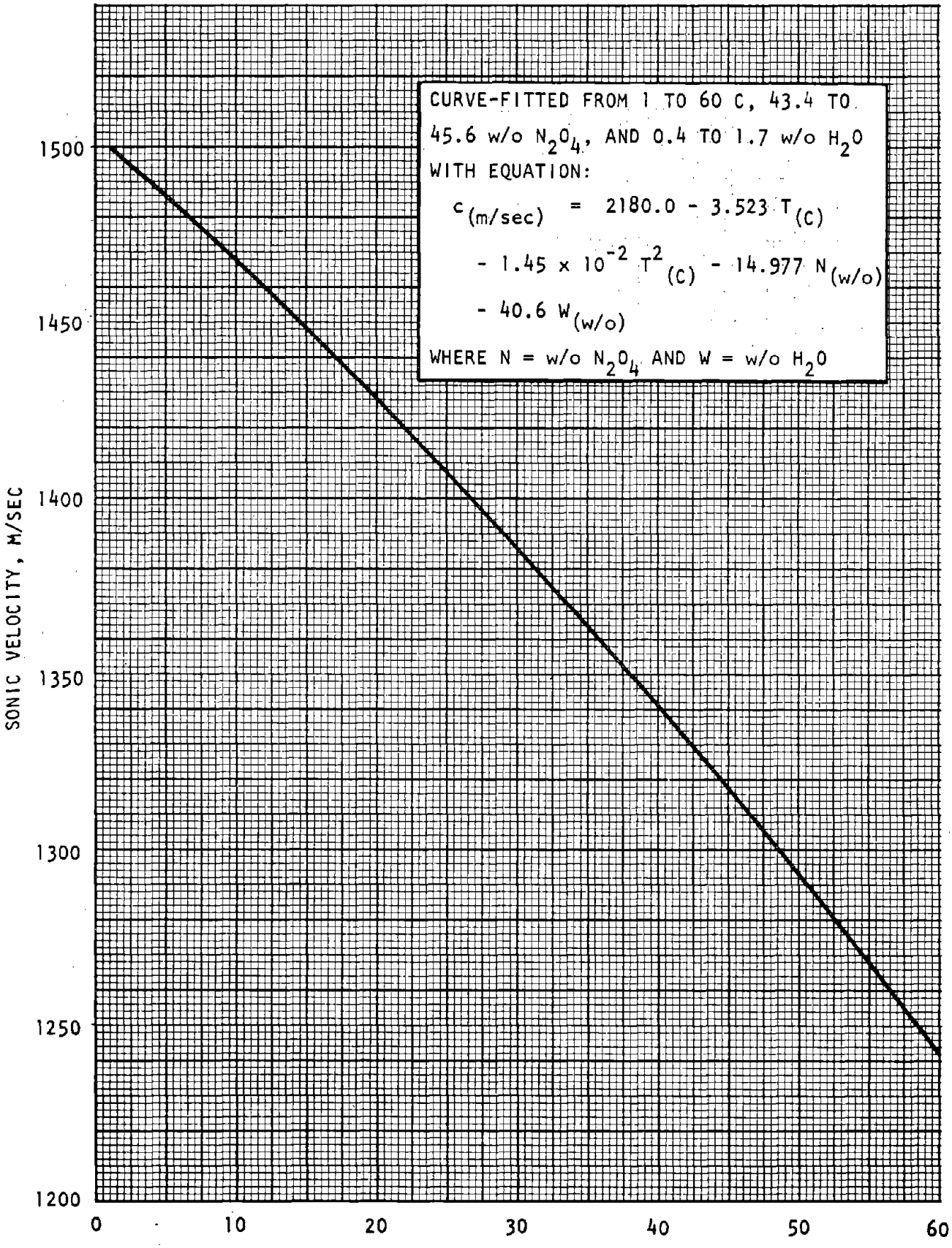

Figure A-6. Sonic Velocity of Saturated Liquid HDA

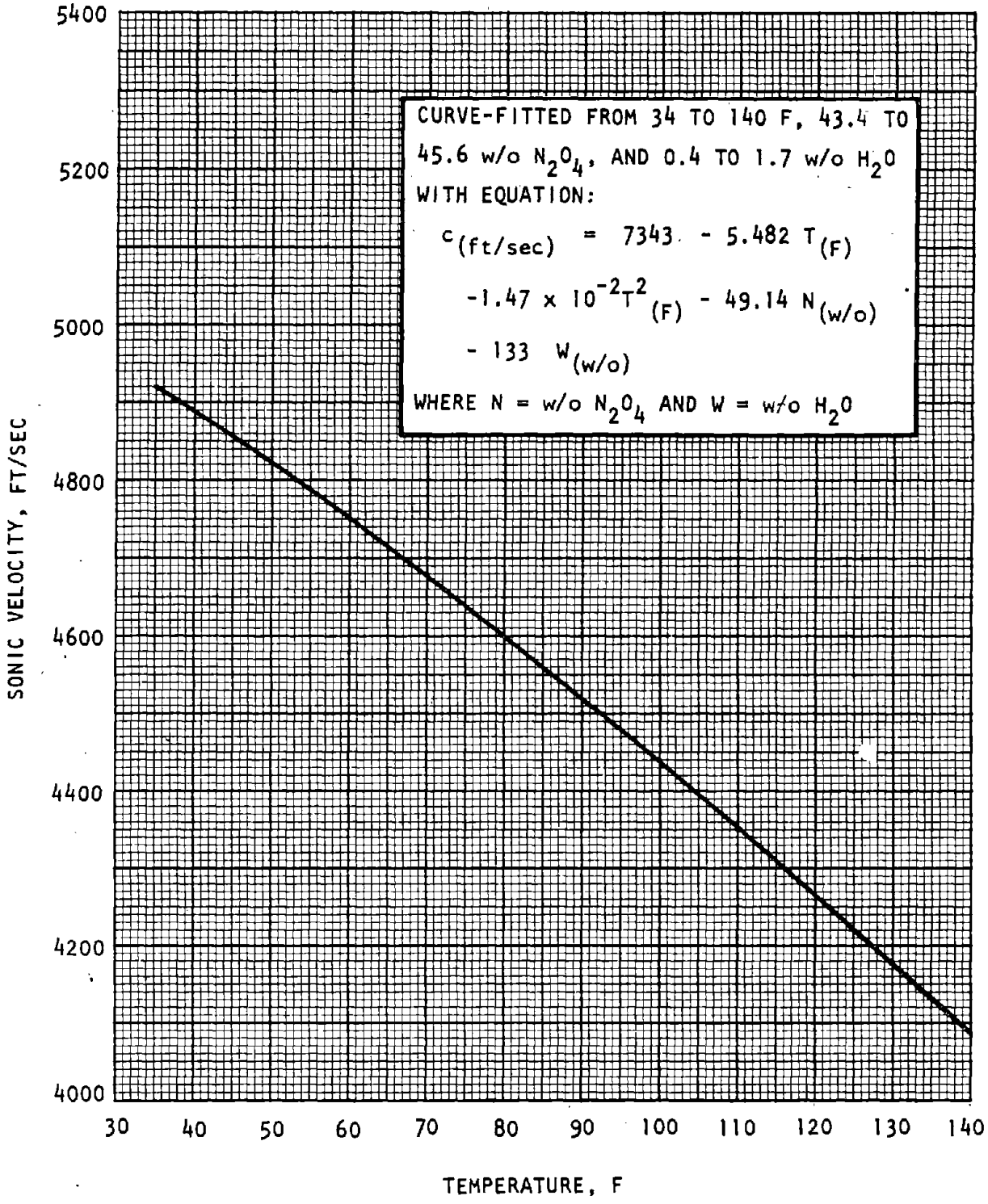

Figure A-6a. Sonic Velocity of Saturated Liquid HDA

REFERENCES

A-1. Chemical Safety Bulletin No. 6, Fuming Nitric Acids, Bell Aerospace Company, Buffalo, New York, 19 June 1970

A-2. Report 8096-910082, Model 8096 Maximum Density Acid, Engine Definition Program, Final Report, Volume II Propellant Characterization Program, Bell Aerospace Company, Buffalo, New York, 1 September 1970.

APPENDIX B

PHYSICAL PROPERTIES OF NITROUS OXIDE

Physico-chemical properties of nitrous oxide, which had been previously determined in experimental and/or analytical investigations, were evaluated and compiled during another Rocketdyne project. This project was preliminary, and its scope did not permit a complete search of the available data and information or allow the preferred practice of always going back to primary data sources, rather than using some secondary sources. Despite these limitations (and the need for a comprehensive handbook for nitrous oxide), the data are given here to assist current users of this material.

The physical and thermodynamic properties of nitrous oxide are presented in Tables B-1 through B-4 and Fig. B-1 through B-9. A brief discussion of the available properties data and analytical estimates used to prepare the tables and graphs given in this section is presented in the following paragraphs.

MELTING POINT AND TRIPLE POINT

The value of the normal melting point (182.26 K) determined in recent, carefully performed experiments (Ref. B-1) was chosen for Table B-1. Two earlier determinations agree closely with this value: 182.4 F (Ref. B-2) and 182.5 K (Ref. B-3). No measurements of the triple point were found. It is probably a few hundredths of a degree Kelvin lower than the normal melting point and is therefore shown in Table B-1 as equal to the normal melting point, expressed to one decimal place.

NORMAL BOILING POINT AND VAPOR PRESSURE

Vapor pressure data and critical compilations were taken from Ref. B-1, B-4, B-5, B-6, B-7, and B-8, all of which were in good agreement. A plot of vapor pressure versus temperature (Fig. B-1) was constructed from these correlated values. The normal boiling point given in Table B-1 was also obtained from this correlation; it agrees within 0.06 K with the individual values given in Ref. B-1, B-5, and B-6.

CRITICAL PROPERTIES

The recommended critical properties of nitrous oxide given in Table B-1 are those from Ref. B-4. The values selected in an earlier review article (Ref. B-9) were not much different (T_c = 36.5 C, P_c = 71.7 atm, ρ_c = 0.457 g/cc).

DENSITY

Reference B-4 gives good, extensive density data over fairly wide ranges of temperature and pressure. These data were used to construct Fig. B-2, along with the values from Ref. B-8 (taken from Ref. B-7) to extend the saturated vapor curve below -60 F, the generalized compressibility factors from Ref. B-10 to extend the vapor curves above +302 F, and the method of Ref. B-11 to extend the compressed liquid curves below -22 F. The saturated liquid and vapor density curves in Fig. B-2 also agree well with values given in Ref. B-12, B-13, and B-14. The saturated liquid density values given in Ref. B-8 (from Ref. B-7, which itself is a secondary source) are substantially higher than the curve in Fig. B-2, although the saturated vapor density values agree well with Fig. B-2.

GAS P-V-T PROPERTIES

Figure B-2 presents density curves for pressures of 1000 and 2000 psia. Figure B-3, Table B-2, and Table B-3 summarize experimental compressibility data for nitrous oxide from Ref. B-4.

HEATS OF FORMATION AND VAPORIZATION

Reference B-1 reports an experimental value of the heat of vaporization at the normal boiling as 3958 ±3 cal/mole. Reference B-4 gives data for heat of vaporization above -30 C. These data, plus values between -88 and -30 C estimated by the method of Ref. B-15 (using a value of the exponent which fits the experimental data) were used to prepare Fig. B-4. The heat of formation of the ideal gas given in Table B-1 was taken from Ref. B-16. This value,

corrected for non-ideality by the method of Ref. B-11 was used with the heat of vaporization from Fig. B-4 to estimate the heat of formation of the liquid at 298.15 K, as given in Table B-1.

HEAT CAPACITY

The only source of experimental data for the specific heat of solid or liquid nitrous oxide is Ref. B-1. The liquid data, which cover only the temperature range from 183.55 to 187.13 K, were used to define the low-temperature end of the saturated liquid curve in Fig. B-5. Constant pressure specific heat data for gaseous nitrous oxide are primarily derived from spectroscopic and molecular structural measurements. The values from Ref. B-16 and the recent critical review of Ref. B-17 are almost identical, and were used to define the zero pressure (ideal gas) curve in Fig. B-5. The following empirical equations, representing recommended values, are given in Ref. B-17:

$$c_p^o = 0.103451 + 4.89293 \times 10^{-4}T - 5.19278 \times 10^{-7}T^2 + 2.44839 \times 10^{-10}T^3$$

(for temperatures between 200 and 600 K)

$$c_p^o = 0.149343 + 2.67192 \times 10^{-4}T - 1.47619 \times 10^{-7}T^2 + 3.01604 \times 10^{-11}T^3$$

(for temperatures between 600 and 1500 K)

where the ideal gas heat capacity, c_p^o, is given in cal/g-K (identical to the value in Btu/lb-R) and T is in degrees Kelvin. Values of gaseous N_2O heat capacity at elevated pressures were estimated from the ideal gas values by the method of Ref. B-18. Very approximate values of heat capacity for the saturated vapor, saturated liquid, and compressed liquid were estimated from the sparse information included in Ref. B-11, and the saturated liquid curve was forced through the available experimental data near the normal boiling point. These estimates, shown as dashed curves in Fig. B-5, should be regarded as preliminary only (especially below about 300 F), and used only until more experimental data become available.

RATIO OF HEAT CAPACITIES

Good experimental data for c_p/c_v are available for a temperature of 25.3 C and pressures up to 5.3 atm (Ref. B-19). These results, extrapolated to zero pressure, agree well (0.09-percent higher) with reliable results obtained by spectroscopic methods. Reference B-20 reports comparable data for higher pressures, up to about 31 atm. Reference B-13 gives values at 1 atm pressure for several temperatures; however, these are substantially higher at 25 C (1.30 viz. 1.278) than the apparently reliable value of Ref. B-19. Consequently, the values of Ref. B-13 were not used. Figure B-6 was constructed by use of the applicable data point from Ref. B-19 and the technique of Ref. B-21 (as given in Ref. B-22). These estimates, shown as dashed curves in Fig. B-6, should be regarded as preliminary and used only until additional experimental data become available.

ENTROPY AND ENTHALPY

Figure B-7 was reproduced from Ref. B-23, as given in Ref. B-24, and was apparently developed as a part of the effort which also lead to Ref. B-4. Table B-4 gives ideal gas thermodynamic properties from Ref. B-16. Some values are also compiled in Ref. B-25.

VISCOSITY

The 14.7-psia curve in Fig. B-8 was plotted by use of the experimental data of Ref. B-26 below 540 R and the data of Ref. B-27 above 540 R. The values of viscosity at 2000 psia were estimated from the experimental 1-atm values by use of the residual viscosity correlation of Ref. B-28. No data were found for viscosity of liquid nitrous oxide, which may be due to the short normal liquid range (4.3 R). Since without experimental data liquid viscosity estimates are very unreliable, no values were generated.

THERMAL CONDUCTIVITY

No data were found for the thermal conductivity of liquid nitrous oxide. The 1-atm curve (Fig. B-9) was plotted from the recommended values of Ref. B-17 (also reported in Ref. B-29), in which the values were chosen from Ref. B-30 below about 360 K and from Ref. B-31 for higher temperatures. The only available experimental data for gaseous thermal conductivity at elevated pressures were from Ref. B-32. Unfortunately, these data at 1-atm disagree with all other data (Ref. B-17). Despite the possible negative implications for the high-pressure data of Ref. B-32, these were judged to be better than purely theoretical estimates and were used to prepare the solid portions of the high-pressure curves in Fig. B-9. These curves were extended to temperatures above 800 R by the correlation of Ref. B-33.

TABLE B-1. PHYSICAL PROPERTIES OF NITROUS OXIDE

Property	Value		Figure Number	Reference Number
	Metric	English		
General Identification				
Identification	Nitrous Oxide			1966
Molecular Formula	N_2O			Atomic Weights
Molecular Weight	44.0128			
Melting Point	182.3K (-90.9C)	328.1R (-131.6F)		B-1
Triple Point	182.3K (-90.9C)	328.1R (-131.6F)		See text
Normal Boiling Point	184.7K (-88.5C)	332.4R (-127.3F)		B-1,B-5,B-6
Critical Properties:				
Temperature	309.58K(36.43C)	557.25R(97.58F)		B-4
Pressure	71.60 atm	1052 psia		B-4
Density	0.452 g/cc	28.25 lb/ft^3		B-4
Volume	2.210 cc/g	0.0354 ft^3/lb		B-4
Z_c		0.274		
Phase Properties				
Vapor Pressure	6.80 atm at 225.0K	100 psia at -54.6F	B-1	See text
Density:				
Liquid	1.228 g/cc at NBP	76.60 lb/ft^3 at NBP	B-2	B-4
Gas	Approx. 2.8 g/l at NBP, 1.987 g/l at 273.15K, 1 atm	0.17 lb/ft^3 at NBP, 0.1235 lb/ft^3 at 32F, 1 atm	B-2	B-7
			B-2	B-24
PVT Properties (gas)	See Figures B-2 and B-3, Tables B-2 and B-3			B-4
Surface Tension	1.75 dyne/cm at 293.15K	1.00×10^{-5} lbf/in at 68F		B-34

TABLE B-1 (Continued)

Property	Value		Figure Number	Reference Number
	Metric	English		
Thermodynamic Properties				
Heats of:				
Formation				
Liquid	17.1 Kcal/mole at 298.15K	700 Btu/lb at 77F		See text
Ideal Gas	19.61 ±0.1 Kcal/mole at 298.15K	802 Btu/lb at 77F		B-16
Fusion	1.563 Kcal/mole at MP	63.9 Btu/lb at MP		B-1
Vaporization	3.958 Kcal/mole at NBP	161.9 Btu/lb at NBP	B-4	B-1
	1.543 Kcal/mole at 298.15K	63.1 Btu/lb at 77F	B-4	B-4
Heat Capacity (const.press)				
Solid	13.98 cal/mole-K at 180K	0.318 Btu/lb-F at -135.7F		B-1
Liquid	18.57 cal/mole-K at NBP	0.420 Btu/lb-F at NBP	B-5	B-1
Gas	9.230 cal/mole-K at 298.15K I.G.	0.2097 Btu/lb-F at 77F, I.G.	B-5	B-16
Ratio of Heat Capacities	1.278 at 298.15K, 1 atm	1.278 at 77F, 1atm	B-6	B-19
Entropy	See Figure B-7 and Table B-4			B-16, B-23
Enthalpy	See Figure B-7 and Table B-4			B-16, B-23
Transport Properties				
Viscosity	See text			
Liquid				
Gas	9.22×10^{-3} cp at NBP, saturated, 14.8×10^{-3} cp at 298.15K, 1 atm	6.20×10^{-6} lbm/ft-sec at NBP, saturated 9.95×10^{-6} lbm/ft-sec at 77F, 1 atm	B-8	B-26

TABLE B-1. (Concluded)

Property	Value		Figure Number	Reference Number
	Metric	English		
Thermal Conductivity				
Liquid	See text			
Gas	2.09×10^{-5} cal/sec-cm-K at NBP, saturated	5.05×10^{-3} Btu/hr-ft-F at NBP, saturated	B-9	B-17, B-29
	4.11×10^{-5} cal/sec-cm-K at 298.15K, 1 atm	9.93×10^{-3} Btu-hr-ft-F at 77F, 1 atm		
Sonic Velocity				
Gas	263 in/sec at 273.15K, 1 atm	863 ft/sec at 32F, 1 atm		B-34
Diffusion Coefficient	1.75×10^{-5} sq cm/sec at 20C (Dilute solution of gas in water)	6.8×10^{-5} sq ft/hr at 68F (Dilute solution of gas in water)		B-24
Electromagnetic Properties				
Dielectric Constant				
Liquid	1.97 at -130F (-90C)			B-36
Gas	1.001028 at 77F (20C), 1 atm			B-37
Magnetic Susceptibility	-0.429×10^{6}, c.g.s.			B-35

TABLE B-2. NITROUS OXIDE LOW PRESSURE EXPERIMENTAL COMPRESSIBILITY ISOTHERMS (REPRINTED FROM REF. B-4)

Pressure, Atm.	Volume, Liters/G. Mole	$z = PV/RT$	Pressure, Atm.	Volume, Liters/G. Mole	$z = PV/RT$
	−30° C.			30° C.	
9.9068	1.7830	0.8853	10.3712	2.2639	0.9440
7.2631	2.5233	0.9184	7.4627	3.2055	0.9614
5.2663	3.5700	0.9421	5.3329	4.5358	0.9722
3.7875	5.0511	0.9591	3.7997	6.4158	0.9800
2.7088	7.1507	0.9706	2.7013	9.0806	0.9861
1.9309	10.1163	0.9790	1.9171	12.8535	0.9903
1.3730	14.3137	0.9851	9.1635	2.5827	0.9512
			6.5720	3.6526	0.9653
8.4645	2.1310	0.9040	4.6943	5.1716	0.9757
6.1674	3.0159	0.9321	3.3415	7.3139	0.9828
4.4496	4.2665	0.9516	2.3736	10.3525	0.9879
3.1929	6.0387	0.9663	1.6826	14.6558	0.9910
2.2781	8.5445	0.9756	1.1925	20.7255	0.9938
1.6218	12.0907	0.9828	8.1798	2.9103	0.9566
1.1515	17.1071	0.9874	5.8551	4.1179	0.9691
			4.1768	5.8243	0.9782
9.5308	6.0493	0.8903	2.9719	8.2477	0.9850
6.9747	2.6372	0.9220	2.1082	11.6631	0.9887
			1.4958	16.5087	0.9927
	−15° C.			60° C.	
8.3072	2.3524	0.9228	8.0016	3.2029	0.9665
6.0117	3.3298	0.9450	5.7136	4.5324	0.9766
4.3174	4.7096	0.9603	4.0644	6.4139	0.9831
3.0877	6.6684	0.9719	2.8868	9.0761	0.9881
2.2003	9.4325	0.9800	2.0474	12.8424	0.9916
1.5641	13.3499	0.9858	9.9677	2.5479	0.9578
1.1094	18.8947	0.9895	7.1362	3.6054	0.9703
10.3084	1.8566	0.9035	5.0900	5.1022	0.9794
7.5104	2.6272	0.9315	3.6187	7.2199	0.9853
5.4196	3.7169	0.9511	2.5682	10.2167	0.9895
3.8861	5.2597	0.9651	1.8207	14.4562	0.9926
2.7744	7.4451	0.9750	8.9511	2.8409	0.9620
1.9754	10.5329	0.9824	6.3966	4.0327	0.9728
1.4032	14.9050	0.9874	4.5573	5.7068	0.9808
			3.2382	8.0750	0.9861
	0° C.		2.2983	11.4267	0.9904
8.2453	2.5483	0.9376	1.6289	16.1693	0.9933
5.9366	3.6075	0.9553			
4.2546	5.1048	0.9688		75° C.	
3.0348	7.2234	0.9778	10.0417	2.7527	0.9676
2.1572	10.2198	0.9836	7.1621	3.8951	0.9765
1.5318	14.4596	0.9884	5.0969	5.5120	0.9834
1.0868	20.4673	0.9922	3.6203	7.7996	0.9884
			2.5668	11.0376	0.9917
9.8028	2.1157	0.9253			
7.0882	2.9934	0.9468		100° C.	
5.0916	4.2372	0.9623	8.6398	3.4614	0.9767
3.6386	5.9953	0.9732	6.1473	4.8982	0.9834
2.5932	8.4844	0.9814	4.3685	6.9313	0.9880
1.8429	12.0034	0.9870	3.0957	9.8079	0.9916
1.3068	16.9812	0.9904	2.1934	13.8788	0.9942
			10.3202	2.8871	0.9731
	15° C.		7.3534	4.0853	0.9811
8.2859	2.7016	0.9467	5.2246	5.7809	0.9864
5.9522	3.8237	0.9623	3.7068	8.1810	0.9904
4.2565	5.4079	0.9738	2.6271	11.5758	0.9932
3.0308	7.6565	0.9812			
2.1535	10.8305	0.9866		125° C.	
1.5284	15.3251	0.9908	7.9811	4.0255	0.9834
1.0841	21.6982	0.9945	5.6682	5.6964	0.9883
			4.0172	8.0603	0.9911
10.2745	2.1489	0.9341	2.8473	11.4066	0.9941
7.4117	3.0409	0.9535	2.0157	16.1399	0.9958
5.3119	4.3046	0.9670			
3.7910	6.0891	0.9766		150° C.	
2.6990	8.6173	0.9838	8.1284	4.2106	0.9857
1.9161	12.1931	0.9884	5.7692	5.9583	0.9900
1.3581	17.2573	0.9914	4.0878	8.4320	0.9927
0.9622	24.4282	0.9938	2.8967	11.9317	0.9954
			2.0520	16.8840	0.9978
9.1777	2.4280	0.9424			
6.6021	3.4365	0.9593	9.7801	3.4928	0.9838
4.7224	4.8617	0.9710	6.9447	4.9428	0.9886
3.3669	6.8812	0.9796	4.9243	6.9947	0.9920
2.3927	9.7320	0.9851	3.4873	9.8971	0.9940
1.6988	13.7796	0.9898	2.4711	14.0050	0.9967
1.2047	19.4842	0.9932	1.7492	19.8187	0.9984

TABLE B-3. SMOOTHED COMPRESSIBILITY DATA FOR GASEOUS NITROUS OXIDE (REPRINTED FROM REF. B-4)

Pressure, Atm.	Vol., Ml./G.	$z = PV/RT$	Pressure, Atm.	Vol., Ml./G.	$z = PV/RT$	Pressure, Atm.	Vol., Ml./G.	$z = PV/RT$	Pressure, Atm.	Vol., Ml./G.	$z = PV/RT$
	−30° C.			15° C.			36.45° C.			40° C.	
6	70.533	0.9336	6	86.201	0.9628	25	20.074	0.8695	68	4.610	0.5370
7	59.686	0.9217	8	63.811	0.9503	30	16.144	0.8391	70	4.234	0.5077
8	51.540	0.9096	10	50.351	0.9373	35	13.313	0.8073	72	3.838	0.4733
9	45.179	0.8970	12	41.350	0.9237	40	11.158	0.7733	74	3.377	0.4281
10	40.058	0.8837	15	32.331	0.9028	45	9.450	0.7368	76	2.758	0.3591
11	35.848	0.8699	20	23.266	0.8662	50	8.045	0.6969	78	1.955	0.2612
12	32.301	0.8551	25	17.774	0.8272	55	6.843	0.6521	80	1.737	0.2380
	−15° C.		30	14.035	0.7838	60	5.776	0.6004	85	1.[illegible]	0.2294
			35	11.281	0.7350	65	4.752	0.5352	90	1.506	0.2321
6	75.903	0.9463	40	9.131	0.6799	68	4.098	0.4828			
8	55.796	0.9275	42	8.362	0.6538	70	3.555	0.4312		44° C.	
10	43.674	0.9075	44	7.628	0.6248	71	3.173	0.3903			
12	35.557	0.8866		30° C.		72	1.792	0.2235	68	5.039	0.5795
14	29.725	0.8647				74	1.636	0.2097	70	4.715	0.5582
15	27.377	0.8533	6	91.243	0.9687	76	1.567	0.2063	72	4.386	0.5341
16	25.317	0.8417	8	67.691	0.9582	78	1.527	0.2063	74	4.059	0.5080
18	21.876	0.8182	10	53.537	0.9473	80	1.498	0.2076	76	3.722	0.4784
20	19.019	0.7904	12	44.096	0.9363	90	1.409	0.2197	78	3.360	0.4432
	0° C.		15	34.629	0.9191	100	1.3547	0.2347	80	2.969	0.4017
			20	25.132	0.8894	120	1.2913	0.2685	82	2.526	0.3503
6	81.102	0.9556	25	19.403	0.8583	140	1.2[illegible]	0.3030	85	2.000	0.2875
8	59.840	0.9401	30	15.532	0.8245	160	1.21[illegible]	0.3371	90	1.705	0.2595
10	47.062	0.9242	35	12.738	0.7889	180	1.1906	0.3713	95	1.592	0.2558
12	38.510	0.9075	40	10.614	0.7512	200	1.1695	0.4052	100	1.626	0.2581
15	29.922	0.8814	45	8.895	0.7083	220	1.1512	0.4388	105	1.479	0.2627
20	21.268	0.8353	50	7.467	0.6606	240	1.1354	0.4721	110	1.443	0.2685
25	16.959	0.7835	55	6.204	0.6038	260	1.1215	0.5052			
28	13.633	0.7496	58	5.470	0.5614	280	1.1086	0.5378			
29	12.934	0.7366	60	4.964	0.5270	300	1.0967	0.5700			
30	12.266	0.7226	62	4.391	0.4817	315	1.0886	0.5941			

	50° C.		75° C.			100° C.		125° C.		150° C.	
Pressure, Atm.	Vol., ml./g.	$z = PV/RT$	Vol., ml./g.	$z = PV/RT$	Pressure, Atm.	Vol., ml./g.	$z = PV/RT$	Vol., ml./g.	$z = PV/RT$	Vol., ml./g.	$z = PV/RT$
8	72.797	0.9667	79.053	0.9744	8	85.225	0.9801	91.343	0.9845	97.423	0.9880
10	57.719	0.9581	62.808	0.9677	10	67.818	0.9749	72.785	0.9806	77.694	0.9849
15	37.580	0.9357	41.140	0.9508	15	44.609	0.9619	48.018	0.9704	51.381	0.9770
20	27.498	0.9129	30.287	0.9333	20	32.998	0.9467	35.617	0.9597	38.196	0.9684
30	17.344	0.8637	19.408	0.8971	30	21.352	0.9208	23.215	0.9383	25.020	0.9515
40	12.208	0.8106	13.945	0.8594	40	15.522	0.8925	17.001	0.9162	18.424	0.9342
50	9.070	0.7528	10.644	0.8200	50	12.012	0.8634	13.273	0.8941	14.468	0.9170
60	6.905	0.6877	8.421	0.7785	60	9.668	0.8339	10.789	0.8721	11.834	0.9001
70	5.254	0.6105	6.815	0.7350	70	7.990	0.8040	9.017	0.8503	9.955	0.8834
80	3.562	0.5129	5.592	0.6593	80	6.728	0.7737	7.688	0.8286	8.551	0.8672
90	2.559	0.3823	4.622	0.6409	90	5.745	0.7433	6.656	0.8071	7.460	0.8511
100	1.824	0.3028	3.835	0.5909	100	4.961	0.7131	5.833	0.7858	6.591	0.8355
110	1.613	0.2945	3.197	0.5419	110	4.321	0.6833	5.163	0.7651	5.883	0.8204
120	1.513	0.3014	2.692	0.4977	120	3.793	0.6543	4.611	0.7454	5.297	0.8058
130	1.449	0.3127	2.320	0.4648	130	3.359	0.6278	4.149	0.7266	4.805	0.7919
140	1.404	0.3263	2.064	0.4452	140	3.002	0.6041	3.760	0.7092	4.390	0.7791
150	1.368	0.3407	1.886	0.4359	150	2.709	0.5841	3.430	0.6932	4.033	0.7669
160	1.339	0.3557	1.763	0.4346	160	2.472	0.5685	3.152	0.6795	3.729	0.7563
170	1.315	0.3710	1.674	0.4384	170	2.281	0.5574	2.914	0.6675	3.465	0.7468
180	1.293	0.3863	1.607	0.4456	180	2.129	0.5508	2.714	0.6581	3.235	0.7381
190	1.274	0.4018	1.552	0.4543	190	2.008	0.5484	2.543	0.6509	3.035	0.7310
200	1.258	0.4176	1.508	0.4647	200	1.908	0.5486	2.396	0.6457	2.861	0.7254
220	1.230	0.4492	1.440	0.4882	220	1.757	0.5557	2.164	0.6414	2.576	0.7183
240	1.207	0.4808	1.388	0.5132	240	1.652	0.5698	1.992	0.6440	2.353	0.7159
260	1.188	0.5106	1.349	0.5404	260	1.573	0.5878	1.862	0.6522	2.178	0.7179
280	1.170	0.5438	1.317	0.5682	280	1.510	0.6080	1.761	0.6643	2.038	0.7235
300	1.154	0.5746	1.287	0.5949	300	1.462	0.6304	1.681	0.6795	1.928	0.7334
315	1.145	0.5987	1.266	0.6144	315	1.428	0.6468	1.632	0.6928	1.860	0.7429

TABLE B-4. IDEAL GAS THERMODYNAMIC PROPERTIES OF NITROUS OXIDE

DINITROGEN MONOXIDE (N_2O) (REPRINTED FROM REF. B-16)

(Ideal Gas) Molecular Weight = 44.016 (1959 Atomic Weights)

T, °K.	cal. mole^{-1}deg.$^{-1}$			kcal. mole^{-1}			
	C_p°	S°	$-(F^\circ-H^\circ_{298})/T$	$H^\circ-H^\circ_{298}$	ΔH_f°	ΔF_f°	Log K_p
0	.000	.000	INFINITE	- 2.290	20.430	20.430	INFINITE
100	7.015	43.988	59.924	- 1.594	20.084	21.573	- 47.145
200	8.033	49.108	53.353	- .849	19.786	23.185	- 25.334
298	9.230	52.546	52.546	.000	19.610	24.896	- 18.248
300	9.250	52.609	52.546	.017	19.608	24.928	- 18.159
400	10.201	55.400	52.921	.992	19.530	26.716	- 14.596
500	10.953	57.761	53.659	2.051	19.520	28.514	- 12.463
600	11.565	59.813	54.517	3.178	19.558	30.311	- 11.040
700	12.070	61.635	55.406	4.360	19.623	32.097	- 10.021
800	12.486	63.275	56.289	5.589	19.710	33.873	- 9.253
900	12.830	64.766	57.149	6.855	19.810	35.638	- 8.654
1000	13.113	66.134	57.980	8.155	19.920	37.391	- 8.171
1100	13.348	67.394	58.779	9.476	20.036	39.132	- 7.774
1200	13.544	68.565	59.547	10.821	20.158	40.863	- 7.442
1300	13.707	69.655	60.283	12.184	20.279	42.583	- 7.158
1400	13.845	70.676	60.989	13.562	20.404	44.293	- 6.914
1500	13.961	71.635	61.667	14.952	20.530	45.996	- 6.701
1600	14.060	72.540	62.319	16.353	20.657	47.691	- 6.514
1700	14.145	73.395	62.945	17.764	20.783	49.377	- 6.347
1800	14.218	74.205	63.548	19.182	20.908	51.054	- 6.198
1900	14.282	74.976	64.130	20.607	21.032	52.728	- 6.065
2000	14.337	75.710	64.690	22.038	21.155	54.392	- 5.943
2100	14.385	76.411	65.232	23.474	21.277	56.049	- 5.833
2200	14.428	77.081	65.755	24.915	21.396	57.703	- 5.732
2300	14.466	77.723	66.262	26.359	21.513	59.350	- 5.639
2400	14.499	78.339	66.752	27.808	21.630	60.993	- 5.554
2500	14.529	78.932	67.228	29.259	21.742	62.630	- 5.475
2600	14.556	79.502	67.689	30.713	21.853	64.262	- 5.401
2700	14.580	80.052	68.137	32.170	21.962	65.894	- 5.333
2800	14.602	80.583	68.572	33.629	22.069	67.517	- 5.270
2900	14.621	81.095	68.995	35.090	22.174	69.140	- 5.210
3000	14.639	81.591	69.406	36.553	22.275	70.757	- 5.154
3100	14.655	82.072	69.807	38.018	22.376	72.371	- 5.102
3200	14.670	82.537	70.198	39.484	22.473	73.981	- 5.052
3300	14.684	82.989	70.579	40.952	22.568	75.591	- 5.006
3400	14.696	83.427	70.950	42.421	22.661	77.196	- 4.962
3500	14.707	83.853	71.313	43.891	22.752	78.797	- 4.920
3600	14.718	84.268	71.667	45.363	22.841	80.400	- 4.881
3700	14.727	84.671	72.013	46.835	22.928	81.995	- 4.843
3800	14.736	85.064	72.351	48.308	23.013	83.591	- 4.807
3900	14.745	85.447	72.682	49.782	23.097	85.183	- 4.773
4000	14.752	85.820	73.006	51.257	23.177	86.774	- 4.741
4100	14.760	86.185	73.323	52.733	23.257	88.365	- 4.710
4200	14.766	86.541	73.633	54.209	23.334	89.951	- 4.680
4300	14.772	86.888	73.937	55.686	23.411	91.537	- 4.652
4400	14.778	87.228	74.236	57.163	23.485	93.120	- 4.625
4500	14.784	87.560	74.528	58.641	23.558	94.703	- 4.599
4600	14.789	87.885	74.815	60.120	23.630	96.288	- 4.574
4700	14.794	88.203	75.096	61.599	23.700	97.860	- 4.550
4800	14.798	88.515	75.373	63.079	23.768	99.441	- 4.527
4900	14.802	88.820	75.644	64.559	23.836	101.011	- 4.505
5000	14.806	89.119	75.911	66.039	23.902	102.590	- 4.484
5100	14.810	89.412	76.172	67.520	23.966	104.156	- 4.463
5200	14.814	89.700	76.430	69.001	24.030	105.733	- 4.444
5300	14.817	89.982	76.683	70.483	24.092	107.305	- 4.425
5400	14.820	90.259	76.932	71.965	24.154	108.872	- 4.408
5500	14.823	90.531	77.176	73.447	24.213	110.446	- 4.388
5600	14.826	90.798	77.417	74.929	24.272	112.010	- 4.371
5700	14.829	91.060	77.654	76.412	24.329	113.575	- 4.354
5800	14.831	91.318	77.888	77.895	24.386	115.142	- 4.338
5900	14.834	91.572	78.117	79.378	24.441	116.706	- 4.323
6000	14.836	91.821	78.344	80.862	24.495	118.267	- 4.308

Dec. 31, 1960; Dec. 31, 1964

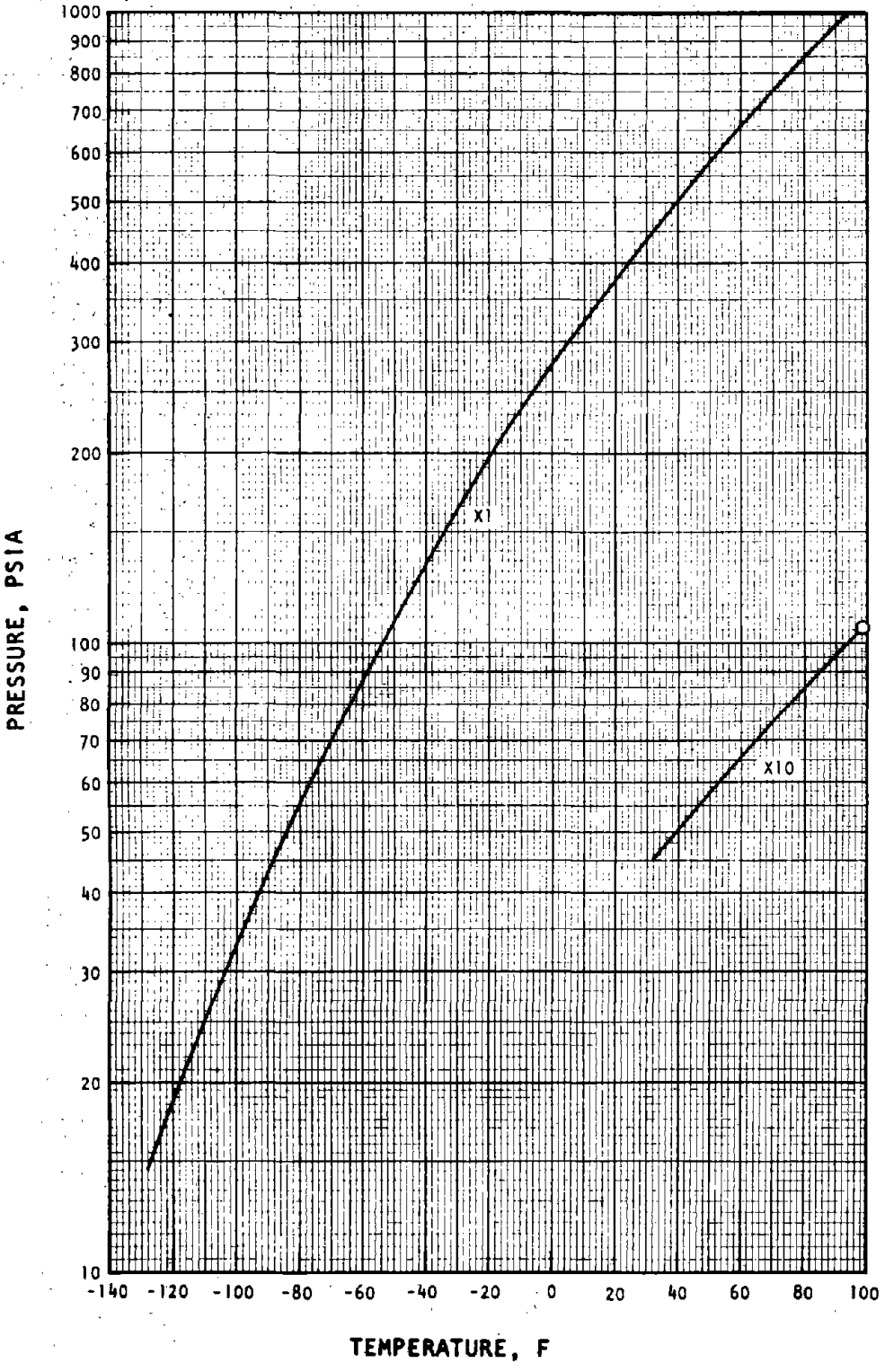

Figure B-1. Vapor Pressure of N_2O

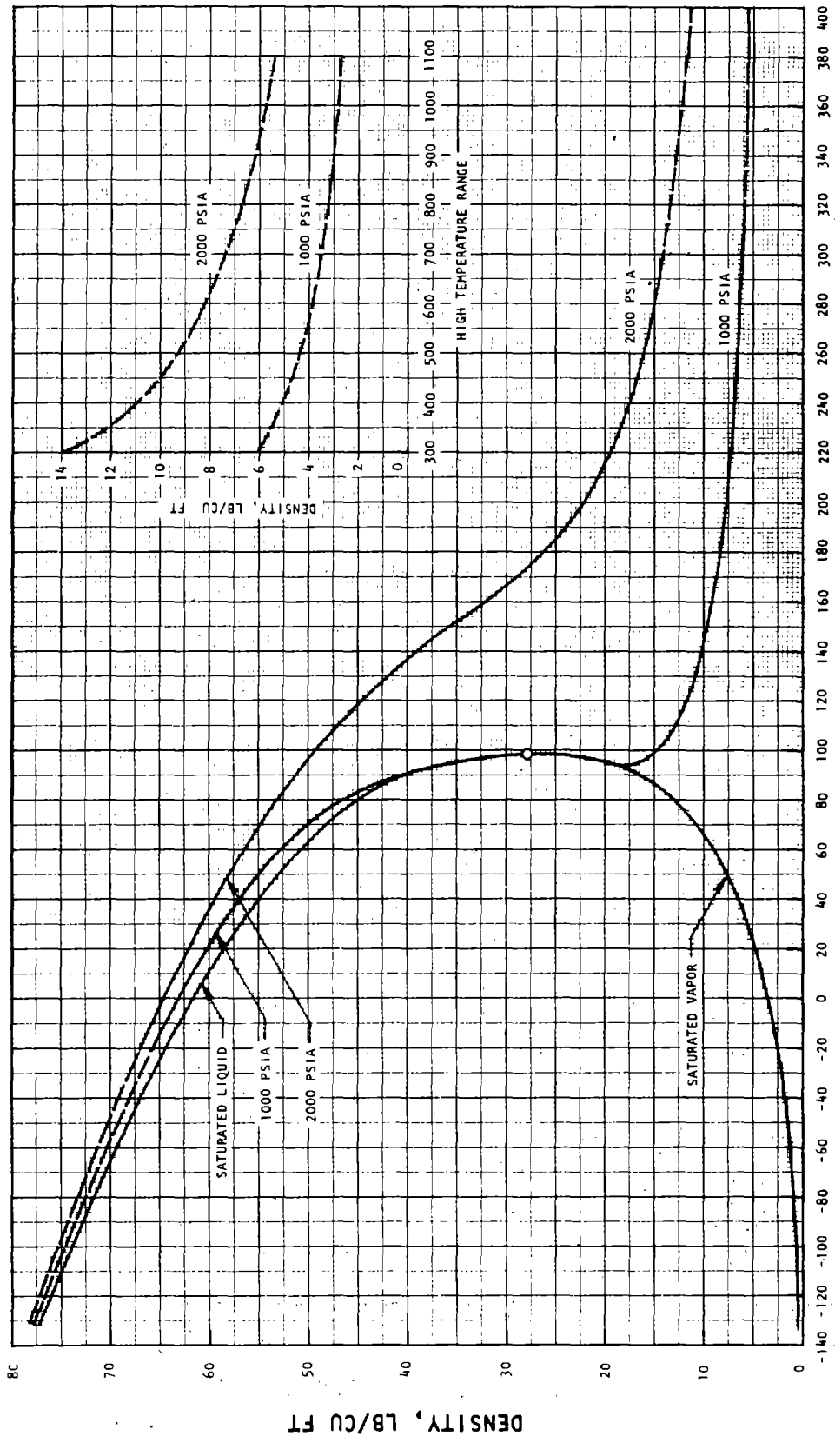

Figure B-2. Density of N_2O Liquid and Vapor

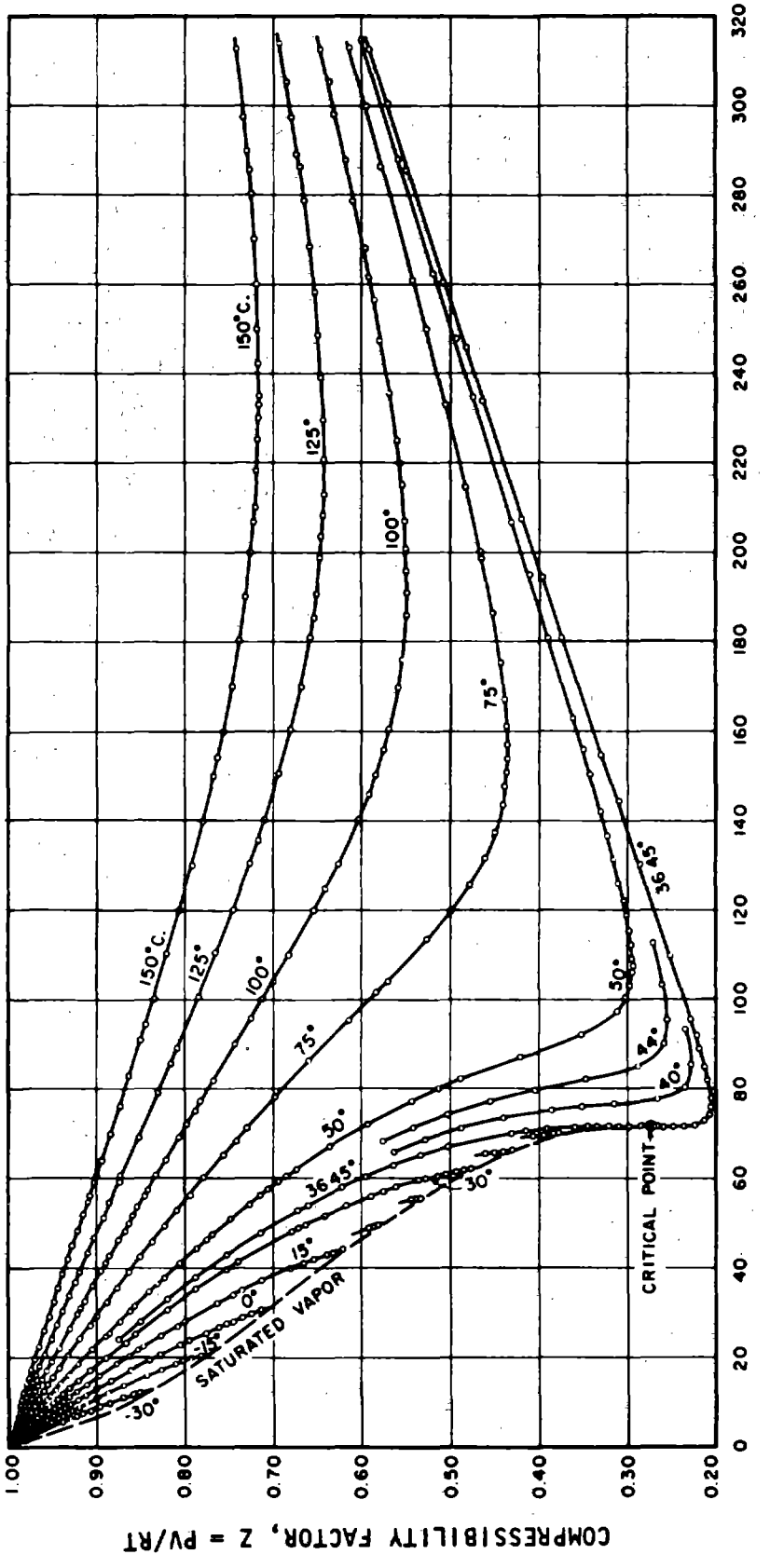

Figure B-3. Compressibility Factors of Nitrous Oxide (Reprinted from Ref. B-4)

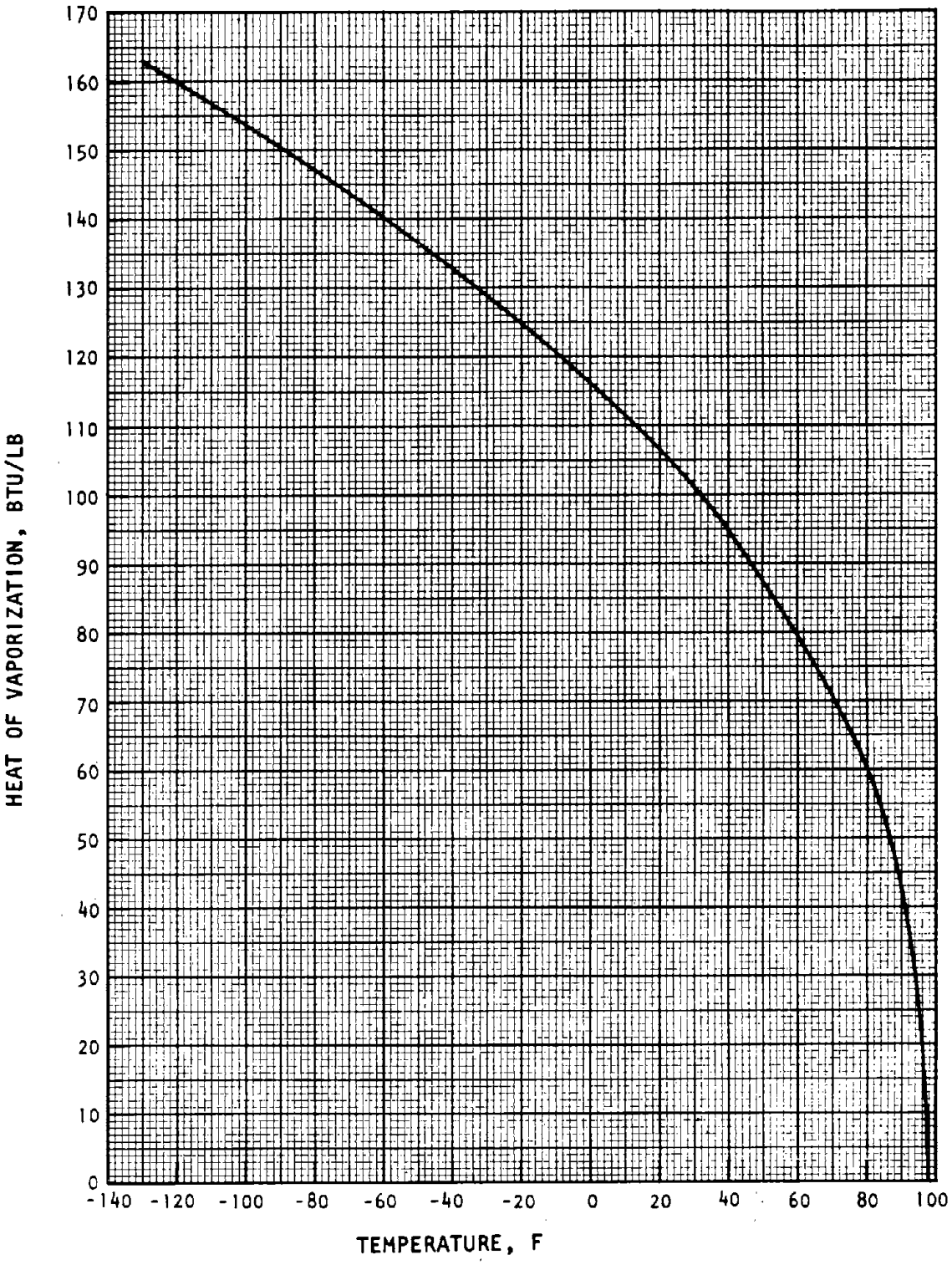

Figure B-4. Latent Heat of Vaporization of N_2O

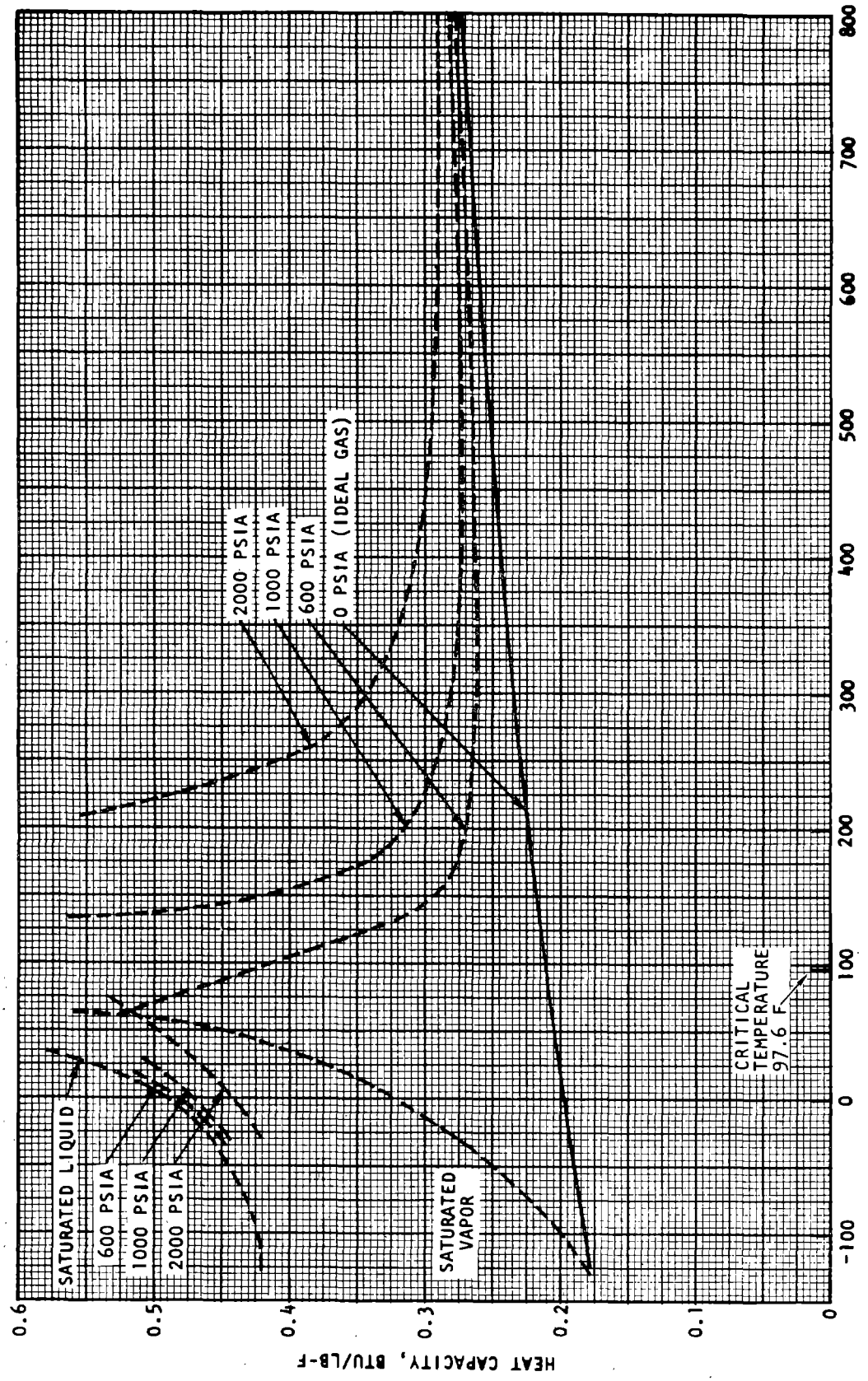

Figure B-5. Heat Capacity at Constant Pressure of Nitrous Oxide

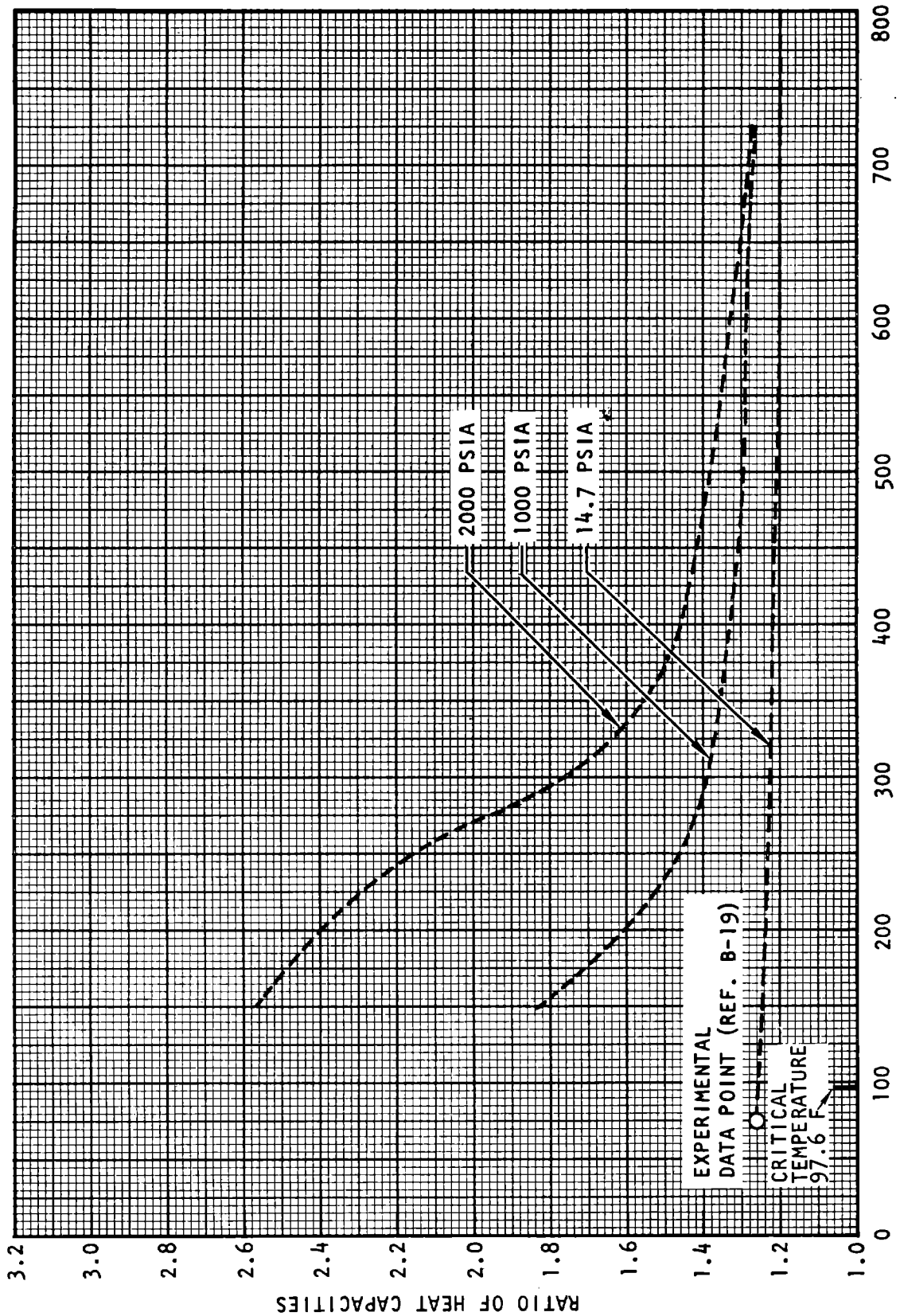

Figure B-6. Ratio of Heat Capacities, C_p/C_v, for Nitrous Oxide

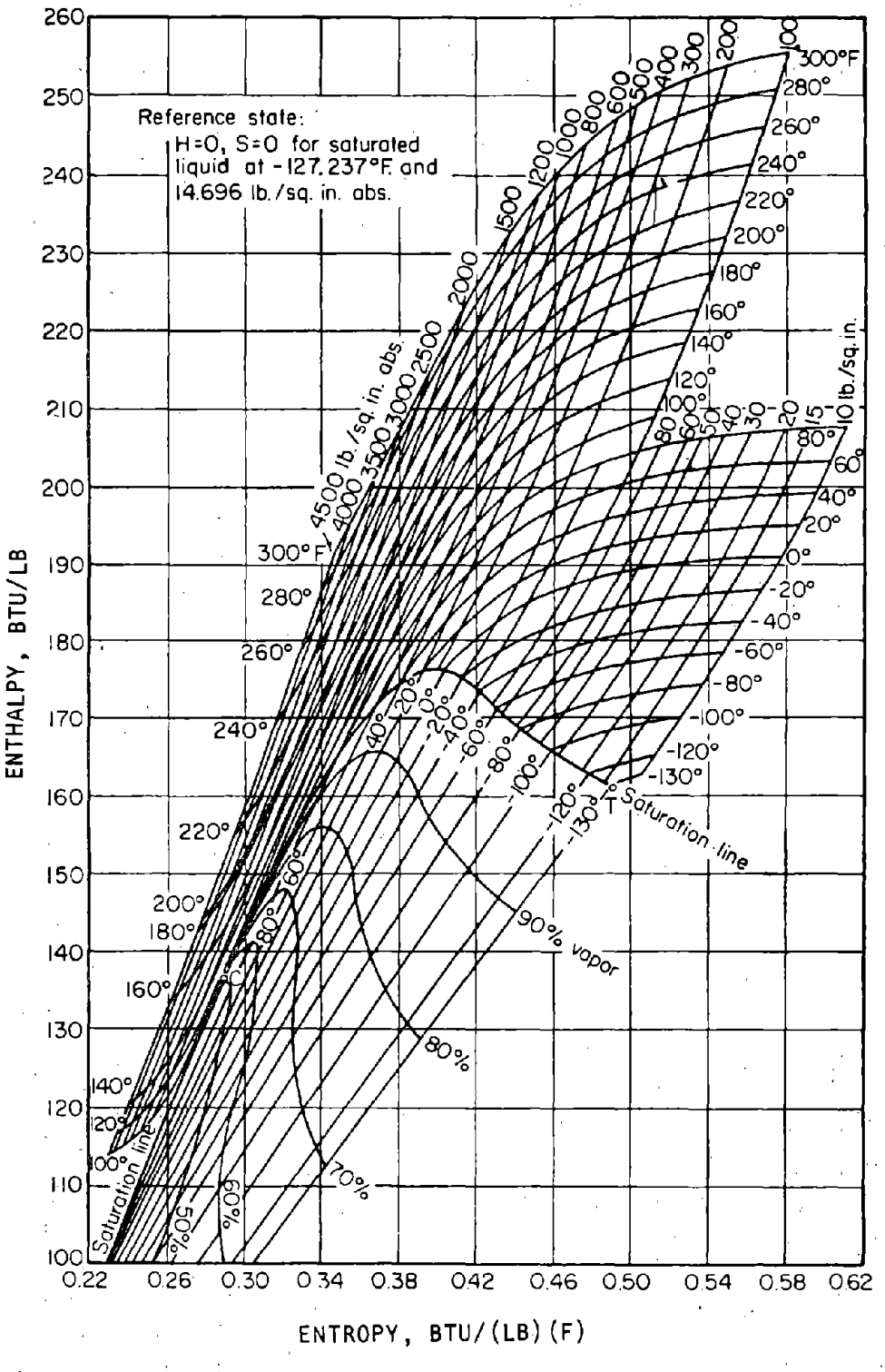

Figure B-7. Enthalpy-Entropy Diagram for Nitrous Oxide (Reprinted from Ref. B-23, as given in Ref. B-24)

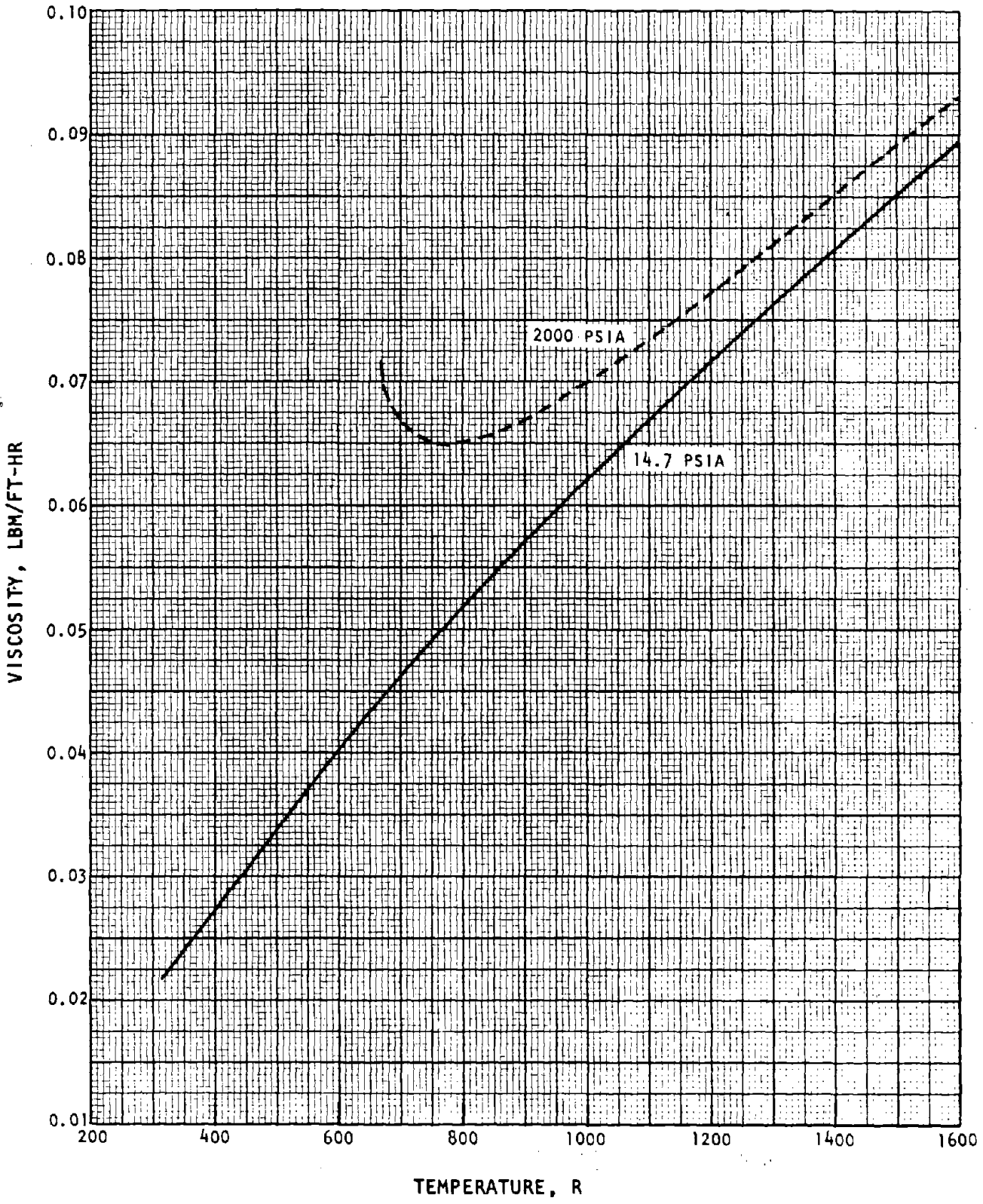

Figure B-8. Viscosity of Gaseous Nitrous Oxide

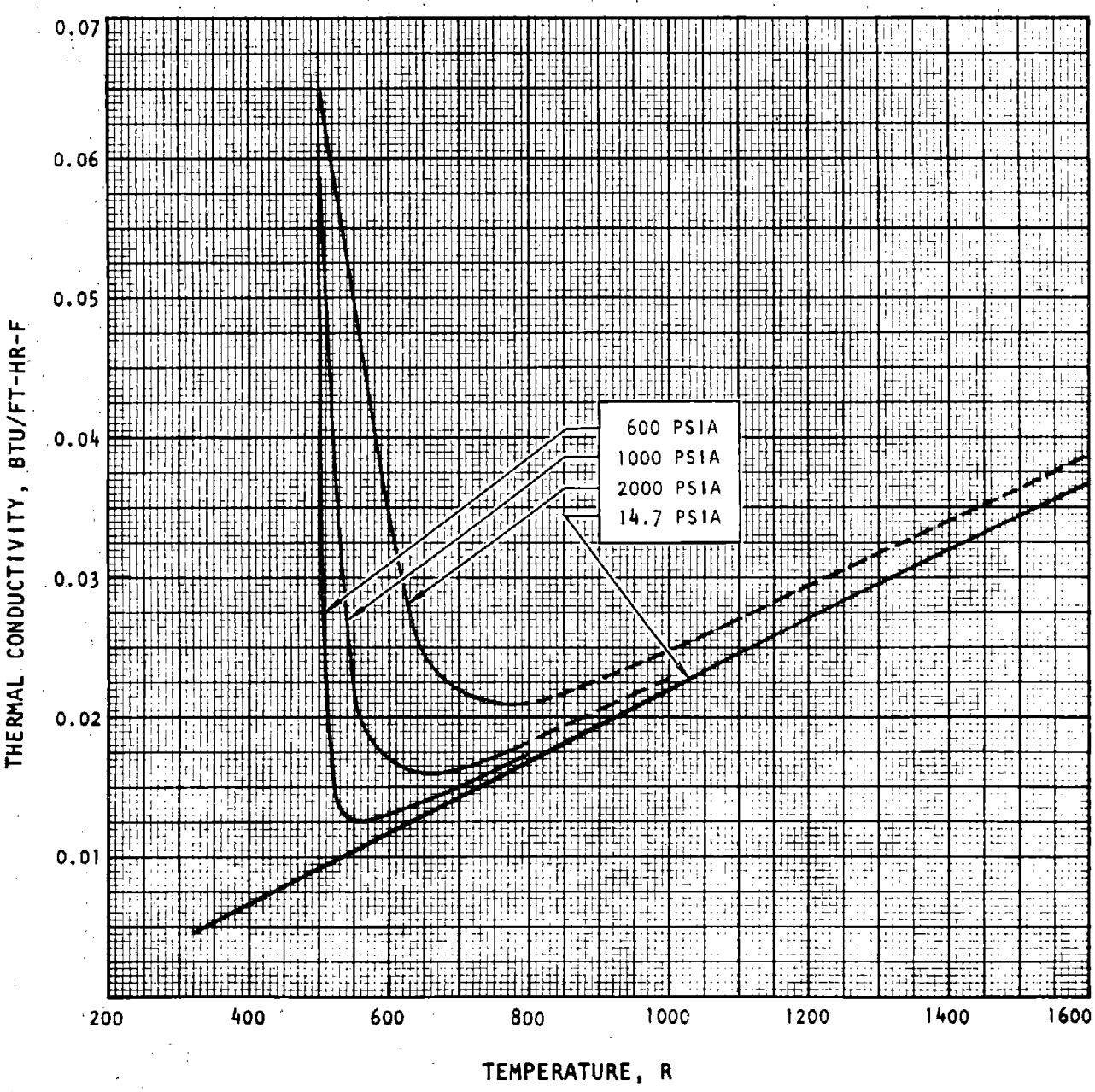

Figure B-9. Thermal Conductivity of Gaseous Nitrous Oxide

REFERENCES

B-1. Blue, R. W., and W. F. Giauque, "The Heat Capacity and Vapor Pressure of Solid and Liquid Nitrous Oxide. The Entropy from its Band Spectrum," J. Amer. Chem. Soc., 57, 991 (1935).

B-2. Clusius, Hiller, and Vaughen, Z. physik, Chem., B8, 427 (1930).

B-3. Burrell and Robertson, J. Amer. Chem. Soc., 37, 2691 (1915).

B-4. Couch, E. J., K. A. Kobe, and L. J. Hirth, "Volumetric Behavior of Nitrous Oxide," J. of Chem. and Eng. Data, 6(2), 229 (April 1961).

B-5. Hoge, H. J., J. Res. Nat. Bur. Standards, 34, 281 (1945).

B-6. Stull, D. R., "Vapor Pressure of Pure Substances," Ind. and Engr. Chem. 39, 517 (April 1947).

B-7. Regrigerating Data Book, A.S.R.E., 1957.

B-8. Matheson Gas Data Book, The Matheson Company, Inc., Newark, California, 4th Edition, 1966.

B-9. Kobe, K. A., and R. E. Lynn, Jr., "The Critical Properties of Elements and Compounds," Chem. Rev., 52, 117 (1953).

B-10. Viswanath, D. S., and G. Su, "Generalized Thermodynamic Properties of Real Gases," A.I.Ch.E. J., 11 (2), 202 (March 1965).

B-11. Lydersen, A. L., R. A. Greenkorn, and O. A. Hougen, Generalized Thermodynamic Properties of Pure Fluids, Report No. 4, Engineering Experiment Station, University of Wisconsin, Madison, October 1953.

B-12. Cailletet, L., and E. Mathias, Comp. rend., 102, 1202 (1886).

B-13. International Critical Tables, McGraw-Hill Book Co., New York, 1928.

B-14. Grunmach, L., Ann. Physik, 15, 401 (1904).

B-15. Watson, J. M., Ind. and Engr. Chem., 35, 398 (1943).

B-16. JANNAF Thermochemical Tables, The Dow Chemical Company, Midland, Michigan, 31 December 1964 (for nitrous oxide page).

B-17. Data Book, Thermophysical Properties Research Center, Purdue University Lafayette, Indiana, current (but undated) sheets supplied to Rocketdyne in August 1971.

B-18. Edmister, W. D., Petrol. Refiner, 27(11), 609 (1948).

B-19. Katz, L., W. F. Leverton, and S. B. Woods, "The Resonance Method of Measuring the Ratio of the Specific Heats of a Gas, C_p/C_v. VI. Carbon Dioxide, Nitrous Oxide, and Methane," Canadian J. of Res., 27(Sec. A), 39 (1949).

B-20. Clark, A. L., and L. Katz, "Resonance Method of Measuring the Ratio of the Specific Heats of a Gas, C_p/C_v. Part III. Sulphur Dioxide and Nitrous Oxide," Canadian J. of Res., 19 (Sec. A, No. 9), 111 (September 1941).

B-21. Reid, R. C., and J. R. Valbert, Ind. Eng. Chem. Fundamentals, 1, 292, (1962).

B-22. Reid, R. C., and T. K. Sherwood, The Properties of Gases and Liquids, McGraw-Hill Book Company, New York, 2nd Edition, 1966.

B-23. Couch, E. J., and K. A. Kobe, University of Texas Report on Contract DAI-23-072-ORD-685, 1 June 1956.

B-24. Perry, J. H., et al (editors), Chemical Engineers' Handbook, McGraw-Hill Book Company, New York, 4th edition, 1963.

B-25. Bowman, R. E., et al, "Properties of Oxides of Nitrogen," Liquid Propellants Handbook, The Battelle Memorial Institute, Columbus, Ohio, 1956.

B-26. Johnston, H. L., and K. E. McCloskey, "Viscosities of Several Common Gases Between 90°K and Room Temperature," J. of Phys. Chem., 44, 1038 (1940).

B-27. Raw, C. J. G., and C. P. Ellis, "High-Temperature Gas Viscosities. I. Nitrous Oxide and Oxygen," J. of Chem. Phys., 28, 1198 (June 1958).

B-28. Jossi, J. A., L. I. Stiel, and G. Thodos, A.I.Ch.E.J., 8, 59 (1962).

B-29. Liley, P. E., "The Thermal Conductivity of 46 Gases at Atmospheric Pressure," Proc. 4th Symp. Thermophys. Prop., J. R. Moszynski (ed.), A.S.M.E., New York, 1968.

B-30. Johnston, H. L., and E. R. Grilly, J. Chem. Phys., 14, 233 (1946).

B-31. Choy, P., and C. J. G. Raw, J. Chem. Phys., 45, 1413 (1966).

B-32. Richter, G. N., and B. H. Sage, "Thermal Conductivity of Fluids, Nitrous Oxide," J. Chem. and Eng. Data, 8(2), 221 (April 1963).

B-33. Stiel, L. I., and G. Thodos, A.I.Ch.E.J., 10, 26 (1964).

B-34. Verslag koninklijke Academie van Wetenschappen te Amsterdam, Verschaffelt, No. 18, 1895, p. 74.

B-35. Handbook of Chemistry and Physics, The Chemical Rubber Co., Cleveland, Ohio, 50th Edition, 1969-1970.

B-36. Maryott, A.A., and E. R. Smith, Table of Dielectric Constants of Pure Liquids, NBS 61-514, National Bureau of Standards, Washington, D. C., 10 August 1951.

B-37. Watson, H. E., G. Gundu-Rao, and K. L. Ramaswamy, "The Dielectric Coefficients of Gases, Part II. The Lower Hydrides of Carbon and Silicon, Oxygen, Nitrogen, Oxides of Nitrogen and Carbon, and Fluorides of Silicon and Sulphur," Proc. Royal Soc. (London), 143, 579 (1933).